To the Graduate Council:

I am submitting herein a dissertation written by Huqiu Zhang entitled " A Study of Fluorinated Diamond-oid Cage Molecules: Alcohols, Esters, and Other Carbonyl Compounds." I have examined the final copy of this dissertation for form and content and recommend that it be accepted in partial fulfillment of the requirements for the degree of Doctor of Philosophy, with a major in Chemistry.

James L. Adcock, Major Professor

We have read this dissertation
and recommend its acceptance:

Accepted for the council:

Associate Vice Chancellor and
Dean of The Graduate School

A STUDY OF FLUORINATED DIAMOND-OID CAGE MOLECULES: ALCOHOLS, ESTERS, AND OTHER CARBONYL COMPOUNDS

A Dissertation

Presented for the

Doctor of Philosophy

Degree

The University of Tennessee, Knoxville

Huqiu Zhang

May, 1995

DEDICATION

To my parents,

and also Yimin, Shee Shee, and Donna

ACKNOWLEDGMENTS

I wish to take this opportunity to express my sincere gratitude and deepest appreciation to my research advisor, Dr. James L. Adcock, for his guidance and trust. Without his advice and support, this work would never have been started or finished.

I thank the other members from this research group: Dr. Shyam B. Mathur, Dr. Purnendu Mukhopadhyay, Dr. Andrei Gakh, Dr. Humin Luo, and Mr. Haoqiang Huang for their help.

I also thank Dr. Albert A. Tuinman and Dr. Scott Kriger for the mass spectra measurement; Dr. Spiro Alexandratos for the access to some of the research equipment; Advance THermal AnalysiS (ATHAS) laboratory for the DSC measurement of starting materials.

Special thanks are extended to the other members of my dissertation committee, Dr. Spiro Alexandratos, Dr. Richard Pagni and Dr. Engin H. Serpersu for their aid and cooperation.

Financial supports from the Environmental Protection Agency of the United States and the Department of Chemistry of the University of Tennessee, Knoxville are gratefully acknowledged.

Finally, I wish to thank my husband, Yimin Jin, whose love and support have made this all worthwhile.

ABSTRACT

Aerosol direct fluorination of adamantyl acetate gives 1-F-adamantyl trifluoroacetate and 1-[2-hydryl-F-adamantyl] trifluoroacetate in almost a 1:1 ratio. Aerosol direct fluorination of 1,3-adamantyl bis-acetate gives 1,3-[2-hydryl-F-adamantyl] bis-trifluoroacetate. The hydrolysis of 1-F-adamantyl trifluoroacetate and 1-[2-hydryl-F-adamantyl] trifluoroacetate gives correspondent perfluorinated alcohols. 2-[2-Hydryl-adamantyl] alcohol is also synthesized by a reduction of perfluorinated adamantanone. The acidities of F-adamantan-1-ol, 2-hydryl-F-adadamantan-1-ol, and 2-hydryl-F-adamantan-2-ol are measured by acid-base titration. The *pKa* values are 5.2, 6.3 and 9.4, respectively. The rates of acetylation reaction of these alcohols correlate with their acidities. The tendency to form hydrogen bonds with hydrogen-bond acceptor solvent depends on the acidity and the steric hindrance of these alcohols.

A series of 1-[2-hydryl-F-adamantyl] esters are synthesized. They are: 1-[2-hydryl-F-adamantyl] methanesulfonate, 1-[2-hydryl-F-adamantyl] trifluoroacetate, 1-[2-hydryl-F-adamantyl] acetate, 1-[2-hydryl-F-adamantyl] benzoate, 1,3-[2-hydryl-F-adamantyl]bis-trifluoroacetate,and1,3-[2-hydryl-F-adamantyl]bis-benzoate. Two-center and three-center C−H hydrogen bonds are found in these ester system. A linear correlation between the chemical shifts and the $^{2}J_{H-F}$ coupling constants is observed along with an unusual high field shift of C−H stretching frequencies in these hydrogen-bond systems. A significant deviation from the linear correlation is found in 1-[2-hydryl-F-adamantyl] methanesulfonate.

F-2,6-Adamantanedione is synthesized by aerosol direct fluorination of 2,6-adamantanedione. Photochemical reaction of F,6-adamantanedione gives F-tricyclo[3.3.0.$0^{3,7}$]octane. It is a three-step reaction, the shortest way to approach the bisnoradamantane structure starting with commercially available adamantane.

A series of perfluorinated cage orthoesters are synthesized using aerosol direct fluorination without significant rearrangement products. They are: 4-methyl-2,6,7-trioxabicyclo[2.2.2]octane, 1,4-dimethyl-2,6,7-trioxabicyclo[2.2.2]octane, 1-ethyl-4-methyl-2,6,7-trioxabicyclo[2.2.2]octane, 2,4,10-trioxaadamantane, and 1-methyl-2,4,10-trioxaadamantane.

Hydrolysis of 1-chloro-F-adamantane and 1,3,5-trichloro-F-adamantane in the presence of KOH and catalyst, 18-crown-6, give 1-hydryl-F-adamantane and 1,3,5-trihydryl-F-adamantane, respectively. The normal strong oxidizing reagents do not oxidize 1-hydryl-F-adamantane. 5-Hydryl-F-adamantan-2-one is synthesized by reducing 5-chloro-F-adamantan-2-one to *E, Z*-2,5-dihydryl-F-adamantan-2-ol, and oxidizing the alcohols.

CONTENTS

List of Figures

List of Tables

Chapter 1 Introduction

1.1 Organic Fluorine Compounds

Fluorine was isolated just over a century ago. However, research about the chemistry of fluorine-containing compounds began in earnest a half century ago. Fluorinated organic compounds can be separated into two categories: (1) highly fluorinated compounds, in which all or at least most of the hydrogen initially bonded to carbon atoms has been replaced by fluorine; and (2) low-fluorinated compounds, in which only a few of the hydrogen atoms have been replaced by fluorine. The first category of compounds is chemically low in reactivity and is used for fire extinguishants, coolants, lubricants, blood substitutes, polymers, etc.. The second category of compounds is widely used in biochemistry, and the medical and pharmaceutical industries.

The first category of compounds comprises the main research subject in our laboratory. This thesis work will therefore focus on the syntheses of perfluorinated organic compounds and the introduction and chemistry of the various types of functional groups that may be attached to these perfluorinated groups.

Fluorine is the most electronegative element, with a Pauling electronegativity of 4 as compared to 3.5 for oxygen, 3.0 for chlorine and nitrogen, and 2.8 for bromine.[1] It is this property that is the origin of the difference between fluorinated compounds and hydrogenated compounds. A high electronegativity means a strong electron-withdrawing effect. When fluorine replaces hydrogen in a hydrocarbon

Table 1 Carbon-Halogen Bond Lengths and Bond Dissociation Energies in Halomethanes

	CH_3X	CH_2X_2	CHX_3	CX_4
F	1.385 Å 456 kJ mol^{-1}	1.358 Å 510 kJ mol^{-1}	1.332 Å 535 kJ mol^{-1}	1.317 Å 543 kJ mol^{-1}
Cl	1.782 Å 350 kJ mol^{-1}	1.772 Å 339 kJ mol^{-1}	1.767 Å 325 kJ mol^{-1}	1.766 Å 301 kJ mol^{-1}
Br	1.939 Å 289 kJ mol^{-1}	1.934 Å 267 kJ mol^{-1}	1.930 Å 259 kJ mol^{-1}	1.942 Å 235 kJ mol^{-1}

compound, the electron density distribution will be changed, which results in a changed chemical reactivity as well. Fluorine forms the strongest single bond to carbon in organic compounds (Table 1).[2] Table 1 indicates that as more fluorine atoms replace hydrogen atoms in a methane structure, the C–F bonds become shorter and the bond dissociation energies become higher. Therefore, perfluorocarbon compounds are very stable and have a strong resistance toward any kind of chemical reactions. Fluorine has the smallest atomic volume next to hydrogen. The Van der Waals radii of related elements are shown in Table 2.[3] Fluorine is the only element in the periodic table which can replace hydrogen without notable steric consequences. Therefore, only fluorine can completely replace hydrogen to form a new series of compounds, the fluorocarbon compounds. Considering the similar

Table 2 Van der Waals Radii of Some Elements

X	H	F	Cl	Br	O	N	C	B
r (Å)	1.06	1.40	1.75	1.87	1.42	1.46	1.53	1.65

steric demand and high C–F bond energy, perfluorocarbon compounds are as stable as hydrocarbon compounds. The above properties enable the perfluorinated organic compounds to be thermally stable and chemically inert.

While the perfluorinated organic compounds are resistant to almost all chemical reagents, the functional groups that are attached to perfluorocarbon groups, such as ester or carbonyl groups, will show a great enhancement in reactivities. The electron densities around these functional groups are drastically altered by a perfluoroalkyl group relative to an alkyl group. The fluorine atoms that sit next to these reaction centers will have a strong inductive electron withdrawing effect. As a result, these reaction centers will show stronger acidity, both as Lewis acids and Bronsted acids. The simplest example is acetic acid, CH_3COOH. It has a *pKa* value of 4.75.[4] However, the *pKa* value is 2.68 for fluoroacetic acid in which one fluorine atom replaces one hydrogen atom, 1.48 for difluoroacetic acid in which two fluorine atoms replace two hydrogen atoms, and 0.70 for trifluoroacetic acid in which all three hydrogens are replaced by fluorines.[5] The acidity of trifluoroacetic acid is about 10^5 stronger than that of acetic acid. Introducing three fluorine atoms in acetic acid has a strong inductive effect on the carboxylic group. After losing a proton atom, the

negatively charged acetate species will be strongly stabilized by the neighboring fluorine atoms. Therefore the acidity of trifluoroacetic acid is greatly enhanced.

The influence of the perfluorinated alkyl group on various functional groups is strong. When these perfluorinated alkyl groups are attached to functional groups, they will show many unusual properties, resulting from the changed polarization such as being more electrophilic. The usefulness of the unique properties of perfluorinated compounds has been recognized for a long time. However, there is not as much known about the chemistry of functionalized perfluorinated compounds as the corresponding hydrocarbon analogues. Therefore this thesis work focuses on the study of perfluorinated compounds with selected functional groups.

1.2 Aerosol Direct Fluorination Method

Fluorine, with its unique physical and chemical properties, can replace sequentially all of the hydrogen in a hydrocarbon compound to form a series of new compounds, culminating in the perfluorocarbon compound. These compounds do not occur naturally; therefore, the entire perfluorocarbon chemistry is based on synthesis. Essentially there are three possible methods for the synthesis of perfluorocarbon compounds. The first method is fluorination with elementary fluorine in a gaseous state.[6] The second method uses fluorine-active metal fluorides.[7] The third method is electrofluorination.[8] Our interest is in fluorination with elementary fluorine. Therefore, only the first method will be discussed here.

Table 3 Reaction Mechanism of Fluorination Reaction

step		reaction	ΔH (kJ mol^{-1})
initiation	1a	$F_2 \rightarrow 2F\cdot$	+157
	1b	$F_2+RH \rightarrow R\cdot+HF+F\cdot$	+17
propagation	2a	$RH+F\cdot \rightarrow R\cdot+HF$	−142
	2b	$R\cdot+F_2 \rightarrow RF+F\cdot$	−285
termination	3a	$R\cdot+F\cdot \rightarrow RF$	−448 ~ −469
	3b	$F\cdot+F\cdot \rightarrow F_2$	−157
	3c	$R\cdot \rightarrow$ Fragmentation	

Fluorine was first isolated by Moissan in 1886. For 50 years after that, the use of elementary fluorine progressed very slowly. This slow pace was mainly due to the unusually high reactivity and corrosiveness of the element. Fluorine, if uncontrolled, reacts violently on contact with any kind of hydrocarbon compounds, often with explosive results. The high exothermicity of the elementary fluorination reaction is due to very weak F−F bond and strong C−F and H−F bonds in the products. The mechanism of elementary fluorination is generally accepted as a radical chain mechanism (Table 3).[5]

Table 3 quantifies the origin of the violent fluorination reaction. First, the dissociation energy for molecular fluorine is very low, only 157 kJ mol^{-1} in step 1a. The dissociation energy is even lower in step 1b, only 17 kJ mol^{-1} and this is much

less than energy released in the propagation steps. Chain reactions can occur through further initiation by energy released in the propagation steps. Therefore, in the associative initiation step, little energy is required. Second, in the propagation step the energy release is larger than the initiation step. The heat generated in the propagation steps are large enough to induce more initiation reactions. Control is essential since the energy released in the termination step is larger than the C–C bond energy. In step 3a, the carbon-fluorine bond formation energy is about 448 to 469 kJ mol^{-1}, surpassing the bond dissociation energy of the carbon-carbon bond, which is about 351 kJ mol^{-1}.[9] Therefore, fragmentation of the carbon skeleton is inevitable if F· radical populations are very high.

The basic problem of direct fluorination involves both kinetics and thermodynamics. The key to solve these problems is to reduce the concentration of input fluorine flow and to remove efficiently the heat that is released from the reaction. Many chemists attempted to solve this problem and succeeded in some aspects before the 1970's. For example, Bockemuler bubbled fluorine diluted with nitrogen through a cold solution of organic compounds in an inert solvent.[10] Mono- and difluorination were achieved, but no perfluorination. After that, Bigelow and coworkers passed fluorine diluted with nitrogen through a reactor containing metals, such as copper gauze.[11] Fairly good perfluorination results were obtained, with yields as high as 62%. The metal, which they claimed as a "catalyst," actually served as a heat sink to absorb the heat released from the reaction. The following work from the same group showed more optimistic results. The hydrocarbon up to C_4

could be successfully perfluorinated; however, it failed to perfluorinate hydrocarbons beyond C_4.[12] Lagow and Margrave invented the LaMar technique. The low-temperature-gradient (LTG) fluorination reactor patented in the late 1970's extended fluorination to ordinary organics. The LTG method was the most successful perfluorination method at that time.[6] This method used a helium diluted fluorine stream and maximized the surface area for the contact of hydrocarbon and fluorine by introducing solid-state stabilization. The reaction temperature was regulated by a liquid nitrogen temperature controller. There were limitations inherent in this reactor. For example, the reaction was slow, and of a "batch" type, which was difficult to commercialize. Additionally, this reactor failed to handle compounds with low solid-state volatility.

The aerosol direct fluorination method (AF) was developed in our laboratory in the early 1980's.[13] A comprehensive review was done by Adcock and Cherry.[14] A schematic drawing of the aerosol direct fluorination reactor is shown in Figure 1. The major difference between the aerosol direct fluorination method and other direct fluorination methods is that AF is a flow process. Organic compounds are evaporated in a hydrocarbon evaporator. Helium gas is the primary carrier gas of hydrocarbon compounds. The preaerosol sodium fluorides are cooled to $-196°C$ and become microscopic nucleating particles. The vaporized hydrocarbons are absorbed on these sodium fluoride particles and exposed to a gradient of increasing fluorine concentration input along the length of a reactor tube having a positive temperature gradient. Fluorination occurs on the surface of these

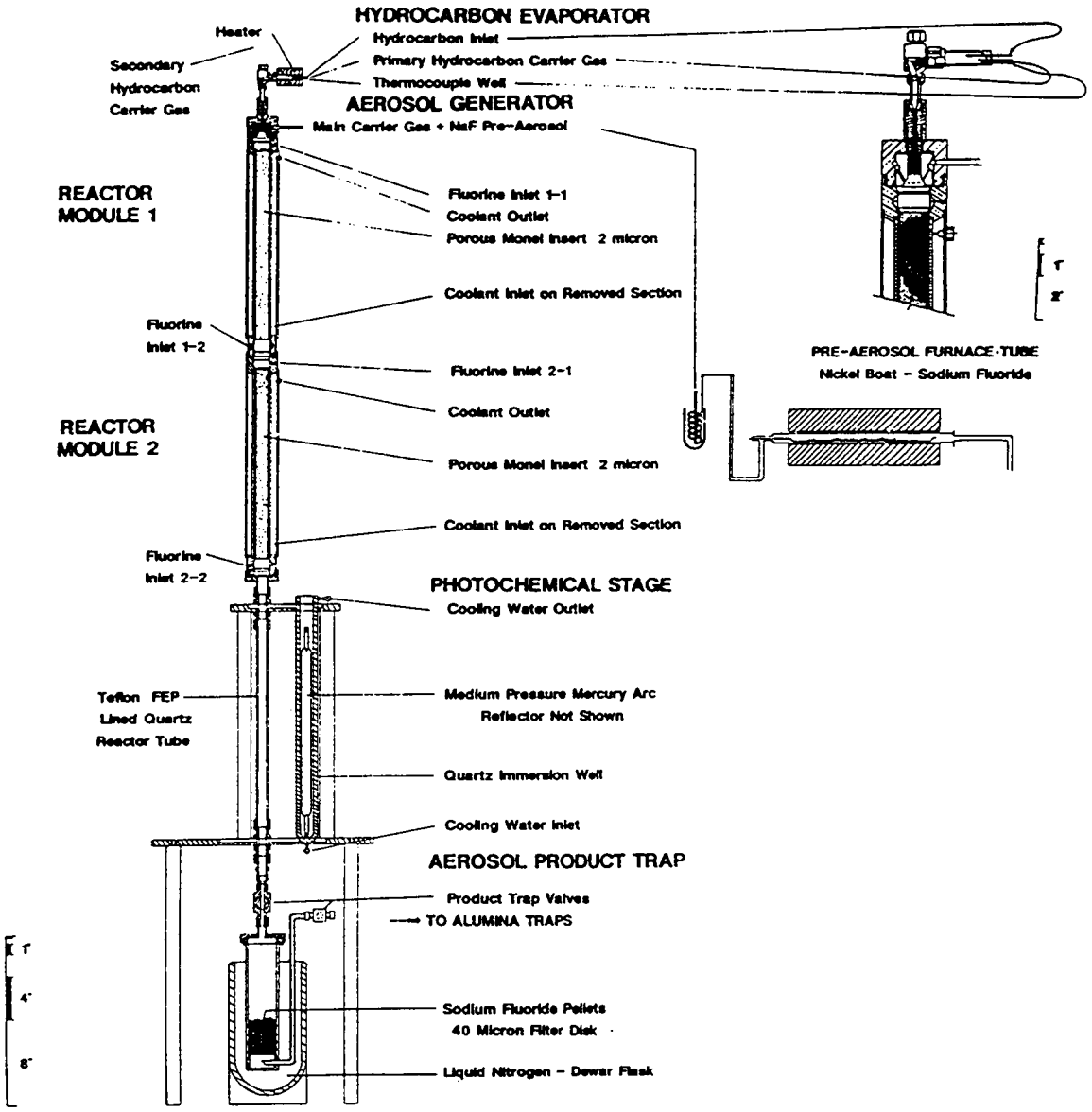

Figure 1 Aerosol Direct Fluorination Reactor[14]

particles, while at the same time they are carried down through the reactor tube by the main helium carrier gas. The final product is collected in a trap which is cooled to −196°C at the bottom of the reactor.

The fluorination occurs in four stages. The first stage has low temperature and low fluorine concentration. This is a reaction-limiting stage. The fluorination reaction is kinetically slower at conditions of low temperature and low fluorine concentration. This initial set of conditions minimizes the possibility of having too many simultaneous hydrogen replacements on one molecule. Consequently, the chances of fragmentation and crosslinking are reduced. In the first stage, the most reactive hydrogen atoms are replaced with fluorine atoms. The second stage should allow an increasing number of efficient collisions of fluorine molecules and hydrocarbon molecules, thus increasing the efficiency of fluorination reaction. The second and third stages have higher temperatures and higher fluorine concentrations. The fourth stage of fluorination is a photochemical stage. Usually the higher the fluorine substitution on the compounds, the more resistant the residual hydrogen atoms become. The last hydrogen atom is the most difficult one to replace with a fluorine atom. In order to replace the remaining hydrogen atoms with fluorine atoms without input of an excess fluorine flow, UV irradiation is applied. The four-stage fluorination increases the efficiency of the fluorine usage, and allows a rough stoichiometric control.

The sodium fluoride nucleating particle serves an important role in the aerosol direct fluorination reaction. These particles act as a heat sink to absorb and

dissipate the heat energy of the fluorination reaction through the sodium fluoride lattice. The fluorination reactor is kept at a low temperature (below 0°C) during the fluorination reaction. The coolant outside the reactor wall cannot, however, prevent a locally high temperature from occurring inside the reactor. In order to efficiently remove the reaction heat from the aerosol particles where the reaction taking place, a high thermal conductivity, inert helium carrier is used. The hydrocarbon compounds are absorbed on the sodium fluoride nucleating particles. The large number of small particles offer a large surface for the absorbed hydrocarbon molecules to react with fluorine. The locally high energy caused by the fluorination reaction can be absorbed by the sodium fluoride lattice. In addition, the hydrocarbon molecules are being held in the solid surface. One side of the molecule is exposed to the fluorine, and the other side of the molecule is protected by the solid surface. Therefore, fluorine can attack one side of the molecules only. Because the absorbed species are fixed on the surface even though there may be a bond scission in a hydrocarbon molecules, recombination is likely to occur. Immobilization minimizes crosslinking caused by the interaction between the carbon radicals that formed during the fluorination reaction by reducing their mobility.

In conclusion, the aerosol direct fluorination method has advantages that the other methods lack. Effective control of reaction exothermicity, fragmentation, and crosslinking results in high yields, high effluent purities, and good fluorine efficiency. Stoichiometric control allows study of reaction pathways and mechanism.

1.3 Aerosol Direct Fluorination of Organic Compounds

The aerosol direct fluorination method has proven to be a successful method to achieve perfluorination of organic compounds. It includes the combined applications of flow process, preaerosol sodium fluoride nucleating particles, fluorine flow gradient, and low-temperature gradient. Since the development of this method, we have perfluorinated many hydrocarbon alkane compounds and hydrocarbons with a variety of functional groups, such as ethers, esters, ketones, and alkyl chlorides. Most functional groups are preserved although rearrangements have been observed.

1.3.1 Alkanes

The aerosol direct fluorination of alkane compounds produces analogous perfluorinated compounds. For example, in the fluorination of neopentane, perfluorinated neopentane is produced in almost quantitative yield.[15] When highly branched hydrocarbon compounds, such as 2,4-dimethylpentane, however, are fluorinated only a small portion of perfluorinated analogues is obtained.[15] The residual hydrogen atoms are found to be located at the highly protected tertiary positions. Therefore, steric effects play an important role in product formation, a role important in other direct fluorination methods.[16] Fluorine will first attack the alkyl groups that have the most hydrogen atoms on them.

The aerosol direct fluorination method is an excellent method to perfluorinate hydrocarbon cage compounds as long as no significant ring strain energy exists. The six-membered ring systems are good precursors for fluorination. The "LTG" direct

fluorination method results in poly-fluorinated "cage" compounds with one or two bridgehead hydrogen residues.[17] However, the aerosol direct fluorination of adamantane[18] and diamantane[19] give the corresponding perfluorinated compounds; all have purities above 74%. In the perfluorination of chain and "cage" hydrocarbon compounds, the aerosol direct fluorination method is very successful.

1.3.2 Ethers

Dialkyl ethers are among those compounds that are most feasible for the aerosol direct fluorination. A large number of different dialkyl ethers including cyclic ethers and "glyme" ethers have been successfully perfluorinated with purities up to 90%.[20] However, when chain orthoesters are subjected to aerosol direct fluorination, an extensive beta scission rearrangement is observed (Scheme 1).[21] The abstraction of hydrogen from the methoxyl group by fluorine results in a rapid loss of the $O=CH_2$ group. The tertiary carbon radical that formed can be stabilized by the other two methoxyl groups. The final product is F-1,1-dimethoxyethane. Generally, aerosol direct fluorination is very good at perfluorination of dialkyl ethers. However, acyclic orthoesters will experience a beta scission rearrangement.

1.3.3 Esters

Two facts influence the aerosol direct fluorination of esters. First, perfluorinated esters undergo F^- catalyzed cleavage to form acid fluorides. Second, the possibility of having hydrogen residue exists when there is highly branched alkyl

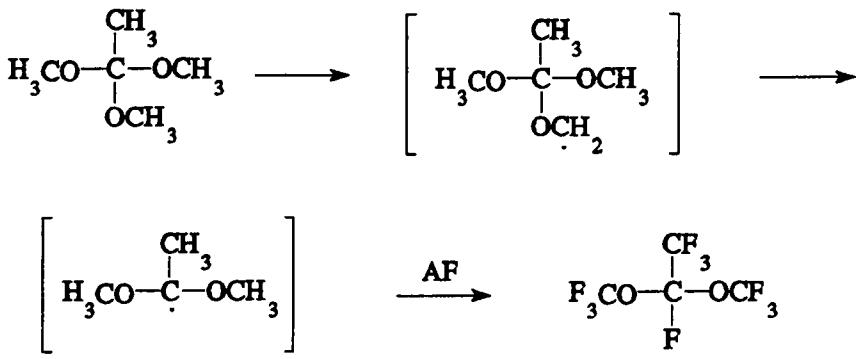

Scheme 1

group on the esters. A series of esters have been subjected to aerosol direct fluorination.[22] These compounds have different alkyl groups attached to the carbonyl part of the molecules and the alkoxyl part of the molecules. The fluorination results show that when the alkyl group becomes more bulky, the carbonyl group is better protected from the attack by fluoride ion, thus enhancing skeletal integrity. However, when there is an isopropyl group attached to either side of the ester, the methine hydrogen residue is likely to exist.

1.3.4 Ketones

The aerosol direct fluorination of ketones usually gives moderate to good yields.[23] In the other fluorination methods, fluoride in potassium fluoride or cesium fluoride will form fluoroxy compounds.[24] However, in aerosol direct fluorination the fluoride in sodium fluoride does not produce any fluoroxy products. This is likely a result of the reduced activity of fluoride ion in the aerosol direct fluorination. While the aerosol direct fluorination successfully perfluorinates the

straight chain and low branched ketones, in the fluorination of highly branched ketones a skeletal rearrangement occurs (Scheme 2).[25]

The aerosol direct fluorination of adamantanone gives perfluorinated adamantanone with a yield above 50% and purity up to 98%.[23b] The UV irradiation of F-adamantanone gives interesting results. CO is eliminated, and a C–C bond is formed (Scheme 3). This provides a good method for the synthesis of smaller cage perfluorinated compounds.

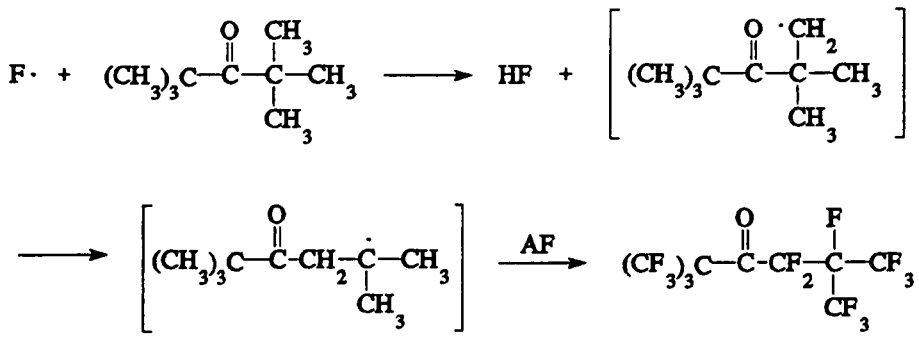

Scheme 2

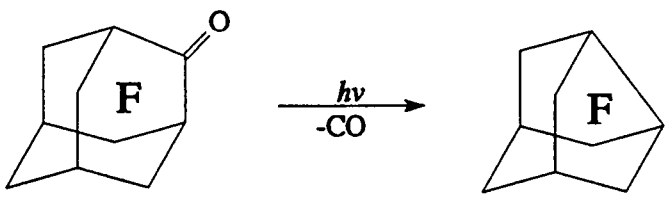

Scheme 3

1.3.5 Alkyl Chlorides

The fluorination of chain alkyl chlorides usually gives good yields of analogous perfluorinated compounds. Rearrangements are observed in some cases. The fluorination of primary alkyl chlorides gives excellent yields without detectable rearrangement products. The secondary alkyl chlorides generally give a mixture of primary and secondary perfluorinated chlorides due to a 1,2-chlorine shift to form more stable radicals during fluorination.[26] The tertiary alkyl chlorides will undergo a complete rearrangement to form primary or secondary chlorides. The formation of a tertiary radical intermediate during the fluorination is the driving force in the rearrangement. The 1,2-chlorine shift is generally observed in the fluorination of secondary or tertiary chain alkyl chloride. In fluorination of adamantyl chlorides, no 1,2-chlorine shift is observed. However, when 2,2-dichloro-adamantane is subjected to fluorination, a unique 1,3-chlorine shift is observed.[27] The formation of tertiary planar radicals and the release of steric energy caused by crowding two chlorine atoms on one carbon atom are the reasons the unfavorable 1,3-chlorine shifts occur.

1.4 A Brief Description of Thesis Work

Perfluorocarbon compounds are very stable compounds, and are inert to most chemical reactions. Fortunately, many functional groups, such as alkyl chloride, esters, and ethers can survive the aerosol direct fluorination intact. Therefore, the synthesis of perfluorinated carbon compounds bearing one or more functional groups is practical. Each of these functional groups with a perfluorinated alkyl group

attached will have interesting chemical properties, such as being differently polarized or more electrophilic. The five major projects in this thesis follow from our continuing interest in the synthesis of perfluorinated organic cage compounds and the study of the chemical and physical properties of these compounds. They are: synthesis of perfluorinated and mono hydryl perfluorinated adamantane alcohols, and the study of their properties; the study of C–H hydrogen-bond system; synthesis of perfluorinated 2,6-adamantanedione and perfluorinated bisnoradamantane; synthesis of perfluorinated cage orthoester derivatives; the reduction and oxidation reaction on bridgehead-substituted F-adamantane.

Chapter 2 Experimental Procedure

2.1 Instrumentation

Synthesis, separation, and characterization of compounds were carried out on the following equipment and instrumentation.

2.1.1 Aerosol Direct Fluorination Reactor

The principle of aerosol direct fluorination was discussed in section 1.2. The detailed reaction procedure will be described here. Nucleating particles of NaF were generated in an electrical furnace heated to above 1050°C. The NaF particles were carried by a flow of helium to a heat exchanger which was kept at −196°C. The chilled NaF particles in the helium stream enter the reactor through an aerosol generator. All the hydrocarbon compounds were introduced to the reactor by liquid solution injection. The hydrocarbon compound (and the solvent)* were evaporated and carried by the primary hydrocarbon carrier (helium) gas into the aerosol generator and then into the reactor. Fluorine diluted with helium gas, enters the reactor through two modules each with two inlets feeding a porous monel diffuser, comprising the reactor wall. In this manner, a fluorine concentration gradient is established over the reactor length. As the fluorination reaction was carried out, the

---

* The solvent was chosen to boil higher then the melting point of the solute to prevent evaporation plugging of the evaporator feed line. Obtaining the most volatile fluorinated solvent possible in the product mixture is a second important consideration.

combined NaF/reactant aerosols were carried down the tubular reactor ending in a stainless steel product trap cooled with liquid nitrogen. Following the fluorination, the product trap was disconnected from the reactor and connected to a vacuum line for further separation.

In a typical run, the hydrocarbon and co-fluorinating solvent ratio was about 1:3.5 (g/g). The solution was injected into the hydrocarbon evaporator by a syringe pump. A 10-ml syringe was used and the injection was controlled at a rate of 1.5 ml/hr. From the weight and the volume of the injection solution, the number of moles of hydrogen atoms can be calculated. From that data, the fluorine flow can be calculated by choice of the proper ratio of hydrogen and fluorine.

Trap to trap fractionation commonly included five traps at different temperatures, commonly −22°C, −45°C, −78°C, −131°C and −196°C, respectively. From the fluorination of adamantane derivatives and all the other compounds in this thesis work, the fluorination products were collected in the −22°C trap along with some perfluorinated solvent which generally passed to colder traps.

2.1.2 Vacuum Line

An all borosilicate-glass vacuum line was used for transfer, fractionation, and storage of fluorinated compounds. All stopcocks were Kontes Hi Vacuum Teflon with non-rotating stems. A Welch Duo-seal (1402B) vacuum pump was used.

2.1.3 Gas Chromatography

All the fluorination products were separated by gas chromatography (GC) on a Bendix 2300 semi-preparative gas chromatograph. This instrument was equipped with a subambient multicontroller, a 7 m × 3/8 inch column, filled with 13% fluorosilicone QF-1 stationary phase on 60−80 mesh, acid-washed chromosorb P conditioned at 225°C for 12 hours. The carrier gas was ultra-high purity helium. Analytic GC separations were carried out on a Hewlett Packard 5890A gas chromatograph using capillary Sp 2100 60 m × 0.25 mm ID fused silica column (Superlco).

2.1.4 Infrared Spectra

Infrared spectra were operated on a Bio-Rad Spc 3200 FTIR spectrophotometer. Gas samples were recorded using a 10 cm gas cell with KCl windows. Liquid and solid spectra were recorded as a thin-film between two KCl plates or in a liquid solution cell with KCl windows.

2.1.5 Nuclear Magnetic Resonance

^{19}F NMR spectra were recorded on a JEOL FX90Q NMR spectrometer with omniprobe and NM-PVTS1 programmable VT system. The operating frequency was 84.74 MHz. $CFCl_3$ was used as solvent and reference. A sample solution held in a 5 mm NMR tube was inserted into a 10 mm NMR tube containing a deuterated solvent to provide a lock. ^{1}H NMR and ^{13}C NMR spectra were recorded on a

Bruker AC-250 NMR spectrometer equipped with a 5 mm switchable $^{1}H/^{13}C$ probe. The operating frequencies were 250.13 MHz for ^{1}H and 62.89 MHz for ^{13}C. Tetramethylsilane (TMS) was used as an internal standard with $CDCl_3$ as lock solvent unless specified otherwise.

2.1.6 Mass Spectra

Mass spectra were recorded on a VG ZAB-EQ Mass Spectrometer. Either positive electron-impact ionization or negative chemical ionization/electron attachment was used as indicated.

2.1.7 Elemental Analysis

Elemental analyses were conducted by E+R Microanalytical Laboratory, Inc., Corona, New York.

2.1.8 Differential Scanning Calorimetry

Differential Scanning Calorimetry (DSC) was used to measure sublimation and melting temperature of pre-fluorination samples. The experiments were carried out on Thermal Analysis 2100 System from TA Instruments, Inc. with a Dual Sample DSC cell and a DSC Autosampler, which was capable of running two samples, one in an opened aluminum pan for sublimation temperature and one in a closed/hermetically sealed aluminum pan for melting temperature, simultaneously. 3–5 mg samples were placed in an aluminum pan and heated at 10 °C/min under

a nitrogen gas flow typically 20 ml/min. Typical DSC curves for a sample in an opened and a closed pan are shown in Figure 2. The opened pan experiment provides a clear picture of sublimation behavior while the closed pan experiment gives the melting temperature.

2.1.9 pH Measurement

pH Values were measured using a Corning pH/ion meter 150, calibrated at pH = 4 and pH = 7. The electrode was a Corning semi-micro combination electrode.

2.2 Commercial Chemicals

All materials used were reagent grade and were used as received except where otherwise noted.

Acetic Acid: Fisher Scientific.

Acetic Anhydride: Mallinckrodt Chemical (99.8%).

Acetone: Mallinckrodt Chemical.

Acetone-d_6: Norell (99.8%D).

Acetonitrile-d_3: Cambridge Isotope Laboratory (99.8%D).

Acetyl Chloride: Aldrich Chemical (98%).

Adamantane: Aldrich chemical (99+%).

1-Adamantanol: Aldrich Chemical (99+%)

2-Adamantanone: Aldrich Chemical (99+%).

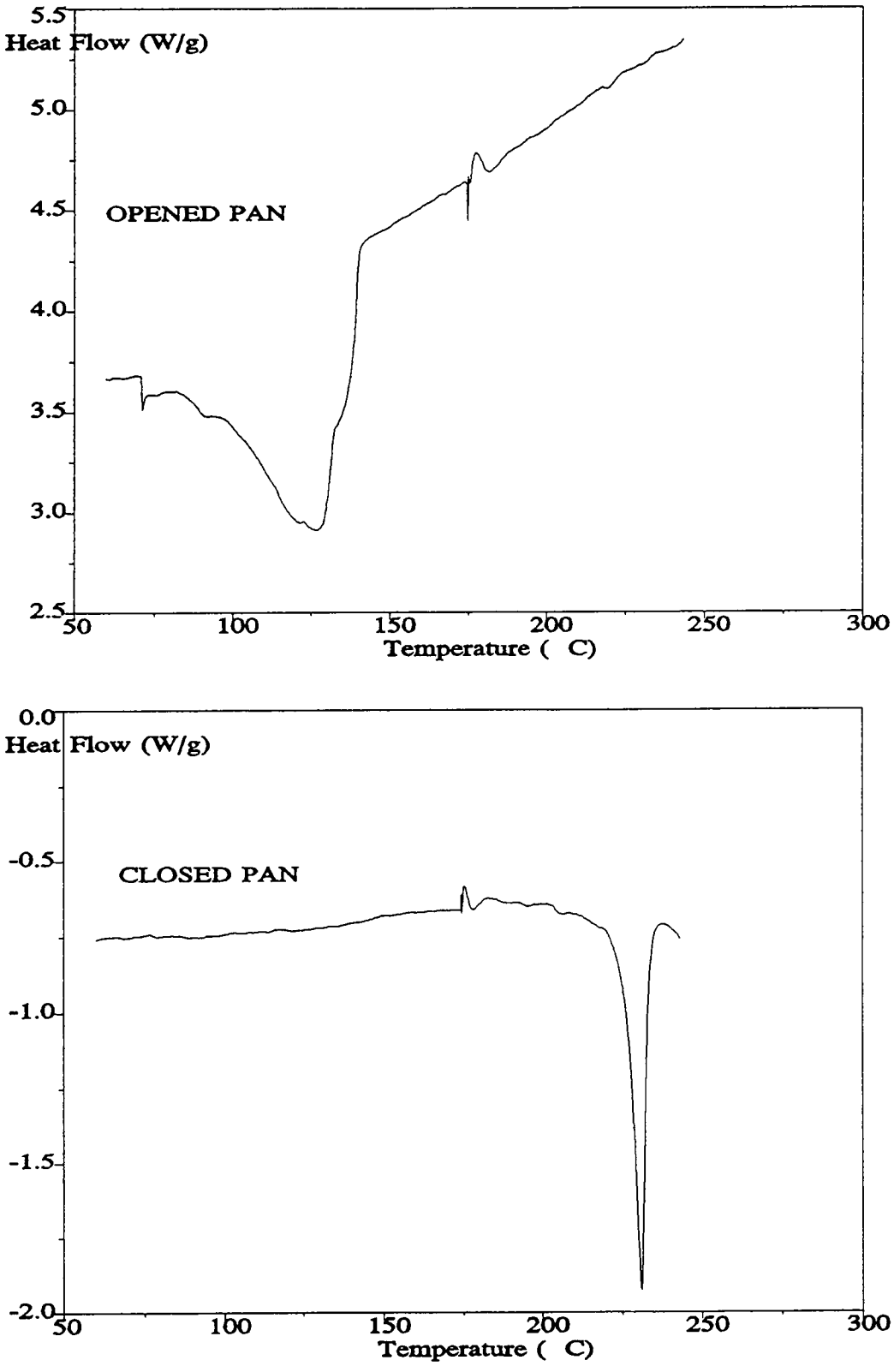

Figure 2 DSC Curves of a Sample in a) Opened Pan and b) Closed Pan.

Aluminum Chloride: Aldrich Chemical (99%).

Benzene: Fisher Scientific.

Benzoyl Chloride: Aldrich Chemical (99+%).

Carbon Tetrachloride: Mallinckrodt Chemical.

1-Chloroadamantane: Lancaster Chemical (99%).

Chloroform: Mallinckrodt Chemical (99.9%).

Chloroform-*d*: Aldrich Chemical (99.8%D).

Chromium(VI) Oxide: Aldrich Chemical (99.9%, powder).

cis, cis-1,3,5-Cyclohexanetriol: Aldrich Chemical (98%).

18-Crown-6: Aldrich Chemical.

Dichloromethane: Mallinckrodt Chemical (99.9%).

Diethyl Ether: Mallinckrodt Chemical (anhydrous).

Ethyl Acetate: Mallinckrodt Chemical.

Fluorine: Air Products, 97% Technical Grade.

Hexanes: Mallinckrodt Chemical.

Hydrochloric Acid: Mallinckrodt Chemical (37%).

Lithium Aluminum Hydride (powder): Aldrich Chemical (95+%).

Magnesium Sulfate (anhydrous): Mallinckrodt Chemical.

Methanesulfonyl Chloride: Aldrich Chemical (99+%).

Methyl Alcohol: Mallinckrodt Chemical (anhydrous).

Methyl Sulfoxide-d_6: Aldrich Chemical (99.9%D).

Molecular Sieves: Mallinckrodt Chemical (4Å).

Phosphorus Pentachloride: Aldrich Chemical (98%).

Phosphorus Trichloride: Aldrich Chemical (98%).

Pyridine: Mallinckrodt Chemical.

Silica Gel 60 Å: American Scientific Products.

Sodium: Fisher Scientific.

Sodium Bicarbonate; Mallinckrodt Chemical.

Sodium Bifluoride (pellets): Harshaw Catalysts.

Sodium Carbonate (anhydrous): Mallinckrodt Chemical.

Sodium Chloride: Mallinckrodt Chemical (Crystal).

Sodium Fluoride: Aldrich Chemical (99.8%).

Sodium Hydroxide: Mallinckrodt Chemical.

Sodium Sulfate Anhydrous: Mallinckrodt Chemical (Granular).

Sulfuric Acid: Mallinckrodt Chemical (96%).

Sulfuric Acid, Fuming 20%: Mallinckrodt Chemical (Approx. 20% Free SO_3).

Tetraethylene Glycol Dimethyl: Aldrich Chemical (99+%).

Tetramethylsilane: Aldrich Chemical (99+%).

Thionyl Chloride: Aldrich Chemical (99+%).

Toluene: Fisher Scientific.

1,1,2-Trichloroethane: Fluka (>98%).

1,2,3-Trichloropropane: Fluka (>99%).

Trichlorofluoromethane (R-11): Pennwalt Corporation.

1,1,2-Trichlorotrifluoroethane (R-113): Aldrich Chemical (99+%).

Triethyl Orthoformate: Eastman Organic Chemical.

Triethyl Orthopropionate: Eastman Organic Chemical.

Trimethyl Orthoacetate: Aldrich Chemical (99%).

1,1,1-Tris(hydroxymethyl)ethane: Aldrich Chemical (99%).

2.3 Synthesis of Hydrocarbon Materials

2.3.1 Synthesis of 1-Adamantyl Acetate

A mixture of 1-adamantanol (3 g) and acetyl chloride (20 ml) was stirred at temperature 0°C for 1 hour and at room temperature for 2 hours. After evaporation of excess acetyl chloride, 4.0 g crude product was obtained; containing 59% of 1-adamantyl acetate and 41% of unreacted starting material. Separation was effected by column chromatography using hexane/acetyl acetate (20:1) as eluent. Characterization of 1-adamantyl acetate: ^{1}H NMR ($CDCl_3$) δ 1.62 (m, 6H), 1.88 (s, 3H), 2.01~2.06 (m, 9H); ^{13}C NMR ($CDCl_3$) δ 170.2, 80.2, 41.3, 36.2, 30.8, 22.6; mp 31-32°C. ^{1}H NMR, ^{13}C NMR spectra and melting point were consistent with data reported in the literature.[28]

2.3.2 Synthesis of Adamantan-1,3-diol

Synthesis of adamantan-1,3-diol followed the literature procedure.[29] Adamantan-1-ol (5.0 g, 0.033 mol) was added to 70% H_2SO_4 (42 ml) and stirred at 85°C for 4 hours. After pouring the mixture on ice, adamantane and unchanged starting material were removed by ether extraction. The aqueous layer was heated

on the steam bath for 2.5 hours. After cooling and the addition of ice, the solution was neutralized with 50% NaOH aqueous solution, saturated with NaCl, then extracted three times with *n*-BuOH. The extracts were combined, dried over anhydrous Na_2SO_4, filtered, and evaporated to dryness. Adamantan-1,3-diol (1.5 g) was obtained as a white solid. The ^1H NMR spectrum and melting point were consistent with data reported in the literature.[29]

2.3.3 Synthesis of 1,3-Adamantyl Diacetate

A mixture of 2.5 g 1,3-adamantanediol and 50 ml acetyl chloride was stirred at temperature 0°C for 15 minutes, at room temperature for 1 hour, under reflux conditions for 2 hours and then at room temperature for another 1 hour. After evaporation of excess acetyl chloride, 3.2 g crude product was obtained, containing 82% of 1,3-adamantyl diacetate and 18% unreacted starting material. Separation was effected by column chromatography using hexane/acetyl acetate (10:3) as eluent. Characterization of 1,3-adamantyl diacetate: ^1H NMR ($CDCl_3$) δ 2.30 (s, 2H), 2.18 (s, 2H), 1.92 (s, 8H), 1.82 (s, 6H), 1.42 (s, 2H); ^{13}C NMR ($CDCl_3$) δ 169.7, 80.0, 44.9, 39.7, 34.5, 30.8, 22.1. The ^1H NMR spectrum was consistent with published data.[30]

2.3.4 Synthesis of 2,6-Adamantanedione

Synthesis of 2,6-adamantanedione followed the literature procedure.[31] Adamantane (14 g, 0.10 mol) was added to fuming sulfuric acid (20% SO_3) (100 ml), with stirring, at 10°C. The temperature was raised gradually to 25°C over about 15

minutes and then maintained at 25 – 28°C by cooling with a cold water bath. After the adamantane dissolved (in about 10 minutes), stirring was continued for additional 10 minutes at 25°C. The mixture was then poured onto crushed ice (300 g) with stirring, and the resulting mixture was subsequently extracted twice with 50 ml portions of CH_2Cl_2 to remove 1-hydroxy-adamantane. The aqueous layer was decanted from some undissolved polymer, and then heated to about 50°C under reduced pressure to remove residual CH_2Cl_2 and SO_2. Heating was continued at atmospheric pressure to 100°C. This temperature was maintained for 2 hours to insure the hydrolysis of the sulfuric acid esters. Water (500 ml) was added, followed by the addition of CrO_3 (7.5 g) in H_2O (25 ml). The mixture was heated at 70°C for 0.5 hour. Upon cooling, the solution was extracted continuously with $CHCl_3$ for 6-8 hours. The extract was dried over anhydrous $MgSO_4$ and evaporated to dryness. The residue was dissolved in CH_2Cl_2 (10 ml). Residual crystals of adamantan-1,3-diol (0.6 g) were filtered off. The filtrate was evaporated to dryness and the residue was separated using column chromatography with Et_2O as eluent. The compounds in order of elution were adamantanone (0.05 g), 2,6-adamantanedione (0.63 g), and 5-hydroxy-adamantan-2-one (4.2 g). ^1H NMR and ^{13}C NMR spectra of 5-hydroxy-adamantan-2-one were consistent with data reported in the literature.[32]

2.3.5 Synthesis of 1,3-Dichloroadamantane and 1,3,5-Trichloroadamantane

Synthesis of 1,3-dichloro-adamantane and 1,3,5-trichloro-adamantane followed the literature procedure.[33] Adamantane (10 g) was dissolved in carbon

tetrachloride (110 ml). Aluminum chloride (10 g) was added to the solution. The mixture was stirred at room temperature for 24 hours. The mixture was cooled to 0°C. Hydrochloric acid (conc., 8 ml) was added to the cooled mixture to destroy any remaining aluminum chloride; this was followed by addition of 150 ml of water. The organic layer was separated, and the water layer was extracted with carbon tetrachloride (2×70 ml). The combined organic solution was washed with an aqueous NaCl (10%) solution, followed by water, and then dried over anhydrous $MgSO_4$. The solution was evaporated and a yellowish solid was obtained (12.5 g). 1,3-dichloroadamantane and 1,3,5-trichloroadamantane were separated by column chromatography (silica gel, hexane). The melting points were 131 – 132°C for 1,3-dichloroadamantane and 101 – 103°C for 1,3,5-trichloroadamantane, which were consistent with data reported in the literature.[34] Because the aerosol fluorination conditions for 1,3-dichloroadamantane and 1,3,5-trichloroadamantane were the same, the fluorination was conducted with the mixture of these two compounds.

2.3.6 Synthesis of 5-Hydroxy-adamantan-2-one

The synthesis followed the same procedure for the synthesis of 2,6-adamantanedione. 5-hydroxy-adamantan-2-one was the major by-product of this procedure. After column chromatograph, 4.2 g of 5-hydroxy-adamantan-2-one was obtained. The ^1H NMR and ^{13}C NMR were consistent with data reported in the literature.[29]

2.3.7 Synthesis of 5-Chloro-adamantan-2-one

Synthesis of 5-chloro-adamantan-2-one followed the literature procedure.[29] 5-Hydroxy-adamantan-2-one (2.0 g) was dissolved in $SOCl_2$ (12 ml) and refluxed for 2 hours. The mixture was evaporated to dryness. The residue was dissolved in CH_2Cl_2 and washed with 0.5N NaOH aqueous solution and 10% aqueous NaCl solution. The organic layer was dried over anhydrous Na_2SO_4 and evaporated to dryness. The residue (2.1 g) was crystallized from hexane. A small insoluble fraction was separated by filtration. White solid was obtained (1.3 g). The ^1H NMR was consistent with data reported in the literature.[29] A ^{13}C NMR ($CDCl_3$) spectrum showed δ 214.4, 64.4, 47.8, 47.3, 46.2, 37.4, 30.4 ppm.

2.3.8 Synthesis of 4-Methyl-2,6,7-trioxabicyclo[2.2.2]octane

The synthesis of 4-methyl-2,6,7-trioxabicyclo[2.2.2]octane followed the literature procedure.[35] In a 250-ml flask with distillation equipment, 1,1,1-tris-hydroxymethylethane (12.0 g, 0.10 mol) and triethyl orthoformate (14.8 g, 0.1 mol) were added. The mixture was heated at 120°C (below the boiling point of starting material) for about 24 hours. During the 24 hours, approximately 17 ml of ethanol was distilled out. The residue was sublimed two times. 7.3 g of white solid was obtained. The ^1H NMR spectrum of 4-methyl-2,6,7-trioxabicyclo[2.2.2]octane was consistent with data reported in the literature.[36]

2.3.9 Synthesis of 1,4-Dimethyl-2,6,7-trioxabicyclo[2.2.2]octane

The synthesis of 1,4-dimethyl-2,6,7-trioxabicyclo[2.2.2]octane followed the literature procedure.[35] In a 250-ml flask with distillation equipment, 1,1,1-trishydroxymethylethane (12.0 g, 0.1 mol) and trimethyl orthoacetate (12.0 g, 0.1 mol) were added. The mixture was heated at 100°C (below the boiling point of starting material) for about 24 hours. During the 24 hours, approximate 8.2 ml of MeOH was distilled out. The residue was sublimed two times. 10.5 g of white solid was obtained. The ^{1}H NMR spectrum of 1,4-dimethyl-2,6,7-tri-oxabicyclo[2.2.2]octane was consistent with data reported in the literature.[36]

2.3.10 Synthesis of 1-Ethyl-4-methyl-2,6,7-trioxabicyclo[2.2.2]octane

The synthesis of 1-ethyl-4-methyl-2,6,7-trioxabicyclo[2.2.2]octane followed the literature procedure.[35] In a 250-ml flask with distillation equipment, triethyl orthopropionate (17.6 g, 0.10 mol) and 1,1,1-trishydroxymethylethane (12.0 g, 0.10 mol) were added. The mixture was heated at 140°C (below the boiling point of starting material) for about 24 hours. During the 24 hours, approximate 17 ml of EtOH was distilled out. The residue was sublimed two times. 11.7 g of white solid was obtained. The ^{1}H NMR spectrum of 1-ethyl-4-methyl-2,6,7-trioxabicyclo[2.2.2]-octane was consistent with data reported in the literature.[36]

2.3.11 Synthesis of 2,4,10-Trioxaadamantane

The synthesis of 2,4,10-trioxaadamantane followed the literature proce-

dure.[37] cis-Phloroglucinol (1.6 g, 12 mmol), triethyl orthoformate (2.2 g, 15 mmol), and absolute EtOH (6.5 ml) with $BF_3 \cdot Et_2O$ (6 drops) were mixed together and shaken occasionally for 2 days. After separating the solvent, the residues were sublimed two times consecutively. 1.1 g white solid was obtained. The ^1H NMR spectrum of 2,4,10-trioxaadamantane was consistent with the published data.[36]

2.3.12 Synthesis of 1-Methyl-2,4,10-trioxaadamantane

The synthesis of 1-methyl-2,4,10-trioxaadamantane followed the literature procedure.[37] cis-Phloroglucinol (1.6 g, 12 mmol), trimethyl orthoacetate (1.8 g, 15 mmol), and absolute EtOH (6.5 ml) with $BF_3 \cdot Et_2O$ (6 drops) were mixed together and shaken occasionally for 2 days. After separating the solvent, the residue was sublimed two times consecutively. 1.8 g of white solid was obtained. The ^1H NMR spectrum was consistent with data reported in the literature.[36]

2.4 Aerosol Direct Fluorination Reactions

2.4.1 Aerosol Fluorination of 1-Adamantyl Acetate

Detailed fluorination parameters are listed in Appendix 1, Table 1-1. A DSC measurement showed that 1-adamantyl acetate starting to evaporate at 100°C. Therefore, $CH_2ClCHCl_2$ was chosen as co-fluorination solvent. 1-Adamantyl acetate (2.4 g) was dissolved in $CH_2ClCHCl_2$ (7.5 g). The solution was injected into the evaporator at a rate of 1.5 ml/hr. After the injection was finished, the crude product was transferred to a vacuum line by vacuum transfer over 24 hours. The product

separated from solvent was fractionated. Two major products were collected using preparative gas chromatograph (column temperature program: 60°C (12 minutes); 30°C/min to 150°C; 150°C (25 minutes); inlet temperature: 190°C; detector temperature: 200°C; retention time: 24.5 minutes and 26.2 minutes). The products were 1-F-adamantyl trifluoroacetate and 1-[2-hydryl-F-adamantyl] trifluoroacetate in an almost 1:1 ratio. 0.58 g of 1-[2-hydryl-F-adamantyl] trifluoroacetate (r.t. = 24.5 min) was collected (yield 9.4%); 0.66 g of 1-F-adamantyl trifluoroacetate (r.t. = 26.2 min) was collected (yield 10.3%). ^{19}F NMR of 1-F-adamantyl trifluoroacetate showed that the chemical shift of the methyl fluorines occurred at δ −74.9 ppm (s, 3F), the chemical shift of the methylene fluorines occurred at δ −114.6 ppm (s,6F) and δ −121.1 ppm (s, 6F), and the chemical shift of the methine fluorines occurred at δ −221.7 ppm (s, 3F). The IR spectrum showed a C=O absorption at 1848 cm^{-1}. ^{19}F NMR of 1-[2-hydryl-F-adamantyl] trifluoroacetate showed that the chemical shift of the methyl fluorines occurred at δ −74.9 ppm (s, 3F), the methylene fluorines occurred at δ −111.7 to −126.2 ppm (m, 10F), one methine fluorine occurred at δ −212.5 ppm (s, 1F), and three others occurred at δ −221.6 to −223.0 ppm (m, 3F). ^{1}H NMR showed a doublet of quartets at δ 6.55 ppm. The coupling constant $^{2}J_{H-F}$ was 46.2 Hz. Long range coupling constant $^{5}J_{H-F}$ was 6.16 Hz. The IR spectrum showed the C−H absorption at 3021 cm^{-1} and the C=O absorption occurred at 1829 cm^{-1}. Because these two compounds were easily hydrolyzed to form their corresponding alcohols, it was difficult to run other analyses on these two compounds. Further characterizations, therefore, were carried out on their respective

hydrolysis products: 1-F-adamantanol and 2-hydryl-1-F-adamantanol. Further detailed characterization may be found in Appendix 2, Tables 2-1 and 2-2.

2.4.2 Aerosol Fluorination of 1,3-Adamantyl Diacetate

Detailed fluorination parameters are listed in Appendix 1, Table 1-2. 1,3-Adamantyl diacetate (1.2 g) was dissolved in $CH_2ClCHClCH_2Cl$ (4.6 g). The solution was injected into the evaporator at a rate of 1.5 ml/hr. After the injection was finished, the crude product was transferred into a vacuum line by vacuum transfer over 48 hours. The product separated from solvent was fractionated. The main product of 1,3-[2-hydryl-F-adamantyl] bis-trifluoroacetate, 0.16 g, was isolated by preparative gas chromatography (column temperature program: 80°C (12 minutes); 30°C/min to 180°C; 180°C (25 minutes); inlet temperature: 220°C; detector temperature: 240°C; retention time: 24 minutes). Based on the injection of 1,3-adamantyl diacetate, the yield was 6%. No perfluorinated 1,3-adamantyl diacetate was collected from preparative GC. ^{19}F NMR showed the chemical shift of methyl fluorines were at δ −74.9 ppm (s, 6F), the chemical shift of methylene fluorines were at δ −112.0 to −121.3 ppm (m, 10F), and the chemical shift of methine fluorines were at δ −218.8 to −221.4 ppm (m, 3F). ^1H NMR showed a doublet of triplets peak with chemical shift at δ 7.7 ppm. The coupling constant $^2J_{H-F}$ was 43.5 Hz. Long range coupling constant $^5J_{H-F}$ was 5.8 Hz. IR spectrum showed the C−H absorption at 3051 cm^{-1} and the C=O absorption at 1832 cm^{-1}. Because 1,3-[2-hydryl-F-adamantyl] bis-trifluoroacetate was easily hydrolyzed to form

the correspondent alcohol, it was difficult to run other analysis with this compound. Therefore, further characterization was obtained from the hydrolysis product, 2-hydryl-F-adamantan-1,3-diol. The detailed characterization is given in Appendix 2, Table 2-3.

2.4.3 Aerosol Fluorination of 2,6-Adamantanedione

Detailed fluorination parameters are listed in Appendix 1, Table 1-3. A DSC measurement showed that 2,6-adamantanedione sublimed at about 150°C. Therefore, $CH_2ClCHClCH_2Cl$ was chosen as co-fluorination solvent. 2,6-Adamantanedione (1.0 g) was dissolved in $CH_2ClCHClCH_2Cl$ (4.3 g). The solution was injected into the evaporator at a rate of 1.0 ml/hr. After the injection was finished, the crude product was transferred onto the vacuum line by vacuum transfer over 48 hours. The product separated from solvent was fractionated. 2,6-F-adamantanedione was the major product collected through preparative gas chromatography (column temperature: 120°C; inlet temperature: 180°C; detector temperature: 200°C; retention time: 10 minutes) 0.60 g pure product was collected. Based on the injection of 2,6-adamantanedione, the yield was 26%. Due to the high symmetry, of this compound, the ^{19}F NMR spectrum was very simple exhibiting only two types of fluorine resonances. The chemical shift of the methylene fluorines occurred at δ −123.8 ppm (s, 8F) and the chemical shift of the methine fluorines occurred at δ −215.9 ppm (s, 4F). IR spectrum showed $\nu_{C=O}$ absorption at 1817 cm^{-1}. Detailed characterization is given in Appendix 2, Table 2-4.

2.4.4 Aerosol Fluorination of 1-Chloroadamantane

The fluorination of 1-chloroadamantane followed the procedure in the literature.[38] 1-Chloroadamantane (2.0 g, 12 mmol) was dissolved in $CH_2ClCHCl_2$ (6.4 g, 43 mmol). The solution was injected into the evaporator at a rate of 1.5 ml/hr. After the injection was completed, the crude product was transferred onto the vacuum line by vacuum transfer over 24 hours. 2.6 g of 1-chloro-F-adamantane was collected through preparative gas chromatography. Based on the injection of 1-chloroadamantane, the yield was 57%. ^{19}F NMR and IR were consistent with data reported in the literature.[38]

2.4.5 Aerosol Fluorination of 1,3-Dichloroadamantane and 1,3,5-Trichloroadamantane

The fluorination of 1,3-dichloroadamantane and 1,3,5-trichloroadamantane mixture followed the procedure in the literature.[27] A mixture consisting of 1,3-dichloroadamantane (1.68 g) and 1,3,5-trichloroadamantane (1.32 g) was dissolved in $CH_2ClCHClCH_2Cl$ (9.6 g). The solution was injected into the evaporator at a rate of 1.5 ml/hr. Following the injection, the crude products were transferred onto the vacuum line by vacuum transfer over 48 hours. Pure samples of 1,3-dichloro-F-adamantane (1.40 g) and 1,3,5-trichloro-F-adamantane (0.94 g) were collected through preparative GC (column temperature program: 180°C (20 minutes); 20°C/min to 200°C; 200°C (20 minutes); inlet temperature: 220°C; detector temperature: 220°C; retention time: 9.5 minutes for 1,3-dichloro-F-adamantane and

14.8 minutes for 1,3,5-trichloro-F-adamantane). ^{19}F NMR of both compounds were consistent with data reported in the literature.[27]

2.4.6 Aerosol Fluorination of Adamantanone

In the literature, the fluorination was conducted by direct sublimation of adamantanone.[23b] However, with direct sublimation, it was difficult to control stoichiometrically the hydrogen and fluorine ratio. Therefore, fluorination of a solution was employed here. Details of the fluorination parameters are listed in Appendix 1, Table 1-4. Adamantanone (2.8 g, 20 mmol) was dissolved in $CH_2ClCHClCH_2Cl$ (10.0 g, 68 mmol). The solution was injected into the evaporator at a rate of 1.5 ml/hr. After the injection was completed, the crude product was transferred onto the vacuum line by vacuum transfer over 24 hours. F-Adamantanone (3.2 g) was collected through preparative GC (column temperature: 160°C; inlet temperature: 200°C; detector temperature: 210°C; retention time: 7 minutes). Based on the injection of adamantanone, the yield was 43% (after GC purification). ^{19}F NMR and IR spectra were consistent with data reported in the literature.[23b]

2.4.7 Aerosol Fluorination of 5-Chloroadamantan-2-one

5-Chloro-F-adamantan-2-one was first synthesized in our laboratory.[39] Detailed fluorination parameters are listed in Appendix 1, Table 1-5. 5-Chloroadamantan-2-one (2.7 g, 15 mmol) was dissolved in $CH_2ClCHClCH_2Cl$ (8.6 g, 58 mmol). The solution was injected into the evaporator at a rate of 1.5 ml/hr.

After the injection was completed, the crude product was transferred onto the vacuum line by vacuum transfer over 48 hours. 5-Chloro-F-adamantan-2-one (1.8 g) was collected through preparative GC (column temperature: 160°C; inlet temperature: 200°C; detector temperature: 210°C; retention time: 8 minutes). Based on the injection of 5-chloroadamantan-2-one, the yield was 30%. ^{19}F NMR spectrum of 5-chloro-F-adamantan-2-one showed that the chemical shifts of methylene fluorines (CF_2) occurred at δ −111.9 ppm to δ −126.3 ppm with unresolved peaks (10F), the chemical shifts of bridgehead fluorines (CF) occurred at δ −211.2 ppm (2F) and δ −219.8 ppm (1F), respectively. ^{19}F NMR spectrum was consistent with previous results from our laboratory.[39]

2.4.8 Aerosol Fluorination of 4-Methyl-2,6,7-trioxabicyclo[2.2.2]octane

Detailed fluorination parameters are listed in Appendix 1, Table 1-6. 4-Methyl-trioxabicyclo[2.2.2]octane (2.2 g) was dissolved in $CH_2ClCHCl_2$ (7.1 g). The solution was injected into the evaporator at a rate of 1.5 ml/hr. After the injection was completed, the crude product was transferred into a vacuum line by vacuum transfer over 24 hours. The product, separated from solvent, was fractionated. F-4-Methyl-2,6,7-trioxabicyclo[2.2.2]octane (0.66 g) was collected through preparative GC (column temperature: 40°C; inlet temperature: 150°C; detector temperature: 150°; retention time: 12 minutes). Based on the injection of 4-methyl-2,6,-7-trioxabicyclo[2.2.2]octane, the yield was 13%. Due to the high symmetry of this compound, ^{19}F NMR spectrum only had three fluorine resonances at δ −85.7 ppm

(methine fluorine), at δ −71.6 ppm (methylene fluorines), and at δ −62.8 ppm (methyl fluorines). A detailed characterization is given in Appendix 2, Table 2-5.

2.4.9 Aerosol Fluorination of 1,4-Dimethyl-2,6,7-trioxabicyclo[2.2.2]octane

Detailed fluorination parameters are listed in Appendix 1, Table 1-7. A DSC measurement showed that 1,4-dimethyl-2,6,7-trioxabicyclo[2.2.2]octane sublimed at 107°C. Therefore, $CH_2ClCHCl_2$ was chosen as co-fluorination solvent. 1,4-Dimethyl-2,6,7-trioxabicyclo[2.2.2]octane (2.1 g) was dissolved in $CH_2ClCHCl_2$ (6.7 g). The solution was injected into the evaporator at a rate of 1.5 ml/hr. After the injection was completed, the crude product was transferred onto the vacuum line by vacuum transfer over 24 hours. The solvent was separated, and the product was fractionated. F-1,4-Dimethyl-2,6,7-trioxabicyclo[2.2.2]octane (0.80 g) was collected through preparative GC (column temperature: 80°C; inlet temperature: 190°C; detector temperature:190°C; retention time: 5 minutes). Based on the injection of 1,4-dimethyl-2,6,7-trioxabicyclo[2.2.2]octane, the yield was 15%. ^{19}F NMR spectrum exhibited three types of fluorine resonances: at δ −70.3 ppm (CF_2 fluorines), δ −62.4 ppm (methyl fluorines), δ −84.9 ppm (methyl fluorines). A detailed characterization is given in Appendix 2, Table 2-6.

2.4.10 Aerosol Fluorination of 1-Ethyl-4-methyl-2,6,7-trioxabicyclo[2.2.2]octane

Detailed fluorination parameters are listed in Appendix 1, Table 1-8. 1-Ethyl-4-methyl-2,6,7-trioxabicyclo[2.2.2]octane (2.2 g) was dissolved in $CH_2ClCHCl_2$.

The solution was injected into the evaporator at a rate of 1.5 ml/hr. After the injection was completed, the crude product was transferred onto a vacuum line by vacuum transfer over 24 hours. The solvent was separated and the product was fractionated. F-1-Ethyl-4-methyl-2,6,7-trioxabicyclo[2.2.2]octane (1.1 g) was collected through preparative GC (column temperature: 50°C; inlet temperature: 150°C; detector temperature: 150°C; retention time: 13.5 minutes). Based on the injection of 1-ethyl-4-methyl-2,6,7-trioxabicyclo[2.2.2]octane, the yield was 18%. ^{19}F NMR spectrum showed three types of fluorine resonances occurred at δ −70.4 ppm (ethylene fluorines), δ −62.3 ppm (methyl fluorines), δ −128.6 ppm (ethyl methylene fluorines), and δ −80.6 ppm (ethyl methyl fluorines). A detailed characterization is given in Appendix 2, Table 2-7.

2.4.11 Aerosol Fluorination of 2,4,10-Trioxaadamantane

Detailed fluorination parameters are listed in Appendix 1, Table 1-9. A DSC measurement showed that 2,4,10-trioxaadamantane sublimed at 127°C. Therefore, $CH_2ClCHClCH_2Cl$ was chosen as co-fluorination solvent. 2,4,10-Trioxaadamantane (0.82 g) was dissolved in $CH_2ClCHClCH_2Cl$ (5.8 g). The solution was injected into the evaporator at a rate of 1.5 ml/hr. After the injection was completed, the crude product was transferred into a vacuum line by vacuum transfer over 24 hours. The solvent was separated and the product was fractionated. F-2,4,10-Trioxaadamantane (0.21 g) was collected through preparative GC (column temperature: 50°C (12 minutes); 30°C/min to 175°C; 175°C (19 minutes); inlet temperature: 180°C; detector

temperature: 180°C; retention time: 12.5 minutes). Based on the injection of 2,4,10-trioxaadamantane, the yield was 11%. ^{19}F NMR showed three types of fluorines resonances: δ −165.7 ppm (3F, bridgehead fluorines, CF), δ −138.8 ppm (6F, methylene fluorines, CF_2), and δ −83.0 ppm (1F, orthoformyl fluorine, CF). The detailed characterization are listed in Appendix 2, Table 2-8.

2.4.12 Aerosol Fluorination of 1-Methyl-2,4,10-trioxaadamantane

The detailed fluorination parameters are listed in Appendix 1, Table 1-10. A DSC measurement showed that 1-methyl-2,4,10-trioxaadamantane sublimed at 93°C. Therefore, $CH_2ClCHCl_2$ was chosen as co-fluorination solvent. 1-Methyl-2,4,-10-trioxaadamantane (0.40 g) was dissolved in $CH_2ClCHCl_2$. The solution was injected into the evaporator at a rate of 1.5 ml/hr. After the injection was completed, the crude product was transferred onto a vacuum line by vacuum transfer over 24 hours. The solvent was separated and the product was fractionated. F-1-methyl-2,4,10-trioxaadamantane (0.13 g) was isolated by preparative GC (column temperature: 50°C (14 minutes; 20°C/min to 100°C; 100°C (8 minutes); inlet temperature: 150°C; detector temperature: 150°C; retention time: 14 minutes). Based on the amount of injection of 1-methyl-2,4,10-trioxaadamantane, the yield was 14%. ^{19}F NMR showed three types of fluorines resonances at δ −162.8 ppm (methine fluorines), at δ −136.3 ppm (methylene fluorines), and at δ −84.1 ppm (methyl fluorines). Detailed characterization is given in Appendix 2, Table 2-9.

2.5 Other Reactions

2.5.1 Hydrolysis of F-adamantyl Trifluoroacetate Derivatives

The hydrolysis of 1-F-adamantyl trifluoroacetate, 1-[2-hydryl-F-adamantyl] trifluoroacetate, and 1,3-[2-hydryl-F-adamantyl] bis-trifluoroacetate followed the same procedure: the trifluoroacetate was dissolved in 1 ml $CFCl_3$ and exposed to atmospheric moisture for three days. A white solid remained. 1-F-adamantyl trifluoroacetate (0.54 g) on hydrolysis gave 0.45 g of F-adamantan-1-ol; 1-[2-hydryl-F-adamantyl] trifluoroacetate (0.47 g) on hydrolysis gave 0.37 g of 2-hydryl-F-adamantan-1-ol; 1,3-[2-hydryl-F-adamantyl] bis-trifluoroacetate (0.16 g) on hydrolysis gave 0.097 g of F-adamantan-1,3-diol. A mixture of F-adamantan-1-ol and 2-hydryl-F-adamantan-1-ol was purified by preparative GC (column temperature: 160°C; inlet temperature: 200°C; detector temperature: 210°C; retention time: 14.3 minutes and 16.7 minutes). The ^{19}F NMR spectrum of F-adamantan-1-ol was simple with only two fluorine resonances: a methine fluorine resonance at δ −224.3 ppm and the methylene fluorine resonances at δ −123.0 ppm. The ^{19}F NMR of 2-hydryl-F-adamantan-1-ol was much more complicated. All the methylene fluorine resonances were unresolved with a chemical shift range of δ −116.4 to −127.1 ppm. The resonance of the methine fluorines beta to the hydrogen occurred as a single peak with chemical shift at δ −213.7 ppm. The other two methine fluorine resonances and the geminal fluorine to the hydrogen occurred as unresolved peaks with a chemical shift range of δ −222.5 to −226.3 ppm. ^1H NMR of 2-hydryl-F-adamantan-1-ol exhibited a doublet of quartets with a chemical shift at δ 5.23 ppm.

$^2J_{H-F}$ was 48.2 Hz and $^5J_{H-F}$ was 6.2 Hz. The ^{19}F NMR spectrum of F-adamantan-1,3-diol was also complicated. The methylene fluorine resonances occurred as unresolved peaks ranging between δ −120.3 and −123.9 ppm. Two methine fluorine resonances and that of the fluorine geminal to the hydrogen occurred as unresolved peaks between δ −221.9 and −225.7 ppm. The ^1H NMR spectrum showed a doublet of triplets with a chemical shift at δ 5.02 ppm; $^2J_{H-F}$ was 47.9 Hz and $^5J_{H-F}$ was 6.3 Hz. Detailed characterizations are listed in Appendix 2, Tables 2-10, 2-11, and 2-12.

2.5.2 $LiAlH_4$ Reduction of F-Adamantanone

The reduction reaction followed a general procedure. GC purified F-adamantanone (0.30 g) was dissolved in dry Et_2O (5 ml) . The solution was added dropwise into a $LiAlH_4$/dry Et_2O (0.10 g/10 ml) solution at 0°C over 10 minutes and with stirring at 0°C continuously for 2 hours. The mixture was allowed to stand at room temperature overnight. Absolute EtOH (2 ml) was added and the mixture was poured into a H_2SO_4 and H_2O (5 g/10 ml) solution. The organic layer was separated. The water solution was extracted with Et_2O, and the organic layers were combined and dried over anhydrous Na_2SO_4. The Et_2O was evaporated, giving 0.28 g of 2-hydryl-F-adamantan-2-ol as a white solid; the yield was 93%. 2-Hydryl-F-adamantan-2-ol was purified by preparative GC (column temperature: 150°C; inlet temperature: 220°C; detector temperature: 220°C; retention time: 12.6 minutes). Alternatively, if F-adamantanone was used directly from the aerosol direct fluorination reaction without GC purification, the final purification could be carried

out by dissolving the reduced reaction mixture with aqueous 0.5 M NaOH. 2-Hydryl-F-adamantan-2-ol formed the sodium salt and dissolved in water solution. Et_2O was used to extract water-insoluble materials. Then the water solution was neutralized with 70% aqueous H_2SO_4 and a white solid precipitated out. Pure 2-hydryl-F-adamantan-2-ol could be extracted to $CF_2ClCFCl_2$ solvent (this method also could be used to purify F-adamantan-1-ol and 2-hydryl-F-adamantan-1-ol). ^{19}F NMR and IR spectra were consistent with the previous result from our laboratory.[40] The detailed characterization is listed in Appendix 2, Table 2-13.

2.5.3 Acetylation Reaction of F-Adamantyl Alcohol Derivatives

The acetylation of F-adamantan-1-ol, 2-hydryl-F-adamantan-1-ol, and 2-hydryl-F-adamantan-2-ol followed a general procedure. The alcohol (0.050 g) was dissolved in acetyl chloride (3 ml). The mixture was refluxed for 24 hours. After the excess acetyl chloride was evaporated, the liquid residue was purified by preparative GC. 1-[2-Hydryl-F-adamantyl] acetate (0.036 g) was obtained in 65% yield (column temperature: 120°C (9 minutes); 50°C/min to 180°C; 180°C (20 minutes); inlet temperature: 200°C; detector temperature: 210°C; retention time: 24.4 minutes). 2-[2-Hydryl-F-adamantyl] acetate (0.032 g) was obtained in 58% yield (column temperature: 180°C; inlet temperature: 220°C; detector temperature: 220°C; retention time: 11.2 minutes). When 1-F-adamantyl acetate was purified under the same GC conditions as 1-[2-hydryl-F-adamantyl] acetate, 1/3 of the compound decomposed to form F-adamantan-1-ol which was not isolated. The ^{19}F NMR spectrum of

1-F-adamantyl acetate was almost identical with that of 1-F-adamantyl trifluoroacetate; methylene fluorine resonances at δ −114.7 ppm (s, 6 F) and δ −121.3 ppm (s, 6F), and methine fluorine resonances at δ −221.8 ppm. The ^{1}H NMR spectrum of 1-[2-hydryl-F-adamantyl] acetate exhibited a doublet of quartets at δ 6.69 ppm, $^2J_{H-F}$ = 45.9 Hz and $^5J_{H-F}$ = 6.4 Hz. The ^{1}H NMR of 2-[2-hydryl-F-adamantyl] acetate exhibited a quintet at δ 6.29 ppm, $^5J_{H-F}$ = 5.6 Hz. Detailed characterizations are listed in Appendix 2, Tables 2-14, 2-15, and 2-16.

2.5.4 Synthesis of 1-[2-Hydryl-F-Adamantyl] Benzoate

2-Hydryl-F-adamantyl-1-ol (0.15 g, 0.37 mmol) was dissolved in dry CH_2Cl_2 (2 ml) in a 5 mm NMR tube. Benzoyl chloride (0.062 g, 0.44 mmol) was added and the mixture was shaken well. Then, pyridine (0.058 g, 0.74 mmol) was added. The reaction mixture was kept at room temperature with occasionally shaking of 8 hours. The ^{19}F NMR spectrum of the product mixture showed the absence of starting material. The CH_2Cl_2 was evaporated from the mixture. The residue was dissolved in ethyl acetate and the solution cooled to 0°C. The mixture was washed twice with cold (0°C) 2×5 ml portions of saturated aqueous $NaHCO_3$, and then with saturated aqueous NaCl. The organic layer was dried over anhydrous $MgSO_4$. Toluene was added and the mixture evaporated to dryness. The solid residue was recrystallized from hexane yielding 0.16 g (83%) crystalline product. ^{1}H NMR exhibited a doublet of quartets at δ 6.90 ppm, $^2J_{H-F}$ = 45.5 Hz and $^5J_{H-F}$ = 6.5 Hz. The detailed characterization of 1-[2-hydryl-F-adamantyl] benzoate is listed in Appendix 2, Table

2-17.

2.5.5 Synthesis of 1-[2-Hydryl-F-Adamantyl] Methylsulfonate

2-Hydryl-F-adamantan-1-ol (0.050 g, 0.12 mmol) was dissolved in dry CH_2Cl_2 solvent (1 ml) in a 5 mm NMR tube. Methylsulfonyl chloride (0.017 g, 0.15 mmol) was added. After the mixture was shaken well, pyridine (0.020 g, 0.25 mmol) was added. The reaction mixture was allowed to stand at room temperature with occasional shaking for 48 hours. A ^{19}F NMR spectrum showed that about 2/5 of the starting material remained. Another 0.01 g of methyl sulfonyl chloride and 0.01 g of pyridine were added to the reaction mixture and the resulting mixture allowed to stand at room temperature for another 48 hours. No starting material was detected by ^{19}F NMR spectrum. The CH_2Cl_2 was evaporated from the reaction mixture. The residue was dissolved in ethyl acetate and cooled to 0°C. The solution was washed with an ice-cooled saturated aqueous $NaHCO_3$ solution followed by saturated aqueous NaCl solution. The organic layer was dried over anhydrous $MgSO_4$. Toluene was added and the solution was evaporated to dryness. The ^1H NMR spectrum showed a doublet of quartets at δ 6.28 ppm, $^2J_{H-F}$ = 45.9 Hz and $^5J_{H-F}$ = 6.2 Hz. The detailed characterization is listed in Appendix 2, Table 2-18.

2.5.6 Synthesis of 1,3-[2-Hydryl-F-Adamantyl]bis-benzoate

2-Hydryl-F-adamantan-1,3-diol (0.16 g, 0.40 mmol) was dissolved in dry CH_2Cl_2 (1.5 ml) solvent in a 5 mm NMR tube. Benzoyl chloride (0.14 g, 1.0 mmol)

was added and the tube shaken well; then, pyridine (0.94 g, 1.2 mmol) was added. The reaction mixture was allowed to stand at room temperature with occasional shaking. After 10 hours, ^{19}F NMR showed no remaining starting material. The CH_2Cl_2 was evaporated from the reaction mixture. The residue was dissolved in ethyl acetate and cooled to 0°C. The solution was washed with ice-cooled saturated aqueous $NaHCO_3$ solution followed by saturated NaCl solution. The organic layer was dried over $MgSO_4$. Toluene was added and the solution was evaporated to dryness. The solid residue was recrystallized from hexane. Crystal 1,3-[2-hydryl-F-adamantyl] bis-benzoate (0.15 g) was obtained in 61% yield . The ^1H NMR spectrum showed a doublet of triplets at δ 8.31 ppm, $^2J_{H-F}$ = 42.3 Hz and $^5J_{H-F}$ = 6.1 Hz. The detailed characterization is listed in Appendix 2, Table 2-19.

2.5.7 Synthesis of F-Tricyclo[3.3.0.$0^{3,7}$]octane

The synthesis of F-tricyclo[3.3.0.$0^{3,7}$]octane followed the photochemical procedure in the literature.[23b] F-2,6-adamantanedione (0.10 g, 0.27 mmol) was dissolved in $CFCl_3$ (0.70 g) in a 5 mm NMR tube. The NMR tube was sealed on the vacuum line and irradiated using a 550 W medium-pressure mercury lamp for 2 hours. After irradiation, the NMR tube was connected to the vacuum line and the reaction mixture was separated by trap-to-trap fractionation. A white solid (0.085 g) was collected in the −22°C trap. The F-tricyclo[3.3.0.$0^{3,7}$]octane was near 100% pure and the yield was 98%. F-tricyclo[3,3,0,$0^{3,7}$]octane was further purified by preparative GC (column temperature: 60°C; inlet temperature: 180°C; detector temperature:

180°; retention time: 9.2 minutes). Due to the high symmetry of F-tricyclo[3,3,0,$0^{3,7}$]octane, the ^{19}F NMR spectrum only showed two fluorine resonances: δ −118.1 (quintet, $^4J_{CF2-CF}$ = 5.6 Hz, methylene fluorines) and δ −206.0 (nonet, $^4J_{CF2-CF}$ = 5.6 Hz, methine fluorines). The IR spectrum exhibited no C=O absorption. The detailed characterization is listed in Appendix 2, Table 2-20.

2.5.8 KOH Reduction Reaction of 1-Chloro-F-Adamantane

1-Chloro-F-adamantane (1.00 g, 2.3 mmol), KOH (1.00 g), benzene (5 ml), cyclohexane (5 ml) and 18-crown-6 (0.08 g) were introduced into a 50-ml stainless steel cylinder. The mixture was kept at 120°C with continuous shaking for 48 hours. The organic layer was separated and dried over anhydrous $MgSO_4$. The product was purified through preparative GC. 1-Hydryl-F-adamantane (0.67 g) was obtained in 73% yield. The ^{19}F NMR and ^1H NMR spectra were consistent with data reported in the literature.[38]

2.5.9 KOH Reduction Reaction of 1,3,5-Trichloro-F-adamantane

1,3,5-Trichloroadmantane (0.20 g, 0.42 mmol). KOH (0.60 g), benzene (1.5 ml) and 18-crown-6 (0.018 g) were added to a 50-ml stainless steel cylinder. The mixture was shaken at 120°C for 5 days. The organic layer was separated and dried over anhydrous $MgSO_4$. The product was purified by preparative GC. 0.067 g (43%) of 1,3,5-trihydryl-F-adamantane was obtained. The ^{19}F NMR spectrum was consistent with data reported in the literature.[41]

2.5.10 $LiAlH_4$ Reduction Reaction of 1-Chloro-F-adamantane

1-Chloro-F-adamantane (0.20 g, 0.45 mmol) was dissolved in dry ether (2 ml). The solution was added dropwise into a $LiAlH_4$/ether (0.1 g/3 ml) solution at 0°C within 5 minutes and stirred at 0°C for an additional 1.5 hours, followed by continuous stirring at room temperature overnight. Absolute EtOH (2 ml) was added and the mixture was poured into a H_2SO_4 and H_2O (5 g/10 ml) solution. The organic layer was separated and the water solution was extracted three times with ether and the combined organic solutions were dried over anhydrous Na_2SO_4. The product was purified by preparative GC yielding 0.11 g (61%) of 1-hydr-yl-F-adamantane. The ^{19}F NMR and ^1H NMR spectra were consistent with data reported in the literature.[38]

2.5.11 $LiAlH_4$ Reduction of 5-Chloro-F-Adamantan-2-one

5-Chloro-F-adamantan-2-one (0.20 g, 0.48 mmol) was dissolved in dry ether (5 ml). The solution was added dropwise into a $LiAlH_4$/ether (0.10 g, 2.6 mmol in 10 ml ether) solution at 0°C within 10 minutes, with stirring at 0°C for an additional 1.5 hours followed by stirring at room temperature overnight. Absolute alcohol (2 ml) was added and the mixture was poured into a H_2SO_4 solution (5 g H_2SO_4 and 10 ml H_2O). The organic layer was separated; the water solution was extracted three times with ether. The combined ether solutions were dried over anhydrous Na_2SO_4. After removing the solvent by evaporation, 0.17 g residue was collected. The product was purified by preparative GC (column temperature: 205°C; inlet temperature:

240°C; detector temperature: 240°C; retention time: 10 minutes). The major product collected was a mixture of *E,Z*-2,5-dihydryl-F-adamantan-2-ol in about 60:40 ratio. The ^{19}F NMR spectrum showed the presence of two isomers. The chemical shifts of methylene fluorines (CF_2) occurred at δ −105.5 ppm to δ −122.4 ppm with unresolved peaks (10F). The chemical shifts of the bridgehead fluorines (CF) of the minor isomer which was *Z* isomer occurred at δ −209.3 ppm (2F) and δ −219.2 ppm (1F). The chemical shifts of bridgehead fluorines (CF) of the major isomer occurred at δ −210.0 ppm (2F) and δ-220.8 ppm (1F). ^1H NMR spectrum showed the bridgehead hydrogen (CH) occurred at δ 3.69 ppm and δ 3.63 ppm as two overlapping octet peaks (actually they were decet peaks with the side peaks diminished in the baseline); the ethylene hydrogen (HOCH) occurred at δ 4.83 ppm as two overlapped peaks; the hydroxy hydrogen occurred at δ 3.02 ppm as a broad peak which disappeared upon adding D_2O.[39]

2.5.12 Synthesis of 5-Hydryl-F-Adamantan-2-one

E,Z-2,5-Dihydryl-F-adamantan-2-one (0.050 g, 0.13 mmol), CrO_3 (0.03 g), Ac_2O (0.5 ml), and AcOH (0.5 ml) were combined and stirred at room temperature for 10 minutes The mixture was monitored by ^{19}F NMR. The spectrum showed the absence of alcohol. Pure 5-hydryl-F-adamantan-2-one was isolated. The isomer peaks in the alcohol disappeared and only singlet peaks were shown for each type of methine fluorine. ^{19}F NMR spectrum showed the chemical shifts of the methylene fluorines (CF_2) occurred at δ −108.1 ppm to δ −127.4 ppm (10F) with unresolved

peaks. Only one set of bridgehead fluorines were observed. The chemical shifts occurred at δ −212.8 ppm (2F) and δ −221.5 ppm (1F). The ^{1}H NMR spectrum showed one octet peak at δ 4.96 ppm.[39]

Chapter 3 Results and Discussions

3.1 Perfluorinated and Monohydryl Perfluorinated Adamantane Alcohols

3.1.1 Introduction

Perfluorinated primary and secondary alcohols are unstable, because of the fluorine atoms geminal to the hydroxyl groups. The $-CF_2OH$ and $-CR_2FOH$ groups readily lose hydrogen fluoride to form acid halides and ketones, respectively. However, perfluorinated tertiary alcohols are stable compounds because no fluorine atom is geminal to the hydroxyl group. Perfluoroalkyl groups are strong electron withdrawing groups. When a hydroxyl group is attached to a perfluoroalkyl group, its conjugate base is stabilized.[42] The result is that the acidities of these alcohols are greatly enhanced. For example, the *pKa* value of perfluorotertiary butyl alcohol is 5.4, the same order of acidity as acetic acid.

Unprotected alcohols can not be directly fluorinated using elemental fluorine, because the hydroxyl group will liberate oxygen radicals or form fluoroxy groups which interfere with the free-radical chain reaction and in the later case are extremely unstable at room temperature. There are several methods for the synthesis of perfluorinated alcohols in the literature (Scheme 4). All of them use indirect methods starting with perfluorinated ketones or alkenes.

Perfluorinated esters are highly hygroscopic. In the presence of water, these esters are easily hydrolyzed to form perfluorinated acids and alcohols. This property

$$(CF_3)_2CO \xrightarrow[\text{diglyme}]{CsF,\ 150^oC} CF_3COF + (CF_3)_3COCs \xrightarrow{H_2SO_4} (CF_3)_3COH \quad 34\% \qquad [43]$$

$$CCl_3Li + (CF_3)_2CO \xrightarrow[2)\ H_2SO_4]{1)\ THF/-100^oC} (CF_3)_2C(CCl_3)OH \xrightarrow{SbF_5} (CF_3)_3COH \quad 60\% \qquad [44]$$

$$(CF_3)_2C{=}CF_2 \xrightarrow{NO_2F} (CF_3)_3C{-}N{=}O \xrightarrow{N_2O_4} (CF_3)_3CONO \xrightarrow{H_2O} (CF_3)_3COH \qquad [45]$$

$$(CF_3)_2CO \xrightarrow[2)\ H_2SO_4]{1)\ C_6F_5Li} (CF_3)_2C(OH)C_6F_5 \quad 79\% \qquad [46]$$

Scheme 4

of perfluorinated esters offers a potential synthetic route to the perfluorinated alcohols (Scheme 5). Herein we report the synthesis of perfluorinated and 2-hydryl-perfluorinated adamantanol by the hydrolysis of the corresponding trifluoroacetates.

$$Rf{-}\overset{\overset{O}{\|}}{C}{-}ORf' \xrightarrow{H_2O} Rf{-}\overset{\overset{O}{\|}}{C}{-}OH + HO{-}Rf'$$

Rf ' = 3o Rf ' = 3o

Scheme 5

In earlier work with perfluorinated esters in our laboratory,[22] Cherry found that the successful aerosol direct fluorination of organic esters depended on the

structures of the esters. In some cases, esters lost the alkoxyl groups to form acyl fluoride compounds. However, if a bulky alkyl group was attached on either the carbonyl side or on the alkoxyl side, the cleavage of the ester group was greatly reduced. Later work also showed that careful control of the aerosol fluorination conditions could significantly reduce cleavage of methyl esters.[47]

3.1.2 Synthesis of F-Adamantyl and H-F-Adamantyl Alcohols

Hydrocarbon ester linkages can be easily preserved during aerosol direct fluorinations when a bulky alkyl group is attached to either the acyl side or the alkoxyl side. Perfluorinated esters are generally produced in synthetically useful yields. 1-Adamantyl acetate has a bulky adamantyl group attached to the alkoxyl side; therefore it is a good precursor for the aerosol direct fluorination. In a typical run, 1-adamantyl acetate is dissolved in $CH_2ClCHCl_2$, and the solution slowly injected into the evaporator of the aerosol fluorination apparatus. After the general work up of the reaction mixture and removal of the fluorinated solvent, two major products, 1-F-adamantyl trifluoroacetate (Compound 1) and 1-[2-hydryl-F-adamantyl] trifluoroacetate (Compound 2), are collected as shown in Scheme 6. Depending on the different hydrogen and fluorine ratios that are used in the reactor, the ratio of Compounds 1 and Compound 2 will change. For example, when H:F is 1:3.2, compound 1 and 2 have a ratio of 30:70; When H:F is 1:4.0, compound 1 and 2 have a ratio of 50:50. Under these fluorination conditions, the perfluorinated compound should normally be more than 90% of the products that are collected. However,

here the amount of mono-hydryl residue (Compound 2) is significant. This unusual result may be attributed to an intramolecular interaction between the carbonyl group on the trifluoroacetate and the hydrogen atom at the α-position of the adamantyl group, and as a consequence, the big trifluoroacetyl group blocks fluorine substitution of the last hydrogen atom. Therefore, an anomalously high yield of Compound 2 is obtained.[48] A detailed discussion of this interaction is found in chapter 3.2.

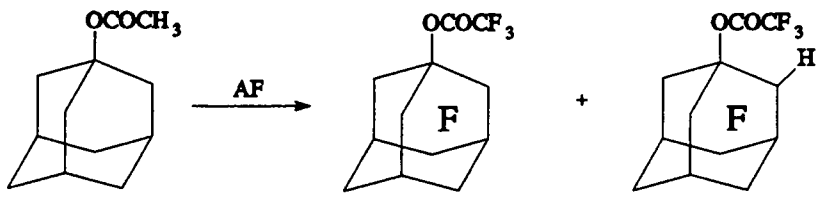

1 2

Scheme 6

The aerosol direct fluorination reaction of 1,3-adamantyl bis-acetate is conducted using $CH_2ClCHClCH_2Cl$ as solvent. After following the general work up procedure of the reaction mixture, the major product, 1,3-[2-hydryl-F-adamantyl] bis-trifluoroacetate, is obtained (Scheme 7). No perfluorinated 1,3-adamantyl bis-trifluoroacetate is collected through preparative GC. This result further supports the premise that there is a relatively strong interaction between the carbonyl groups of the trifluoroacetates and the hydrogen atom at the α position of both. Since there are two trifluoroacetyl group in 1,3-[2-hydryl-F-adamantyl] bis-trifluoroacetate interacting with the α-proton, fluorine attack on that proton is blocked. Since this proton can not be replaced by fluorine, no perfluorinated product is obtained.

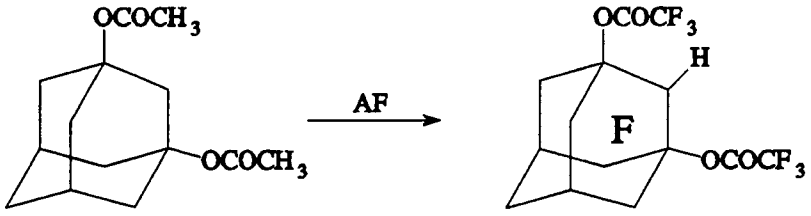

3

Scheme 7

The $-CF_3$ and F-adamantyl groups in Compound 1 and 2 strongly activate the ester groups to nucleophilic attack. The result is that these esters are highly reactive with water. The moisture in the atmosphere is sufficient to hydrolyze these esters. The hydrolysis goes to near completion on leaving the product container open to the atmosphere overnight. The yields for hydrolysis of these esters are quantitative (Scheme 8). The hydrolysis products are F-adamantan-1-ol (Compound 4) and 2-hydryl-F-adamantan-1-ol (Compound 5).

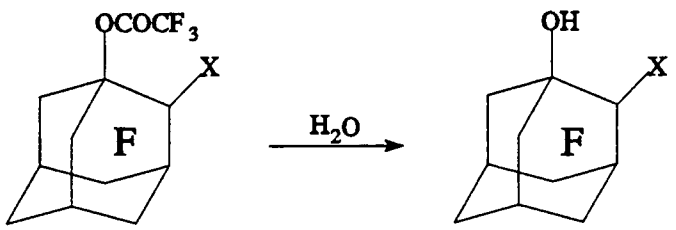

X = F

X = H

4 : X = F

5 : X = H

Scheme 8

F-adamantanone was synthesized in our laboratory in 1992.[23b] The perfluorinated adamantyl group strongly polarizes the carbonyl group. Reduction

of this carbonyl group can easily be achieved by stirring F-adamantanone with $LiAlH_4$-ether solution at room temperature overnight (Scheme 9).[40] The yield of 2-hydryl-F-adamantan-2-ol (Compound 6) is 93%.

(6)

Scheme 9

3.1.3 Acidities and Reactivities

The acidities of perfluorinated and 2-hydryl-F-1-adamantanol have been measured using acid-base titration. For comparison, the acidity of 2-hydryl-F-adamantan-2-ol is also measured. In addition to the acidities, the nucleophilicities of these alcohol toward acetyl chlorides are investigated along with the solvolysis reaction of these alcohols.

When perfluorinated and mono-hydryl F-adamantyl groups are attached to the hydroxyl group as in compounds 4, 5 and 6, they are expected to have relatively high acidities. Actually all three alcohols can be titrated by aqueous NaOH. Due to the low solubilities of these alcohols in water, the titrations are conducted in methanol/water solution (1:1 by volume). The distilled water used to prepare solutions was boiled for 1 hr to eliminate CO_2 gas. In each titration, about 0.10 g (±

0.1 mg) of the fluorinated alcohol is dissolved in 4.00 ml MeOH and 4.00 ml H_2O. NaOH concentration was 0.0459 N. The titration curves are shown in Figure 3.

The acidities of compounds 4, 5 and 6 greatly depend on their structures. In compound 4, there are six β fluorine atoms to stabilize the conjugate base species. It is the strongest acid among the three compounds. The *pKa* value is 5.2, which is in the same range as that of aliphatic acids. Compound 5 has five β-fluorine atoms that can stabilize the conjugate base. The *pKa* value of compound 5 is expected to be somewhat higher than that of compound 4. The experiment yields a *pKa* of 6.3 for compound 5. Compound 6 is a secondary alcohol. It has one α-hydrogen atom and only two β-fluorine atoms. The acidity of compound 6 is much lower than that of compounds 4 and 5. However it is still a much stronger acid than hydrocarbon aliphatic alcohols. The *pKa* value of 9.4 is similar to the acidities of phenols. The inductive effect of the fluorine atoms is severely decreased as they are moved away from the functional group. The acidities of these alcohols depend mostly on the number of β-fluorine atoms.

The difference in acidities among these alcohols led us to investigate the nucleophilicities of these compounds. Kinetic studies were conducted in acetyl chloride solution at 56°C. Each of the alcohols (0.027 g) was dissolved in about 1.0 g (± 0.1 mg) of AcCl in a 5 mm NMR tube. The NMR tube was connected to a drying tube through a rubber septum and was submerged in a water bath to the level of the solvent . Water temperature was controlled at 56.0 ± 0.1°C. For each of the three compounds, the product and reactant ratio of the pseudo first order reactions

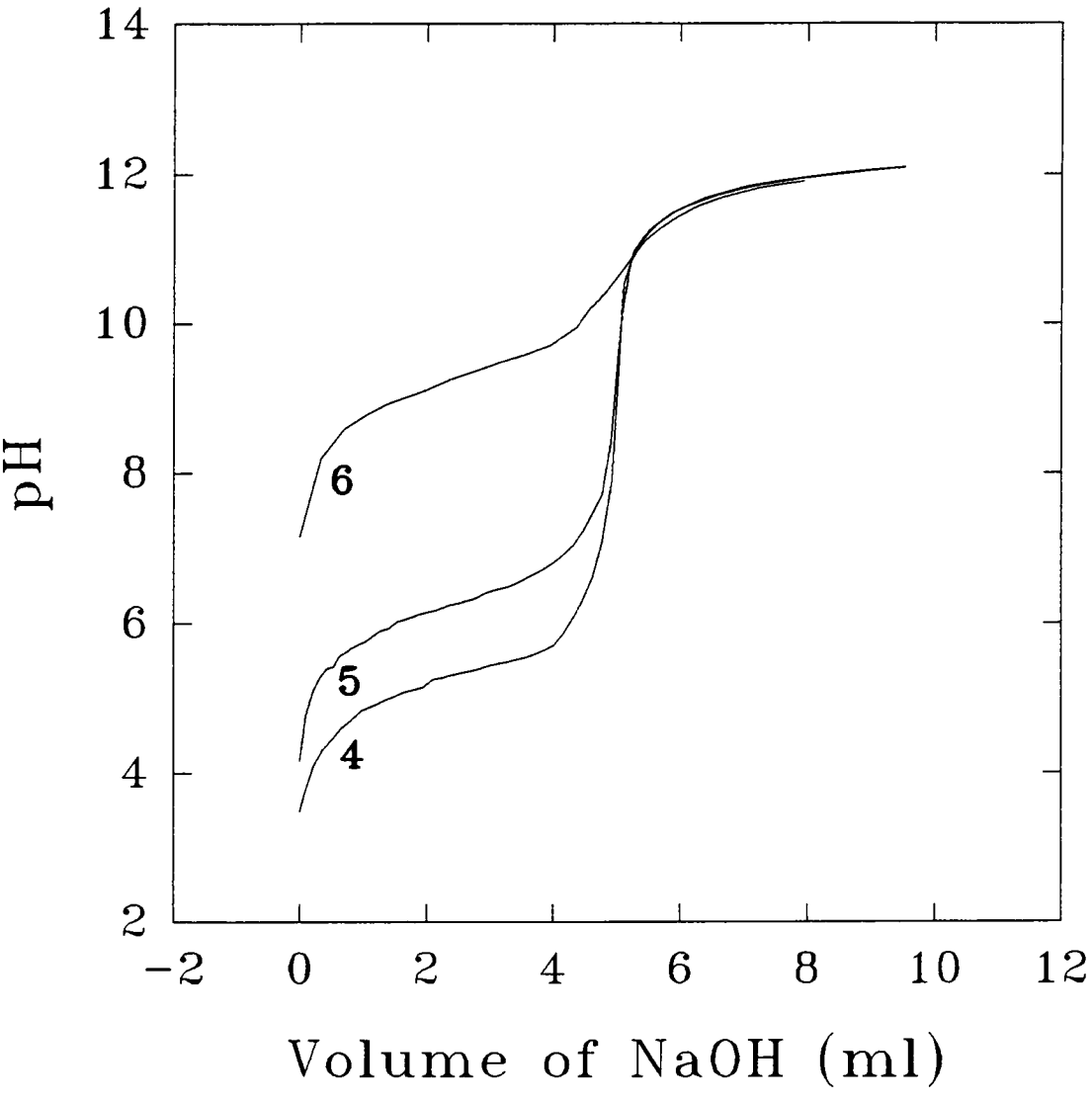

Figure 3 Titration Curves of Compounds 4, 5 and 6

can be measured by integrals obtained from the ^{19}F NMR spectra. For a general reaction (Scheme 10), the [A]/[B] values can be calculated based on the integrals of some well resolved peaks observed from the ^{19}F NMR spectra of the alcohols and acetates. ln([A]/[Ao]) can be derived from equation [A] + [B] = [Ao] and [A]/[B] values. Tables 4, 5 and 6 list the time and corresponding [A]/[B] and ln([A]/[Ao]) values. A plot of −ln([A]/[Ao]) versus time (in minutes) for each compound is

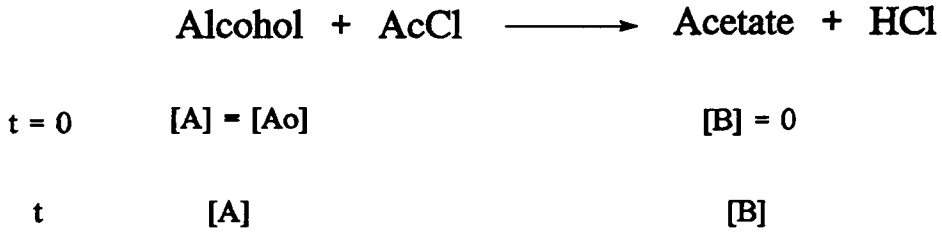

Scheme 10

Table 4 Rate Measurement of Compound 4, F-adamantan-1-ol

time(min)	60	135	195	277	336
[A]/[B]	13.72	5.05	3.31	2.33	1.57
ln([A]/[Ao])	−0.07	−0.18	−0.26	−0.36	−0.49
time(min)	399	484	539	578	
[A]/[B]	1.29	0.97	0.83	0.73	
ln([A]/[Ao])	−0.57	−0.71	−0.79	−0.86	

Table 5 Rate Measurement of Compound 5, 2-Hydryl-F-adamantan-1-ol

time(min)	135	256	352	472	562
[A]/[B]	7.01	3.63	2.73	1.69	1.46
ln([A]/[Ao])	−0.13	−0.24	−0.31	−0.46	−0.52

Table 6 Rate Measurement of Compound 6, 2-Hydryl-F-adamantan-2-ol

time(min)	135	230	320	427	487	547
[A]/[B]	21.76	12.09	8.03	6.95	5.91	5.00
ln([A]/[Ao])	−0.04	−0.08	−0.12	−0.13	−0.16	−0.18

Table 7 *pKa* and Rate Constant at 56°C of Compounds 4, 5 and 6

compound	*pKa*	$k_{obs} \times 10^4$ (min^{-1})
4	5.2	15.4
5	6.3	8.9
6	9.4	3.1

shown in Figure 4. The rate constants derived from the plot are listed in Table 7.

Under pseudo first order reaction conditions, the rate constant depends on the ease of the formation of the nucleophile. Compound 4 is the strongest acid among these three compounds. Its conjugate base is the most stable and the most readily formed species. Therefore compound 4 would be expected to have the highest rate constant as shown in Figure 4. Likewise, compound 5 has a higher rate constant than compound 6. The acidities and the pseudo first order acetylation rate constants of compounds 4, 5, and 6 are in good correlation. That is, the strongest acid has the fastest rate of acetylation.

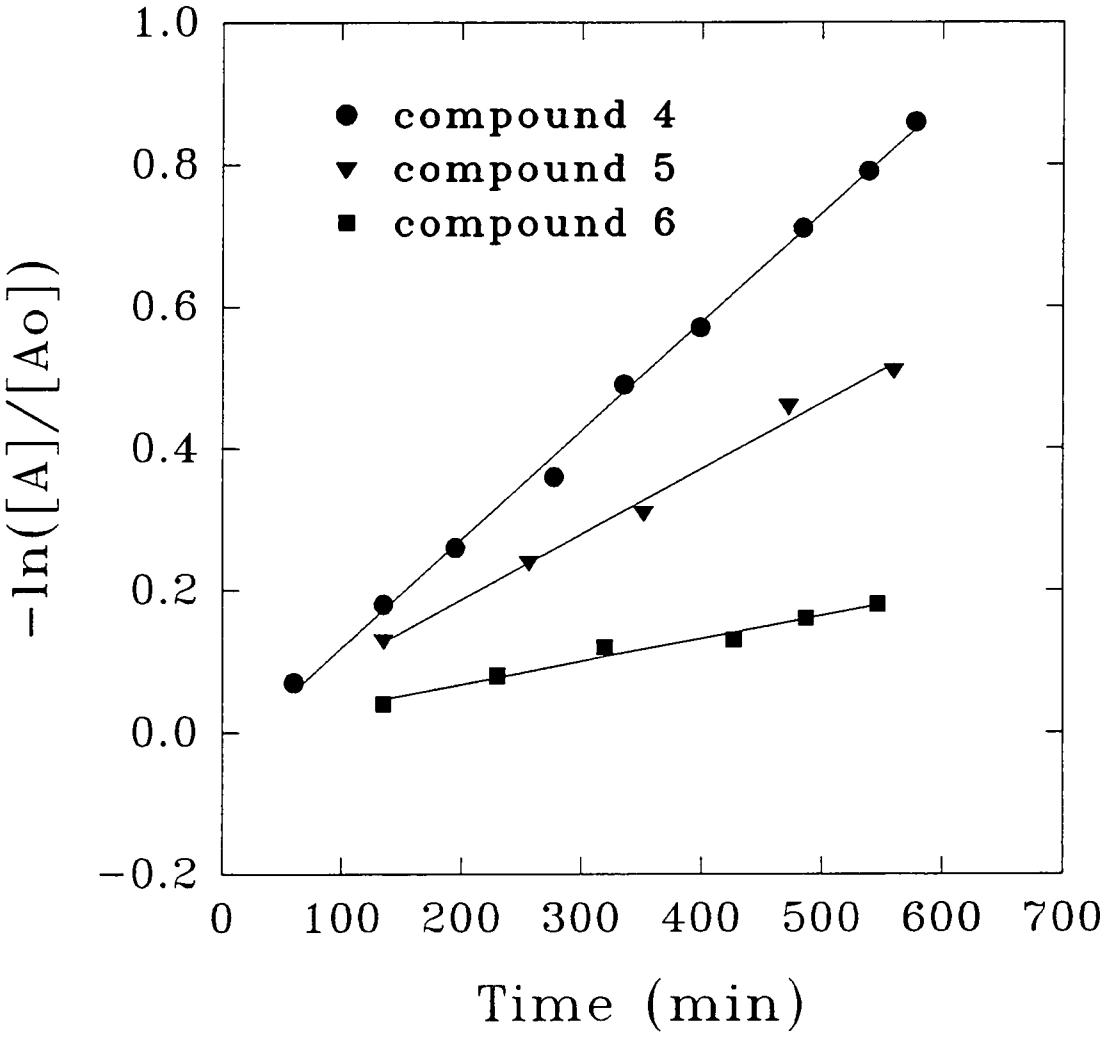

Figure 4 Rate Measurement of Compounds 4, 5 and 6 at 56°C.

3.1.4 Solvolysis

Poly- or perfluorinated alcohols are more acidic than the corresponding hydrocarbon alcohols, and as a consequence they are stronger hydrogen-bond donors than the hydrocarbon alcohols.[49] These poly- or perfluorinated alcohols have been the subjects for many studies involving hydroxyl groups forming hydrogen bonds with different kinds of hydrogen-bond acceptors.[50] Ladika and co-workers[51] have found that when 2,2,2-trifluoroethanol (TFE) and 1,1,1,3,3,3-hexafluoro-2-propanol (HFIP) form hydrogen bonds with t-$BuOCH_3$ molecules, the chemical shifts of methoxy groups in *t*-$BuOCH_3$ changed with the molar ratio of alcohol/ether. The $\Delta\delta$ (change of proton chemical shift of methyl group in *t*-$BuOCH_3$) showed good correlation with the *pKa* value of alcohols. That is the stronger the acid, the larger the $\Delta\delta$ value will be. Here we report the results of a ^1H NMR study of hydrogen bonds between poly- or perfluorinated adamantanol and *t*-$BuOCH_3$.

Because of the relatively high acidities of these alcohols, these compounds easily form hydrogen bonds with hydrogen-bond acceptors. In a *t*-$BuOCH_3/CCl_4$ solution, the addition of any of these fluorinated alcohols will result in the formation of intermolecular hydrogen bonds with the oxygen atom in *t*-$BuOCH_3$. The formation of hydrogen bonds can be detected by measuring the chemical shift change of the methoxy proton in *t*-$BuOCH_3$. Figure 5 shows a plot of the molar ratio of alcohol/ether to the chemical shift changes. For compounds 4 and 5, the *t*-$BuOCH_3$ methoxy proton chemical shift changes correlate well with the acidities. Compound 6 gives different results. According to Ladika's results,[50] the acidities are correlated

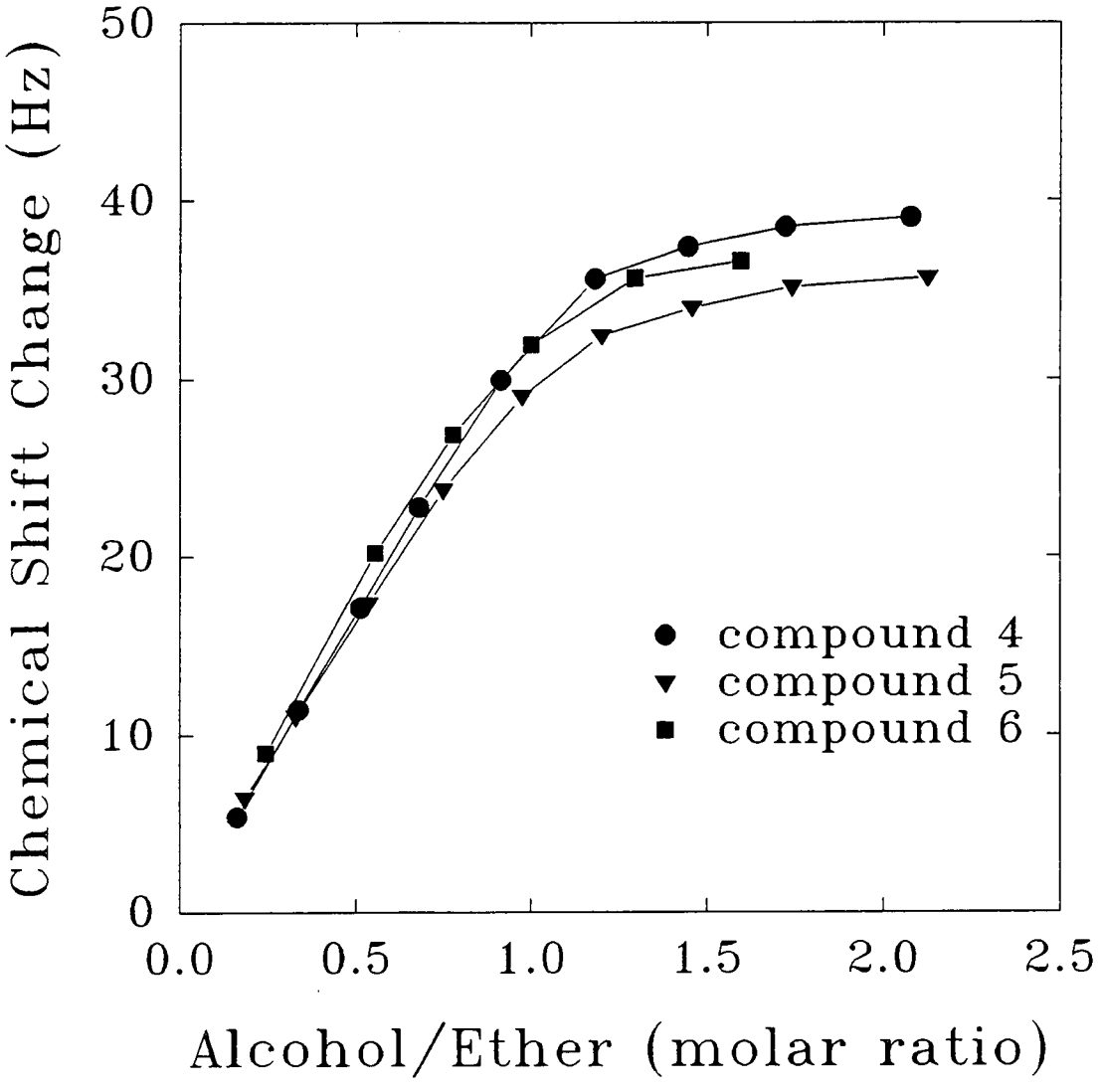

Figure 5 Correlation between Chemical Shift Changes and Molar Ratio of Alcohol/Ether

with the chemical shift changes. A stronger acid will form a stronger hydrogen bond with *t*-$BuOCH_3$; therefore, a higher chemical shift change will be observed. A weaker acid, on the other hand, will form a weaker hydrogen bond with *t*-$BuOCH_3$; thus, a lower chemical shift change will be observed. Therefore, compound 6 will be expected to have a lower curve than compound 4 and 5 due to its lower acidity. However, when alcohol/ether ratio is smaller than 1, compound 6 has a chemical shift change that is larger than either compound 4 or 5. When the alcohol/ether ratio is larger than 1, its curve is located between those of compounds 4 and 5. This unusual result for compound 6 can be rationalized according to the different location of the hydroxyl group. In compounds 4 and 5, the hydroxyl groups are located on the bridgehead carbon atoms. The α-fluorine atoms will cause steric hindrance as any hydrogen-bond acceptor approaches the hydroxyl hydrogen. In compound 6, the hydroxyl group is located on a bridge carbon. As any hydrogen-bond acceptor approaches the hydroxyl hydrogen, the two α-fluorine atoms on the bridge carbon atoms will cause less steric hindrance. Therefore, a reduced steric effect likely causes compound 6 to form stronger intermolecular hydrogen bonds than compounds 4 and 5.

In conclusion, the *pKa* values of F-adamantanol (Compound 4), 2-hydryl-F-adamantanol (Compound 5), and 2-hydryl-F-adamantan-2-ol (Compound 6) are 5.2, 6.3, and 9.4, respectively. As the number of β-fluorine atoms decrease, the acidities decrease. The acetylation rate constants of these three compounds correlate well with their acidities. The relative ability to form intermolecular hydrogen bonds

with *t*-$BuOCH_3$ depend on both the acidity and steric hindrance around the hydroxyl groups of these compounds.

3.2 C–H Hydrogen Bond

3.2.1 Introduction

A hydrogen bond is a bond between a hydrogen atom in a functional group A–H and an atom B or a group of atoms.[52] A usually refer to oxygen, nitrogen, and fluorine. B is oxygen, nitrogen, and fluorine. A hydrogen bond is weaker than a covalent bond. Therefore, the bonds are usually represented by dotted lines.

Considering the structure of a hydrogen bond, there are three types of hydrogen bonds in the literature. The first type is a "two-center" hydrogen bond. The hydrogen has an interaction with only one B atom (structure 1). The second type is a "three-center" (or bifurcated) hydrogen bond. The hydrogen is bonded to two B atoms or two hydrogen atoms are bonded to one B atom (structure 2). The third type is a "four-center" (or trifurcated) hydrogen bond. The hydrogen atom is bonded to three B atoms or three hydrogen atoms are bonded to one B atom (structure 3).[53]

In the 1930's, Glasstone first presented polarization measurement results for the trihalomethanes would form 1:1 complexes with hydrogen-bond acceptors such as ethers and ketones.[54] Later, Gordy confirmed these results by demonstrating that the vibrational spectra of polarized C–H groups were affected by hydrogen-bond acceptor solvents.[55] Thus, the fact that polarized C–H bonds could act as a

(Structure 1)

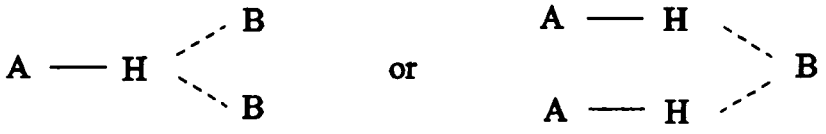

(Structure 2)

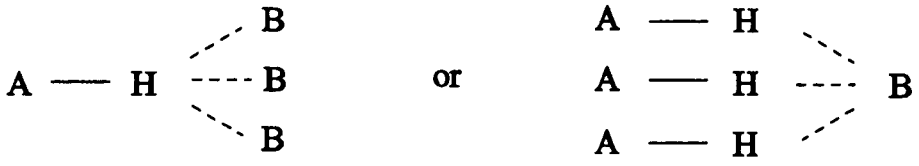

(Structure 3)

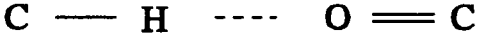

(Structure 4)

hydrogen-bond donors was established. Up to now, the C–H hydrogen bonds discussed in the literature have been "two-center" hydrogen bonds. No "three-center" or "four-center" hydrogen bonds involving C–H groups have been found in the literature.

X-ray crystallography, FT-IR, and ^{1}H NMR are three of the most commonly used tools for the study of hydrogen bonds. Given a C–H group as a hydrogen-bond

donor and a carbonyl group O=C as a hydrogen-bond acceptor (Structure 4), X-ray crystallography and neutron diffraction show that the distance between non-bonded, polarized hydrogen and oxygen atoms are commonly shorter than the sum of their van der Waals radii.[56] In infrared spectra, the polarized C−H stretching frequency is found to shift to a lower frequency. For $C(sp^3)-H$ bond, this shift is in the range of 10~100 cm^{-1}. The C=O stretching frequency also shifts to a lower frequency within the range of 10 ~ 50 cm^{-1}.[57] The ^1H NMR chemical shift of the polarized C−H proton is found to move to a lower field. In an intramolecular hydrogen bond, the low field shift is about 1 ppm.[58] There are many examples in which these three methods have been used to study "two-center" hydrogen bonds.[59] Despite their power, both crystallographic analysis and infrared spectroscopy have limitations. In some cases crystallography cannot distinguish a hydrogen-bond interaction from the effect of crystal-packing forces.[8] In other cases, the reliability of using the C−H stretching frequency as an indicator of a hydrogen bond is questionable. Lorand et. al. have shown that in the cases of F_2CHCN and $C_6H_5CH(NO_2)_2$, the C−H bond (as a hydrogen bond-donor) showed no stretching frequency change.[60] Pinchas even observed an increase in C−H stretching vibrational frequency.[61] The ^1H NMR chemical shift change offers a more reliable indicator of a hydrogen bond than does the IR. The fundamental difference in reliability between ^1H NMR and FT-IR, according to Lorand et.al., is that while IR frequency can be well defined by specific bond distance and bond angle relationships, the ^1H NMR chemical shift measurement takes into account all possible interactions between the hydrogen-bond

donor and the acceptor. For "three-center" or "four-center" hydrogen bonds, however, the study was limited to crystallographic data only. No infrared or ^1H NMR spectra have appeared in the literature.

Not only is ^1H NMR a more reliable tool to detect a hydrogen bond but also, when a hydrogen bond is formed, a correlation between the geminal coupling constant of the C−H group with another NMR active nucleus and the chemical shift of that proton may be observed. Evans discovered that BrClFC−H forms hydrogen bonds with different hydrogen-bond acceptor solvents.[62] The two bond hydrogen-fluorine coupling constant $^2J_{F-H}$ exhibited a linear relationship with the chemical shift variation due to each different solvent. The reason the $^2J_{F-H}$ coupling constants changed with different hydrogen-bond acceptors is not quite clear.

In our work with 1-[2-hydryl-F-adamantyl] trifluoroacetate and 1,3-[2-hydryl-F-adamantyl] bis-trifluoroacetate, we observed that the polarized C−H bonds form "two-center" and "three-center" hydrogen bonds, respectively. In addition to the ^1H NMR and FT-IR spectral evidence, a linear correlation between coupling constants $^2J_{F-H}$ and the chemical shift also is observed. Unexpectedly the C−H stretching frequencies moved to higher frequencies, a "Pinchas Effect".

3.2.2 Two and Three Center C−H Hydrogen Bonds

Because hydryl-substituted perfluorinated compounds have strongly polarized C−H bonds, any hydrogen-bond acceptors which are properly located may form hydrogen bonds with them. In order to quantify evidence for an intramolecular

hydrogen bond, the ^1H NMR spectra of our subject compounds, 1-[2-hydryl-F-adamantyl] trifluoroacetate (Compound 2) and 1,3-[2-hydryl-F-adamantyl] bis-trifluoroacetate (Compound 3), were compared to the ^1H NMR spectra of the reference compounds, 2-hydryl-F-adamantane (Compound 8), 2-hydryl-F-adamantan-1-ol (Compound 5), 2-hydryl-F-adamantan-1,3-diol (Compound 7), and 1-F-adamantyl trifluoroacetate (compound 1). Of these compounds, only 2-hydryl-F-adamantane has been reported in the literature previously.[63] Compounds 1, 2, and 3 were synthesized by aerosol direct fluorination of the corresponding hydrocarbon esters. Compounds 5 and 7 are the hydrolysis products of 2 and 3, respectively.

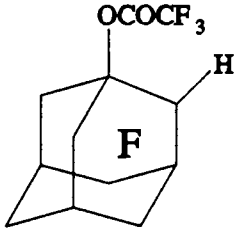

2

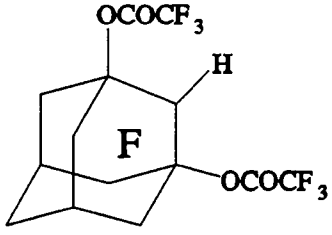

3

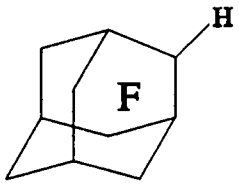

8

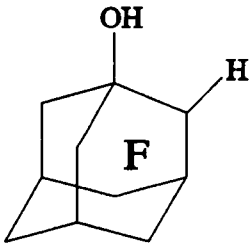

5

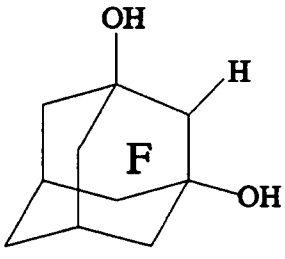

7

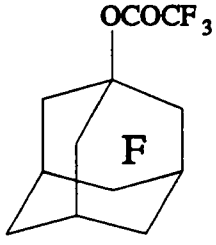

1

Figure 6 shows the 250 MHz ^1H NMR spectra of compounds 2, 3, 5, 7, and 8. The ^1H NMR spectrum of each compound has a doublet peak plus additional lower order splitting. The doublet is caused by the two-bond fluorine-hydrogen coupling, $^2J_{F-H}$. The additional lower order splitting is due to "long-range virtual coupling," a phenomenon that often occurs in polyfluorinated or perfluorinated compounds. A detailed discussion is presented in section 3.3.

In a comparison of the ^1H NMR spectra of compounds 5, 7 and 8 (Table 8), the chemical shifts of the protons in these compounds are in the order of 7, 5 and 8 from high field to low field. The structural differences within these three compounds involve the substitution of fluorine atoms by hydroxyl groups. Compound 8 has two bridgehead fluorine atoms at alpha to the hydrogen atom, compound 5 has one bridgehead α-fluorine substituted by a hydroxyl group, and compound 7 has both α-fluorine atoms substituted by hydroxyl groups. Fluorine has the highest electronegativity among monatomic substituents. Its strong inductive effect is responsible for the low field chemical shift of the proton in compound 8, which is δ 5.45 ppm ($^2J_{H-F}$ = 48.8 Hz). The oxygen linked substituents have a lower electronegativity than that of fluorine. The inductive effect of oxygen is less than that of fluorine. As expected, one hydroxyl group causes the hydrogen chemical shift of 2-hydryl-F-adamantan-1-ol (5) to move to a relatively higher field (δ = 5.23 ppm; $^2J_{H-F}$ = 48.2 Hz), and two hydroxyl groups cause the hydrogen chemical shift of 2-hydryl-F-adamantan-1,3-diol (7) to move to even higher field (δ = 5.02 ppm; $^2J_{H-F}$ = 47.9 Hz). Now comparing compounds 8, 2, and 3, the bridgehead fluorine atom

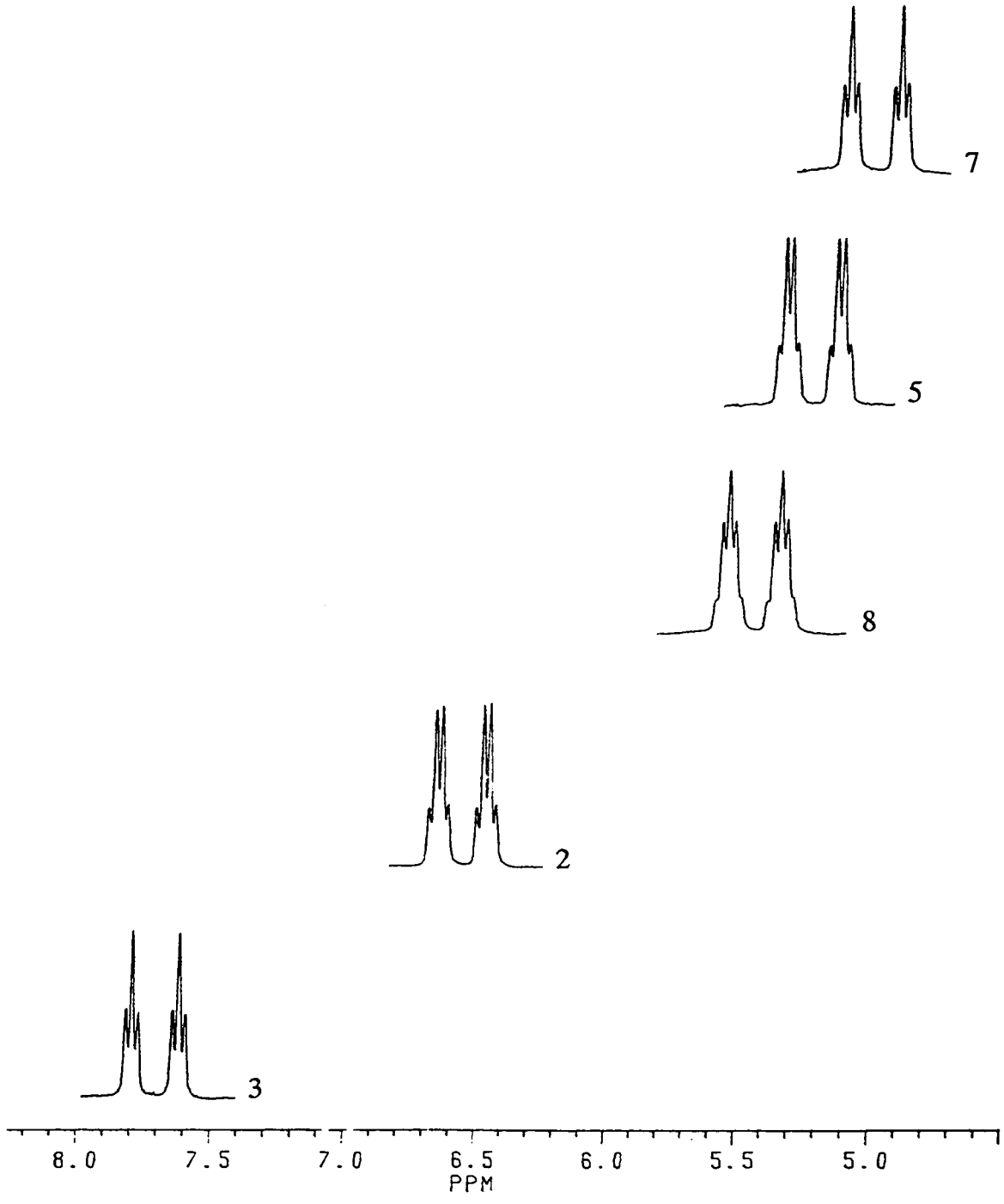

Figure 6 250 MHz NMR Spectra of Compounds 2, 3, 5, 7, and 8.

Table 8 Proton Chemical Shifts and $^2J_{H-F}$ of Compounds 2, 3, 5, 7 and 8.

Compound	δ (ppm)	$^2J_{H-F}$ (Hz)
7	5.02	47.9
5	5.23	48.2
8	5.45	48.8
2	6.55	46.2
3	7.70	43.5

in compound 2 is substituted by a trifluoroacetoxyl group, and the two bridgehead fluorine atoms in compound 3 are substituted by two trifluoroacetoxyl groups. The chemical shift of a proton adjacent to a trifluoroacetoxyl group will be expected to occur in the same region as a proton adjacent to a hydroxyl group. Surprisingly, the proton chemical shift of 1-[2-hydryl-F-adamantyl] trifluoroacetate (2) moves to a significantly lower field (δ 6.55 ppm, $^2J_{H-F}$ = 46.2 Hz). The chemical shift change is 1.10 ppm. An intramolecular C–H hydrogen bond usually cause the proton a low field shift ($\Delta\delta$) of about 1 ppm. Obviously there is a relatively strong interaction between the trifluoroacetoxyl group and the C–H group. Compound 2 is a monohydryl perfluorinated ester. The only C–H bond in this compound is strongly polarized by the perfluorinated adamantyl group, especially by the adjacent fluorine atom. Therefore, this highly polarized C–H bond has a potential to be a hydrogen

bond donor. On the other hand, there is a perfluorinated acetyl group at the α position of the C−H bond. The carbonyl group has the potential to be a hydrogen bond acceptor. Structure 5 depicts 2 as having an intramolecular hydrogen bond which forms a six-membered ring.

The ^{1}H NMR spectrum of 1,3-[2-hydryl-F-adamantyl] bis-trifluoroacetate (3) shows that the proton chemical shift moves to an even lower field (δ = 7.70 ppm), which is 1.15 ppm lower than for compound 2 and 2.25 ppm lower than for compound 8. The two-bond H−F coupling constant become smaller ($^2J_{H-F}$ = 43.5 Hz) than is found in compound 2 ($^2J_{H-F}$ = 46.2 Hz). Structure 6 shows that in compound 3, two fused six-member rings can be formed by an intramolecular hydrogen bond. The likelihood that a three-center hydrogen bond exists is strong.

In order to further confirm the existence of the intramolecular hydrogen bond in the 2-hydryl-F-adamantyl ester system, four more compounds were synthesized. They are 1-[2-hydryl-F-adamantyl] acetate (Compound 9), 1-[2-hydryl-F-adamantyl]

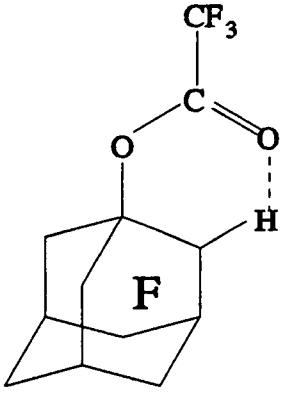

Structure 5

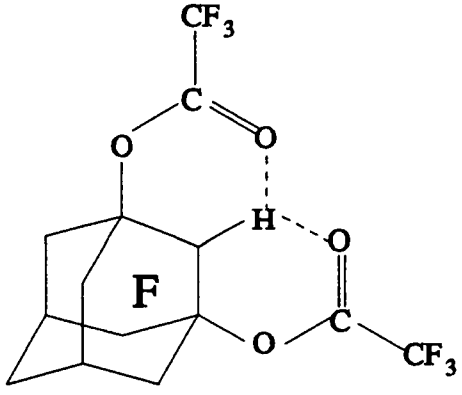

Structure 6

benzoate (Compound 10), 1-[2-hydryl-F-adamantyl] methylsulfonate (Compound 11), and 1,3-[2-hydryl-F-adamantyl] bis-benzoate (Compound 12). ^{1}H NMR spectra show that in all four compounds the proton chemical shift moves to lower field relative to the proton chemical shift in 2-hydryl-F-adamantane (Figure 7).

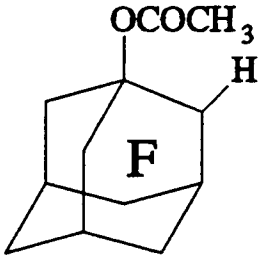

9

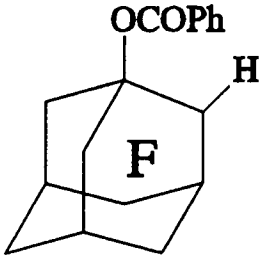

10

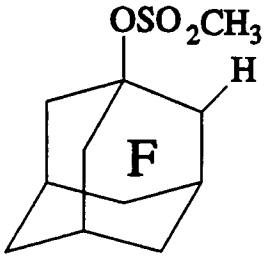

11

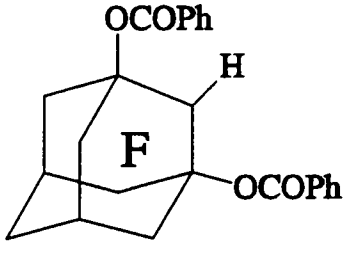

12

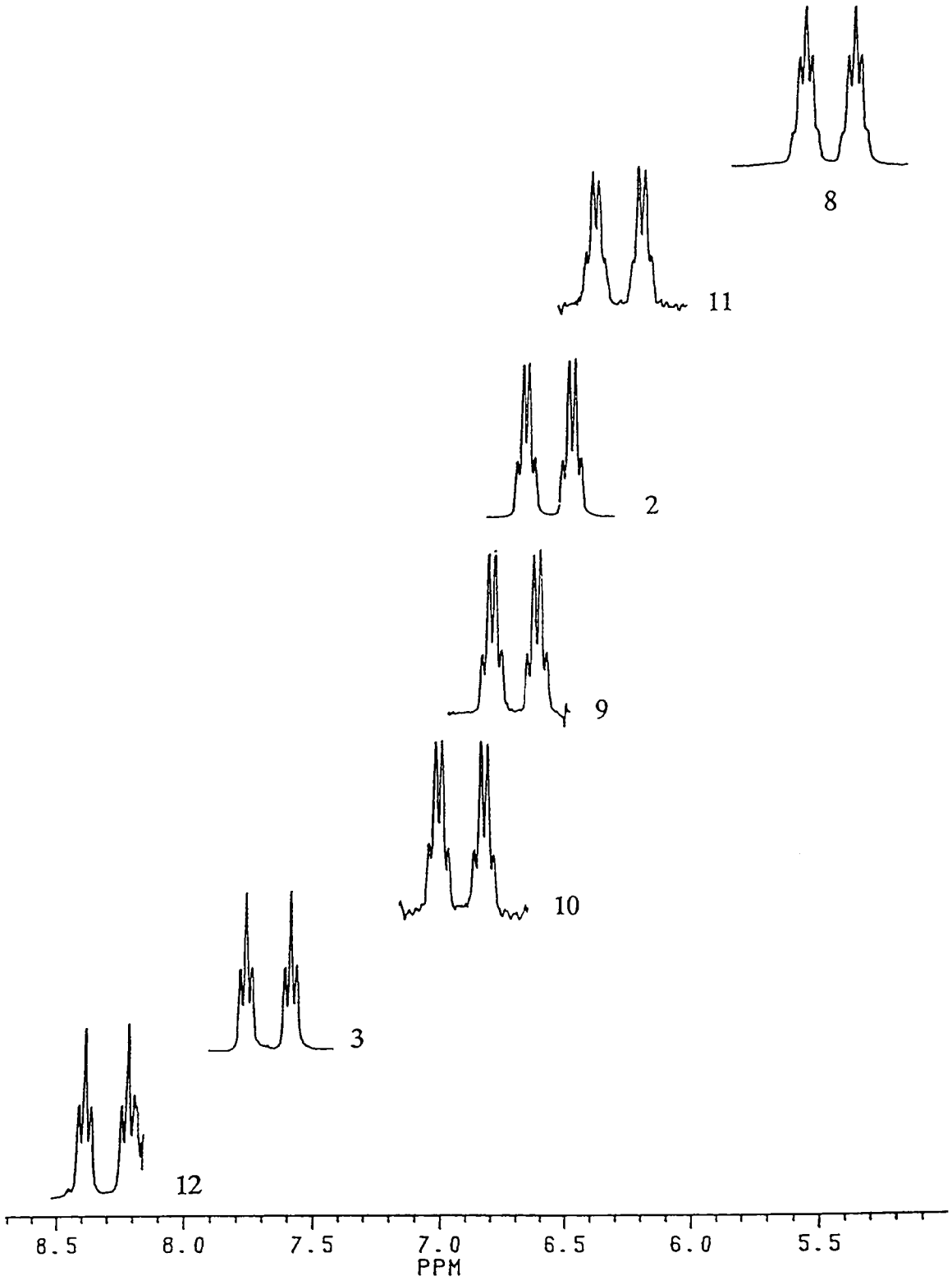

Figure 7 250 MHz ^{1}H NMR of 2-Hydryl-F-adamantyl Esters

In comparison of the ^1H NMR spectra in 1-[2-hydryl-F-adamantyl] trifluoroacetate (2), 1-[2-hydryl-F-adamantyl] acetate (9), and 1-[2-hydryl-F-adamantyl] benzoate (10), the proton chemical shifts are δ 6.55 ppm, 6.69 ppm, and 6.90 ppm, respectively. Due to the strong electron withdrawing effect of the trifluoromethyl group, the carbonyl group in trifluoroacetate is not as strong a hydrogen-bond acceptor as the carbonyl groups in either the hydrocarbon acetate or the benzoate. Therefore, the trifluoroacetate forms the weakest hydrogen bond among these three compounds, and as a consequence, the proton has the highest field chemical shift among these three compounds. Likewise, in the three-center hydrogen-bond system, the carbonyl group in trifluoroacetate is not as strong a hydrogen-bond acceptor as the carbonyl group in benzoate. Therefore, the proton in 1,3-[2-hydryl-F-adamantyl] bis-benzoate has a much lower chemical shift (8.31 ppm) than the proton in 1,3-[2-hydryl-F-adamantyl] bis-trifluoroacetate (7.70 ppm).

Table 9 shows the chemical shift relationship between the two-center hydrogen bond and three-center hydrogen bond. In both the trifluoroacetate and benzoate cases, the chemical shift change that is caused by a three-center hydrogen bond is almost double the chemical shift change that is caused by a two-center hydrogen bond. These results further substantiate the existence of a three-center hydrogen bond in this C−H hydrogen-bond donor system.

Table 9 Chemical Shift of Two-center and Three-center Hydrogen Bond

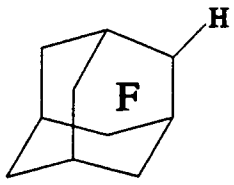	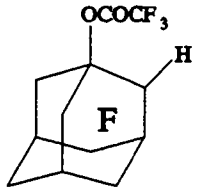	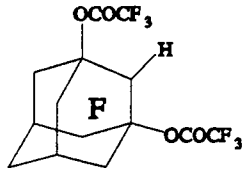
δ 5.45 ppm	δ 6.55 ppm	δ 7.70 ppm
	Δδ 1.10 ppm	Δδ 1.15 ppm
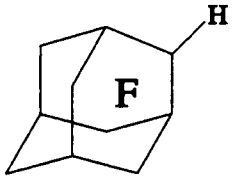	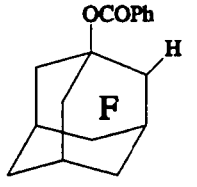	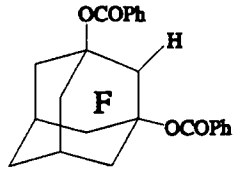
δ 5.45 ppm	δ 6.90 ppm	δ 8.31 ppm
	Δδ 1.45 ppm	Δδ 1.41 ppm

3.2.3 Correlation of Chemical Shifts and $^2J_{H-F}$ Coupling Constants

The chemical shift is a measurement of the electric shielding of a nucleus in a molecule. The coupling constant is a measurement of a change of spin or orbital motion between two nuclei transmitted through valence electrons of the intervening bonds. There are several articles in the literature which try to reveal a relationship between the chemical shifts and coupling constants.[64] Most of these works studied the coupling constants between two nuclei that were bonded together, that is ^1J. The only example considering the ^2J coupling constant was by Evans. In the early 1960's, Evans discovered that HCBrClF forms intermolecular hydrogen bonds with different solvents.[62] The chemical shifts of the proton changed with different hydrogen-bond acceptor solvents. The coupling constants between the proton nucleus and the fluorine nucleus $^2J_{H-F}$ also changed. A linear correlation was found between the chemical shifts and the coupling constants. Evans did not give an explanation.

During our work on the two-center and three-center hydrogen bond system, not only a good linear correlation between chemical shifts and coupling constants is found, but this linear correlation exists for both a two-center and a three-center intramolecular hydrogen bond. Figure 8 shows the linear correlation. In 2-hydryl-F-adamantane (8), no hydrogen bond exists; the chemical shift is 5.45 ppm and the coupling constant is 48.8 Hz. In 1-[2-hydryl-F-adamantyl] trifluoroacetate (2) which has one two-center hydrogen bond, the chemical shift is 6.55 ppm and the coupling constant is 46.2 Hz. In 1,3-[2-hydryl-F-adamantyl] bis-trifluoroacetate (3) which has a three-center hydrogen bond, the chemical shift is 7.70 ppm and the coupling

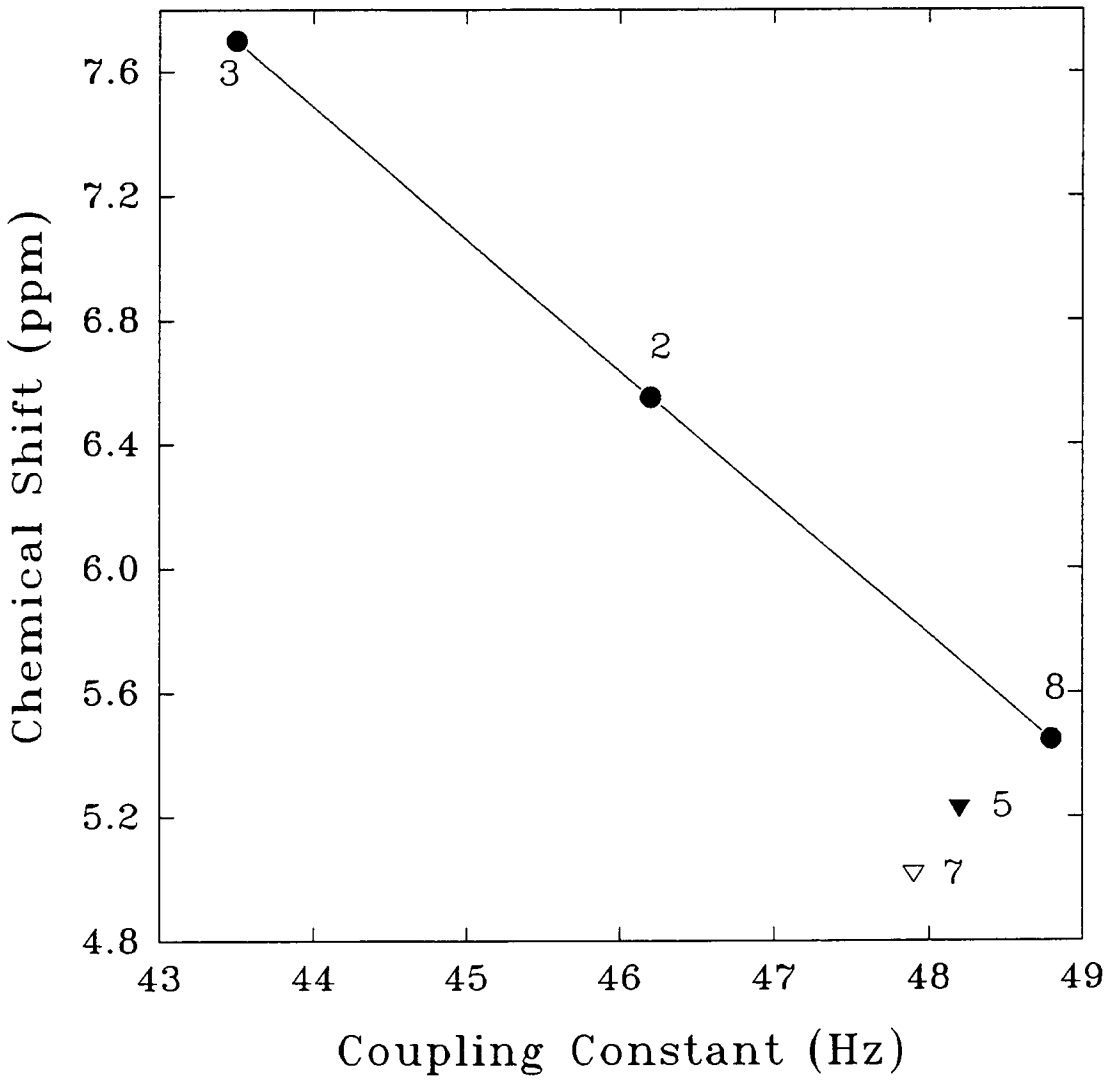

Figure 8 Correlation Between Chemical Shift and Coupling Constants in Two-center and Three-center Hydrogen Bond System (1)

constant is 43.5 Hz. As a comparison, Figure 8 also shows the data for 2-hydryl-F-adamantan-1-ol (5) and 2-hydryl-F-adamantan-1,3-diol (7) which do not have intramolecular hydrogen bonds. In compounds 8, 5, and 7, the change in chemical shifts and coupling constants is caused solely by the substitution of fluorine atoms by hydroxyl groups. These hydroxyl groups interact solely through the intervening σ bonds. There is not a similar linear correlation between compounds 8, 5, and 7. The changed direction of chemical shifts and their relationship to the coupling constants is different from that found in the hydrogen bonded systems. In compounds 8, 2, and 3, the excellent correlation found between the chemical shift and $^2J_{H-F}$ of the reference species (8), two-center (2), and three-center (3) hydrogen bond species seems clearly related to the number of hydrogen bond acceptors.

In further examination of this hydrogen bond system, we found that 1,3-[-2-hydryl-F-adamantyl] bis-benzoate (12), 1,3-[2-hydryl-F-adamantyl] bis-trifluoroacetate (3), 1-[2-hydryl-F-adamantyl] benzoate (10), 1-[2-hydryl-F-adamantyl] acetate (9), 1-[2-hydryl-F-adamantyl] trifluoroacetate (2), and 2-hydryl-F-adamantane (8) follow this same linear correlation (Table 10 and Figure 9). The stronger the hydrogen bond is, the lower field the chemical shift will be and the smaller the $^2J_{H-F}$ will be. This result suggests that the changes in the chemical shifts and the coupling constants depend on the total electron density change around the proton and the fluorine nuclei. No correlation is found between the proton chemical shifts and their long range coupling constants $^5J_{H-F}$.

Table 10 Proton Chemical Shifts and $^{2}J_{H-F}$ Coupling Constants of Compounds 2, 3, 8, 9, 10, 11, and 12.

Compound	δ (ppm)	$^{2}J_{H-F}$ (Hz)	$^{5}J_{H-F}$ (Hz)
12	8.31	42.3	6.1
3	7.70	43.5	5.8
10	6.90	45.5	6.5
9	6.69	45.9	6.4
2	6.55	46.2	6.2
11	6.28	45.9	6.2
8	5.45	48.8	6.0

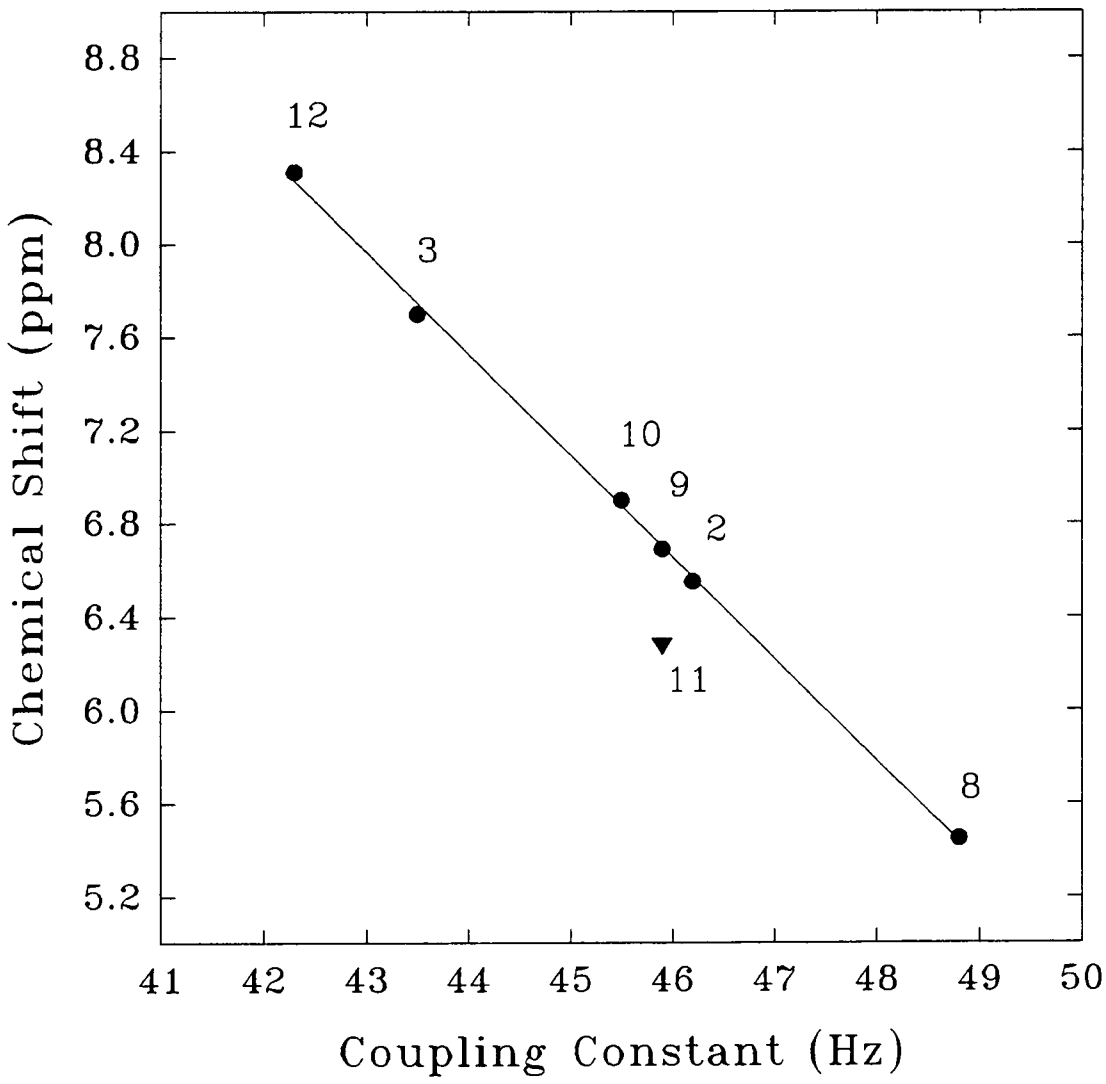

Figure 9 Correlation of Chemical Shifts and Coupling Constants in Two-center and Three-center Hydrogen Bond System (2)

A significant deviation from the correlation is found for 1-[2-hydryl-F-adamantyl] methylsulfonate. The configuration difference between the methylsulfonate and the other esters suggests an explanation of this deviation. Compounds 2, 3, 9, 10, and 12 are carboxylate esters. The configuration of the ester center are planar. In compound 11, the configuration of a sulfonate is near tetrahedral. "Sybyl" molecular modeling calculation results are shown in Table 11, where α is the dihedral angle between C=O (S=O) bond and C−H bond, and d_{H-O} is the distance between the hydrogen and the oxygen. In the carboxylate esters system, the dihedral angle are around 19°, whereas in the methylsulfonate system, the dihedral angle is about 38°.

In all the carboxylate esters, when a hydrogen bond is formed, the lone pair

Table 11 Dihedral angles α and Hydrogen Oxygen Distance d_{H-O}

Compound	α	d_{H-O} (Å)
2	18.7	2.392
9	18.4	2.392
10	19.3	2.380
3	18.0	2.393
11	38.1	2.415

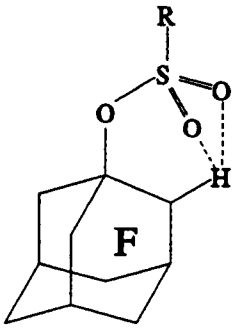

Structure 7

electrons on oxygen point to the hydrogen in almost the same angle while in 1-[2-hydryl-F-adamantyl] methylsulfonate, the lone pair electron on the oxygen point to the hydrogen at a different angle. It is this difference that may cause the deviation of 1-[2-hydryl-F-adamantyl] methylsulfonate from the established correlation.

Structure 7 shows a three-center hydrogen bond in the methylsulfonate ester. The hydrogen may form hydrogen bonds with both oxygen atoms of the sulfonyl group. The possible formation of this type of three-center hydrogen bond needs to be further investigated.

The solvent induced linear correlation between chemical shift and coupling constant, which was found in Evans' compound, HCBrClF, is also observed in 2-hydryl-F-adamantan-1-ol. Figure 10 and Table 12 show the results. The solvent induced intermolecular correlation is not as good as the intramolecular correlation but follows the same pattern. Deviations may be induced by competing intermolecular hydrogen-bonded interaction, due to the hydroxyl groups.

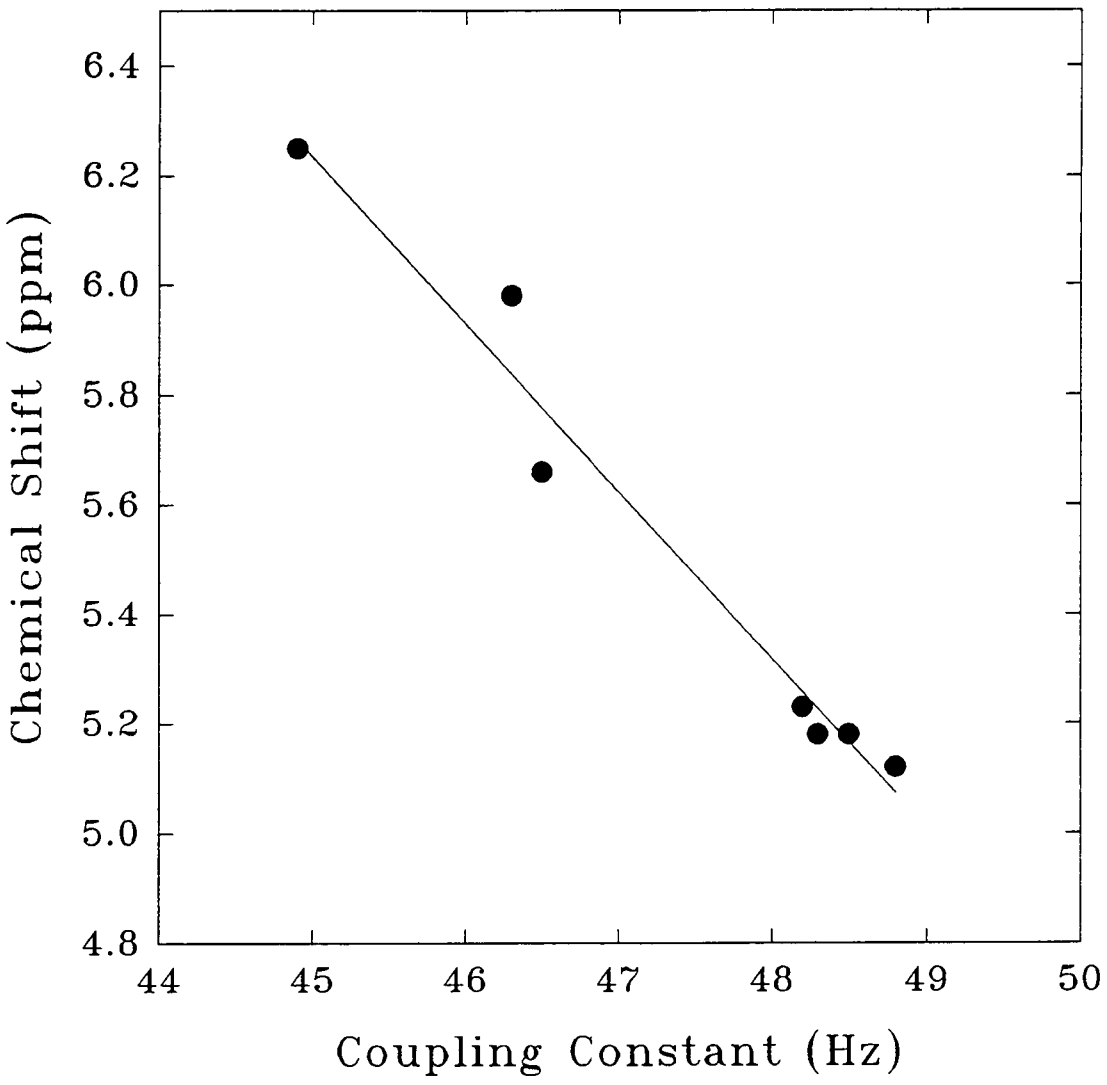

Figure 10 Solvent Induced Chemical Shift Correlate with Coupling Constant in 2-Hydryl-F-adamantan-1-ol

Table 12 Solvent Induced Chemical Shift Correlation with $^2J_{H-F}$ Coupling Constant in 2-Hydryl-F-adamantan-1-ol

Solvent	δ (ppm)	$^2J_{H-F}$ (Hz)
CD_3SOCD_3	6.25	44.9
CD_3COCD_3	5.98	46.3
CD_3CN	5.66	46.5
$CDCl_3$	5.23	48.2
$CFCl_3$	5.18	48.5
CF_3CSCF_3	5.18	48.3
$(C_4F_9)_3N$	5.12	48.8

3.2.4 Infrared Spectroscopic Evidence for a C–H Hydrogen Bond

A hydrogen atom covalently bonded to a highly electronegativity atom (A) will form a very polarized bond, H–A. Because of the electronegativity of atom A, the electron density of the A–H bond will move toward A. The hydrogen atom will appear as a "naked" proton, which easily accepts electrons density from a Lewis base. Any element (B) that has electron lone pairs will interact with this proton. This interaction is a hydrogen bond. Forming a hydrogen bond between H and B will affect the physical properties of the H–A bond. By measuring the change in the H–A bond, we can detect the existence of a hydrogen bond.

In general, when a hydrogen bond is formed between an A–H bond and a C=O bond (Structure 8), the electron density of oxygen will move to the proton. One consequence is that the bond between C and O is weakened; therefore the stretching mode of C=O will move to a lower frequency ($\Delta\nu$ is about 10–50 cm^{-1}). Secondly, as the proton accepts more electron density from oxygen, the hydrogen atom in the A–H bond is pulled toward oxygen, the bond between A and H is weakened, and the stretching mode of A–H moves to a lower frequency ($\Delta\nu$ is about 10–100 cm^{-1}) as well. In most cases, when a polarized C–H bond is involved in a hydrogen-bond system, the C–H stretching frequency will also shift to a lower frequency. For example, Allerhand and Schleyer surveyed a series of compounds with polarized C–H bonds in dimethyl sulfoxide-d_6 and pyridine-d_5 solutions.[65] The C–H bonds are hydrogen bond donors. The oxygen on dimethyl sulfoxide-d_6 and the nitrogen on pyridine-d_5 are the hydrogen-bond acceptors. The C–H

stretching modes in FT-IR shift to lower frequencies. However, Lorand and co-workers found the correlation between the hydrogen-bond formation constants K and the IR shifts ($\Delta\nu$) to be very poor in the system where excellent correlation between formation constants K and the ^1H NMR data were found.[60] In two examples, F_2CHCN and $C_6H_5CH(NO_2)_2$, the stretching frequencies of C–H actually showed no shift ($\Delta\nu=0$) after forming hydrogen bonds. They concluded, that as a tool to detect C–H hydrogen bonds, IR was not as reliable as ^1H NMR.

The controversy about the IR shifts in C–H hydrogen bonds actually started in the 1950's. Pinchas first obtained evidence for an increase in C–H stretching frequencies in various ortho-substituted benzaldehydes which he attributed to an internal hydrogen bond (Structure 8).[66] Later, West and Watley argued that if a hydrogen bond existed, there should be a decrease in the N–O stretching frequency which did not occur.[67] Furthermore, the mesitaldehyde (Structure 9), which had two methyl groups at the ortho positions of an aldehyde group, also had an increased C–H frequency. Therefore, they suggested that the increase in C–H stretching frequencies was not caused by an intramolecular hydrogen bond, but was caused by a steric effect.

The controversy about the IR shifts in C–H hydrogen bonds in ortho-nitro-benzaldehydes remains unresolved. The "Pinchas Effect" lacked critical support because no molecules existed that offered a clear example of the IR effect which also had other supporting spectral evidence. For example, Sammes and Li studied a C–H hydrogen bond system (Structure 10) in depth.[68] However, because too

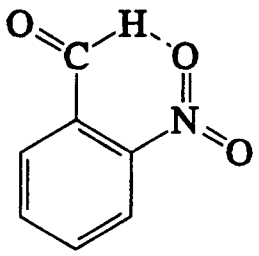

(Structure 8)

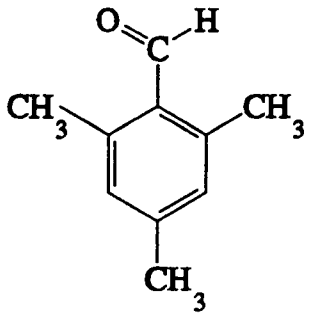

(Structure 9)

many hydrogen atoms existed in this system, the hydrogen-bond C−H frequency was overlapped by other C−H frequencies; therefore, they could not obtain a good IR result from this hydrogen-bond system.

In compounds 1-[2-hydryl-F-adamantyl] trifluoroacetate (2) and 1,3-[2-hydryl-F-adamantyl] bis-trifluoroacetate (3), there is only one C−H bond in each of them. Therefore, no other C−H frequency overlaps with it in the FT-IR spectrum. If there

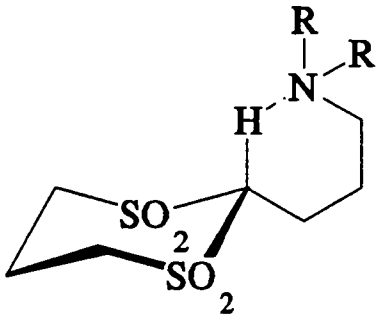

(Structure 10)

is any interaction between this C−H bond and other functional groups, the FT-IR spectrum will clearly show the change in C−H bond stretching frequencies. In fact, we observe an increase in C−H stretching frequencies in both these systems.

The IR spectral data are listed in Table 13. In the reference compound 1-F-adamantyl trifluoroacetate (1), there is no possibility of a hydrogen bond. The C=O stretching frequency is 1848 cm^{-1}. In 1-[2-hydryl-F-adamantyl] trifluoroacetate (2), where one "two-center" hydrogen bond exists, the C=O stretching frequency is found to shift to a lower frequency (1829 cm^{-1}; $\Delta\nu$ 19 cm^{-1}). This shift to lower frequency is also found in 1,3-[2-hydryl-F-adamantyl] bis-tri-fluoroacetate (3), where one "three-center" hydrogen bond is possible. The frequency shifts to 1832 cm^{-1} ($\Delta\nu$ 16 cm^{-1}). The decrease in the C=O stretching frequency of compound (17) is less than that of compound (16). In the "two-center" hydrogen bond, the interaction is between the one hydrogen-bond donor and only one acceptor. In the "three-center" hydrogen bond, the interaction with the hydrogen-bond donor is split between the two acceptor carbonyl groups. For the same hydrogen-bond donor and acceptor, the "three-center" hydrogen-bond energy would be expected to be weaker than the "two-

Table 13 C=O and C−H Stretching Frequencies of Compounds 1, 2, 3 and 8

IR	$\nu_{C=O}$ (cm^{-1})	ν_{C-H} (cm^{-1})
8		2993
1	1848	
2	1829	3021
3	1832	3051

center" hydrogen-bond energy. It seems reasonable that the one C=O stretching frequency in compound (2) will move to a lower frequency than the two C=O's in compound (3).

For the C−H stretching frequency, instead of moving to a lower frequency in both compounds (2) and (3) as usually expected for the hydrogen bond, they move to a higher frequency and increase in intensity. Compound (8) has a C−H stretching frequency of 2993 cm^{-1}, while that of (2) is 3021 cm^{-1}, and that of (3) is 3051 cm^{-1}. Both ^1H NMR and IR $\nu_{C=O}$ frequencies indicate the existence of a C−H hydrogen bond. Therefore, the increases in C−H frequencies caused by C−H hydrogen bonds are real in these systems (Figure 11).

The difference between our system (including the Pinchas system) and the other C−H hydrogen bond system which showed low field shift upon forming a hydrogen bond, is that our hydrogen bonds are intramolecular and the others are intermolecular. In the intermolecular system, hydrogen is on the straight line formed by C and O (Structure 11) within about 15°.[69] Therefore, the C−H stretching mode is in the direction of the lone pair electrons on oxygen. The lone-pair electrons have a direct effect on the stretching mode of the C−H bond (an incipient 3C−4e^- bond molecular orbital system). On the other hand, in the intramolecular system (Structure 12), the C−H···O system is locked in a six-membered ring. The C−H···O angle is smaller than 120° (3C−4e^- bond effect negligible). The C−H stretching mode is not directly affected by the lone-pair electrons on the oxygen. Instead, it is affected by the electronic field created by those lone-pair electrons. We

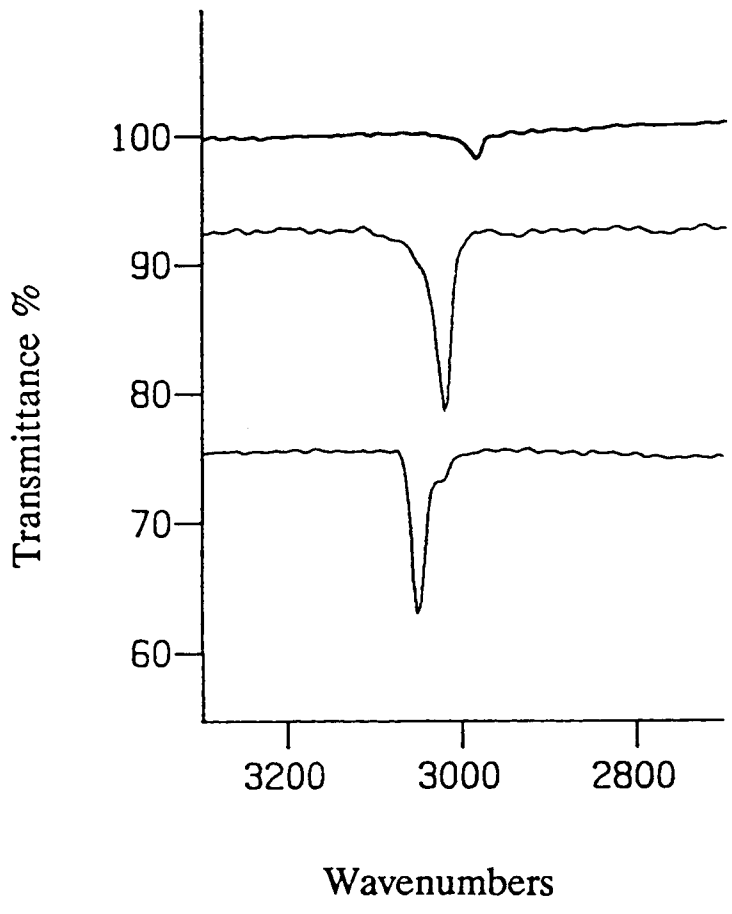

Figure 11 C–H Stretching Frequency High Field Shift

assume it is this difference that causes the different C−H frequency shift between the intramolecular and intermolecular hydrogen bond systems. Further study by X-ray crystallography and molecular modelling is under way.

In conclusion, the ^1H NMR and FT-IR of C=O stretching spectra strongly support the existence of polarized C−H groups as "two-center" and "three-center"

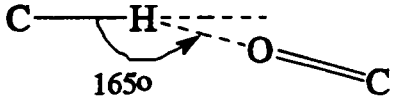

(Structure 11)

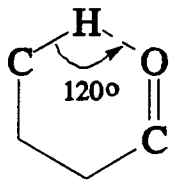

(Structure 12)

hydrogen-bond donors. A linear correlation between coupling constant $^2J_{H-F}$ and the chemical shift is found within the C−H hydrogen bond systems. In an intramolecular C−H hydrogen bond system, the C−H stretching frequencies will shift to either higher frequencies or lower frequencies depending on the angle formed by C−H···O.

3.3 F-2,6-Adamantanedione and F-Tricyclo[3.3.0.$0^{3,7}$]octane (Bisnoradamantane)

3.3.1 Introduction

As precursors, many organic compounds can be perfluorinated by using the aerosol direct fluorination method. Cage hydrocarbon compounds are among those precursors that are especially well suited to the aerosol direct fluorination method. First, cage hydrocarbon compounds usually have high volatilities, which enable them to be evaporated in the reactor. Second, if no strain energy exists, the rigid skeleton

will prevent fragmentation from occurring. Several cage hydrocarbon compounds have previously been successfully perfluorinated in our laboratory, such as adamantane,[18] diamantane,[19] and [2.2.2]-bicyclooctane.[70] These three molecules are notable in that the smallest ring in each system is a six-membered ring. Because a six-membered ring has the lowest strain energy, ring opening does not occur under aerosol direct fluorination conditions. However, for those cage compounds that have a relatively high ring strain energy, such as cubane, ring opening does occur under aerosol direct fluorination conditions.[71] To avoid this problem, we have sought alternative methods leading to smaller ring perfluorinated cage compounds, such as bisnoradamantane (Structure 13).

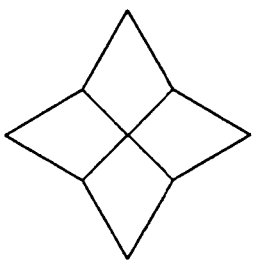

Structure 13

A typical way to obtain a perfluorinated cage compound usually involves the synthesis of its hydrocarbon analogue compound first, then subjecting this compound to aerosol direct fluorination. According to the literature, the synthesis of (hydrocarbon) bisnoradamantane involves multistep synthesis procedures. Two typical synthesis routes are showed in Scheme 11[72] and 12.[73] These are multistep synthesis routes. Because a high probability of ring opening of the

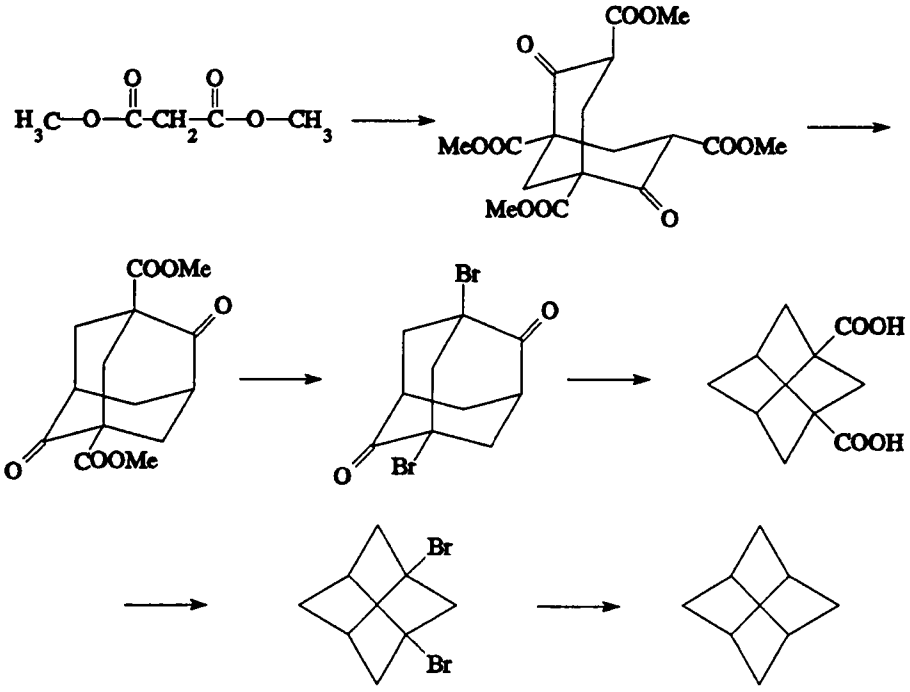

Scheme 11

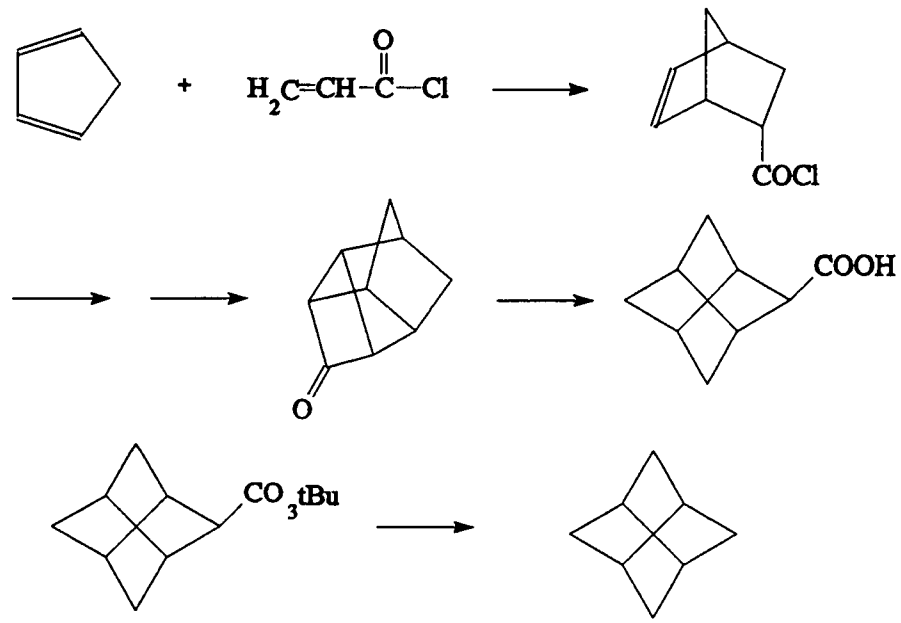

Scheme 12

hydrocarbon bisnoradamantane during aerosol direct fluorination exists due to the ring strain in this system, it is not reasonable to synthesize bisnoradamantane first and then perfluorinate it. An alternative synthesis route to the perfluorinated bisnoradamantane was conceived.

In earlier work Adcock and Luo found that perfluorinated cage ketones easily extrude CO molecules to form carbon-carbon bonds.[23b] Perfluorinated adamantanone under UV irradiation eliminates CO to form F-noradamantane (Scheme 3). We reasoned that if perfluorinated 2,6-adamantanedione could eliminate two CO molecules simultaneously or sequentially, a two-step synthesis of perfluorinated bisnoradamantane will have been achieved starting from the hydrocarbon 2,6-adamantanedione (Scheme 13).

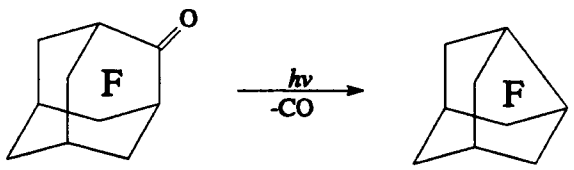

Scheme 3

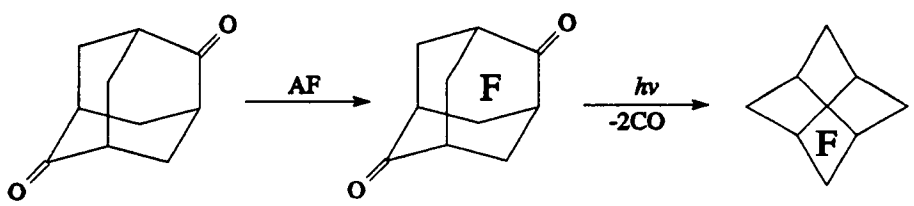

Scheme 13

3.3.2 Perfluorination of 2,6-Adamantanedione

In order to carry out the chemistry of Scheme 13, perfluorinated 2,6-adamantanedione must first be synthesized. There are two one-step methods for the synthesis of 2,6-adamantanedione in the literature.[74] The Morat and Rassat method,[74b] using CrO_3/Ac_2O to oxidize adamantanone to form 2,6-adamantanedione (20%) and 5-acetoxyadamantan-2-one (36%), does not give the reported results in our hands; 5-acetoxyadamantane-2-one is the dominant product, and 2,6-adamantanedione occurs in only trace amounts. The method of Geluk and Schlatmann,[74a] however, which starts with adamantane and 20% oleum, easily produces the reported results.

The selection of a co-fluorinating solvent for fluorination of 2,6-adamantanedione depends on the sublimation temperature of 2,6-adamantanedione. A DSC analysis of an unsealed 2,6-adamantanedione sample shows that sublimation begins at about 140 °C. 1,2,3-trichloropropane has a boiling point around 150 °C, and thus it is a compatible co-fluorinating solvent. The solution can then be injected into the aerosol reactor by a syringe pump giving good stoichiometric control.

Four bridgehead hydrogen atoms in 2,6-adamantanedione are severely deactivated by the two carbonyl groups. As a result these bridgehead hydrogen atoms are harder to substitute with fluorine atoms. In an aerosol fluorination reaction normally sufficient to perfluorinate adamantanes (C–H to F_2 ratio of 1:2 to 1:3), the major products isolated are 1,3 and 1,5-dihydryl-F-2,6-adamantanedione. When the fluorine input is doubled, the major product is F-2,6-adamantanedione.

3.3.3 Perfluorinated Tricyclo[3.3.0.$0^{3,7}$]octane

The irradiation of F-2,6-adamantanedione in a $CFCl_3$ solution using a 550 W medium-pressure mercury lamp results in the elimination of CO molecules. The irradiation reaction is monitored by ^{19}F NMR. Both F-2,6-adamantanedione and tricyclo[3.3.0.$0^{3,7}$]octane are highly symmetrical. Only two sets of equivalent fluorine appear in the ^{19}F NMR for each compound. In an earlier report that F-adamantanone eliminates CO to form noradamantane under UV irradiation[23b] (Scheme 3), the formation of noradamantane can be observed in as little as 10 minutes. During the photochemical reaction of F-2,6-adamantanedione, the formation of bisnoradamantane can be observed from the ^{19}F NMR spectrum within 10 minutes of irradiation, as well. After 2 hours irradiation, no F-2,6-adamantanedione can be detected (Figure 12).

The photochemical reaction of F-2,6-adamantanedione is very clean and almost quantitative. Bisnoradamantane has an all five-membered ring system and two twist-boat configurations exist in the structure. Despite the existence of significant ring strain energy, the elimination of two CO molecules from F-2,6-adamantanedione is as uncomplicated as the elimination of one CO molecule from F-2-adamantanone. The most plausible reason is that the four bridgehead carbon atoms are rigidly held in the proper position. After elimination of CO, the formation of a carbon-carbon bond is inevitable. Therefore, the photochemical elimination of CO to form five-membered rings in perfluorinated compounds is a favorable procedure.

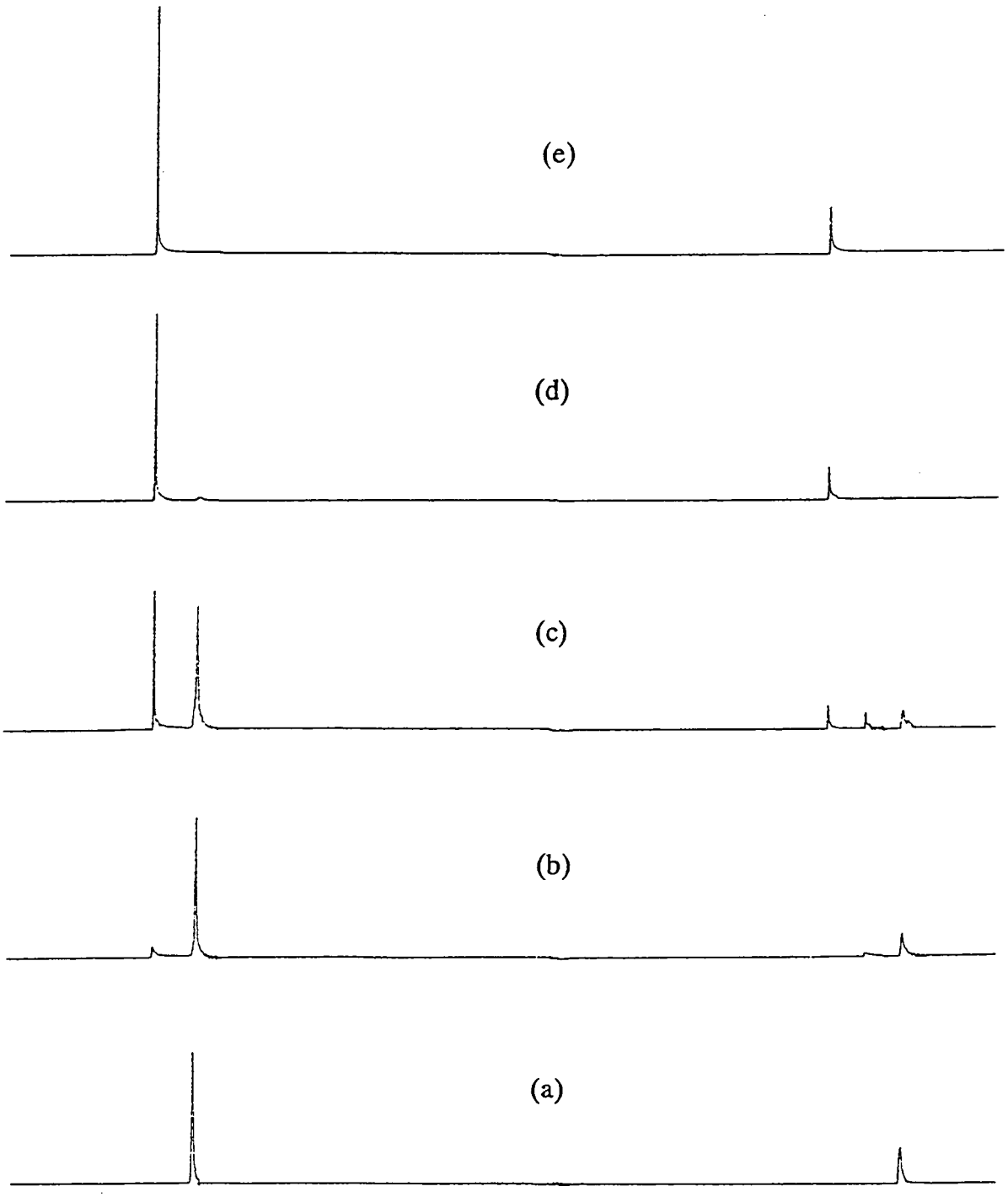

Figure 12 ^{19}F NMR Monitoring Photochemical Reaction of F-Adamantan-2,6-dione with Different Irradiation Time. (a) 0 min (Spectrum of F-Adamantan-2,6-dione); (b) 10 min; (c) 30 min; (d) 80 min; (e) 2 hr. (Spectrum of F-Tricyclo[3.3.0.$0^{3,7}$]octane).

3.3.4 Virtual Coupling in Perfluorinated Cage Compound

Virtual long-range spin-spin coupling was first used to describe proton-proton long-range coupling.[75] Later it was also used to explain fluorine-fluorine long-range coupling in perfluorinated chain compounds.[76] The general concept is that in an AA'X system, nucleus X, although coupled to only one of the AA' nuclei, appears to be coupled to both. The X nucleus appears to "see" the combined spin states of A and A'. The splitting pattern of X in NMR will be a triplet. We find that the virtual coupling is also observed in highly symmetric perfluorinated cage compounds.

The ^{19}F NMR spectrum of F-bisnoradamantane has a unique splitting pattern. The bridgehead fluorine peak appear as 9-line multiplet, and the methylene fluorine peak is a quintet. These phenomena can only be explained as a result of virtual long-range coupling. In polyfluorinated or perfluorinated compounds, the fluorine-fluorine long range coupling is usually stronger than short range couplings. The vicinal fluorine coupling constant, ^3J, is usually near-zero.[77] It has been assumed that the near-zero coupling of vicinal fluorines is caused by the restricted rotation of the carbon-carbon bond.[78] In F-bisnoradamantane (Structure 13), all of the ^3J coupling between the bridgehead fluorines and the methylene fluorines on adjacent carbons ($^3J_{Fa-Fb}$ and $^3J_{Fa'-Fa''}$) will have near-zero coupling due to the rigid "cage" structure. However, all the four-bond couplings (including the coupling between Fb−Fa", Fb−Fb', and Fa−Fa') are expected to be strong. In general, if two identical nuclei have the same chemical shifts, no matter how strong they are

coupled to each other, the coupling constants will be zero. In this structure, all the methylene fluorine atoms, which are separated by four bonds, have the same chemical shifts. Therefore, although they are strongly coupled to each other, the coupling constants $^4J_{Fb-Fb'}$ equal zero. The same reasoning is applied to the zero coupling constants $^4J_{Fa-Fa'}$. If two nuclei strongly couple to each other, and the coupling constants equal zero, the net result is that these two nuclei will combine their separated spin states into one set of spin states. Instead of "seeing" two separate nuclei, other nuclei appear to "see" one single nucleus with a set of spin states. Therefore, the methylene fluorine nuclei combine all the spin states; the bridgehead fluorine nuclei appear to couple to a nucleus with eight states of spin angular momentum. As a result, a multiplet of 9 peaks is observed. On the other hand, the methylene fluorine nuclei appear coupled to a nucleus with a four states of spin angular momentum. The result is a quintet peak. The spacing in the quintet is 2.8 Hz. According to Bovey's description, this spacing should be equal to $1/2(^3J_{Fa-Fb}+^4J_{Fb-Fa'})$. Since $^3J_{Fa-Fb}$ is near-zero, $^4J_{Fb-Fa'}$ should be 5.6 Hz. The virtual coupling does not exist over short distances. For example, in the ^{13}C NMR spectrum of F-bisnoradamantane, the bridgehead carbon atoms have doublets with unresolved peaks, and the methylene carbon atoms have triplets with unresolved peaks.

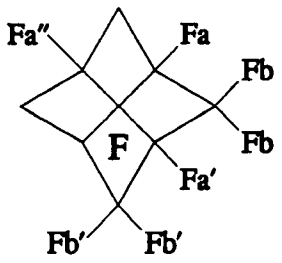

(Structure 13)

3.4 Perfluorinated Cage Orthoesters

3.4.1 Introduction

Orthoesters are compounds with three alkoxyl groups attaching to the same carbon atom (Structure 14). In the orthoester center, the carbon atom bearing three oxygen atoms will exhibit very strong electronic effects due to the high electronegativity of the three oxygen substituents. The tendency to relieve the steric

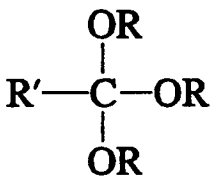

Structure 14

hindrance and high electron density is strong. In many reactions, fragmentation will occur, especially under radical reaction conditions such as occur during aerosol direct fluorination. In earlier work from our laboratory, perfluorination of acyclic orthoesters always resulted in an extensive beta-scission.[21] However, in this work

aerosol fluorination of cage orthoesters, results in the perfluorinated cage orthoesters as the predominant products.

Spin-spin coupling between various nuclei and the factors that influence this phenomenon are of continuing research interest. There are several papers[79] reporting ^{13}C NMR spectra and the corresponding J_{C-F} coupling constants values of monofluorinated compounds in the literature. However, few examples of ^{13}C NMR spectra and the corresponding J_{C-F} coupling constant values for polyfluorinated and perfluorinated compounds are found in the literature. This absence of data in part is due to the limited availability of these compounds but is principally due to the technical challenge of interpreting the NMR spectra. Because the coupling constant $^{1}J_{C-F}$ value is large compared to the chemical shift differences of polyfluorinated and perfluorinated compounds, the ^{13}C NMR spectra usually appear very complicated and are difficult to interpret. In contrast, the ^{13}C NMR spectra and coupling constant J_{C-F} values of the perfluorinated orthoesters (compounds 13 through 17) are relatively easy to interpret due to the high symmetry of these compounds.

3.4.2 Perfluorination of Cage Orthoesters

The precursor cage orthoesters in this study are 4-methyl-2,6,-7-trioxabicyclo[2.2.2]octane (compound 13), 1,4-dimethyl-2,6,7-trioxabicyclo[2.2.2]octane (compound 14), 1-ethyl-4-methyl-2,6,7-trioxabicyclo[2.2.2] octane (compound 15), 2,4,10-trioxaadamantane (compound 16), and 1-methyl-2,4,10-trioxaadamantane (compound 17).

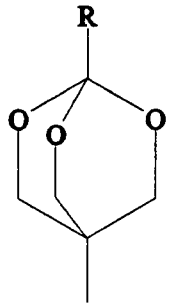

13: R = H

14: R = CH_3

15: R = CH_2CH_3

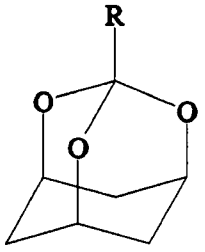

16: R = H

17: R = CH_3

Compounds 13, 14 and 15 were prepared following the method of Doering and Levy.[35] Compounds 16 and 17 were prepared following the method of Bohlman and Sucrow.[37] Of the perfluorinated analogues of compounds 13 through 17, only perfluorinated 14 has been previously reported. Talbott[80] reported a fluorination procedure which produced 1,4-bis(trifluoromethyl)-2,6,7-trioxa-perfluoro-bicyclo[2.2.2]octane (compound 14') from 4-methyl-1-trifluoromethyl-2,6,7-tri-oxabicyclo[2.2.2]octane. No reason was given why the corresponding hydrocarbon 1,4-dimethyl-2,6,7-trioxabicyclo[2.2.2]octane was not a good precursor. In our work, starting materials for fluorination are the corresponding trioxahydrocarbons (compounds 13 through 17). The aerosol fluorination reactions were carried out uneventfully. Although all starting materials are easily sublimed, liquid injection of a 1,1,2-trichloro-ethane solution to introduce samples was chosen so the H:F ratio could more easily be controlled. The major products of each fluorination reaction were the perfluorinated analogues of compounds 13 through 17 (13' through 17') (Schemes 14, 15).

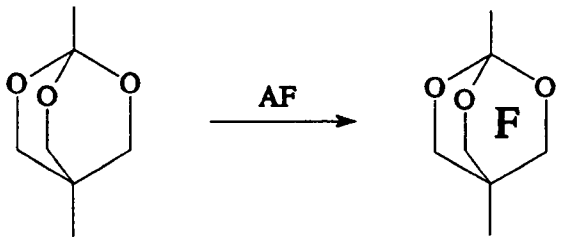

Scheme 14

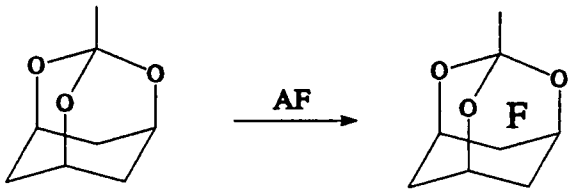

Scheme 15

Aerosol direct fluorination of acyclic orthoesters results in extensive β-scission. The initiation of β-scission occurs on hydrogen-abstraction by fluorine, under free-radical conditions. Mckelvey has given a possible mechanism for this type of hydrogen-abstraction reaction.[81] Mckelvey studied the reaction of 2-methoxy-4-methyltetrahydropyran (Structure 15). Both cis- and trans- isomers will undergo hydrogen abstraction reactions under photochemical excitation. In both structures,

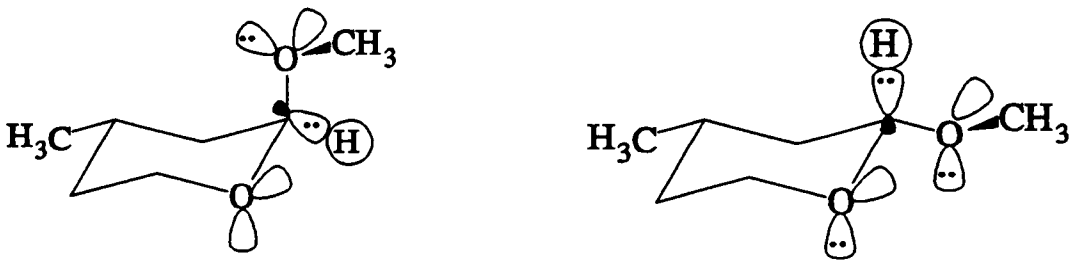

trans *cis*

Structure 15

there is at least one nonbonding orbital on oxygen which is antiperiplanar to the C–H bond being broken. The non-bonding electron pair on oxygen assists the breaking of the C–H bond. The cis-isomer has greater reactivity than the trans-isomer because it has two nonbonding orbitals that are antiperiplanar to the C–H bond. A possible mechanism for the β-scission of acyclic orthoesters is illustrated in Scheme 16. Free rotation about the chain system will allow a nonbonding orbital on oxygen to be antiperiplanar to the C–H bond being broken. Therefore, hydrogen abstraction on one methoxyl carbon is favorable. A rearrangement results in formation of a radical on the center carbon of the orthoester by breaking a beta bond and eliminating OCH_2. The newly formed radical center on the carbon atom bearing two alkoxyl groups is stabilized. Thus the steric strain is released, and a carbon radical with lower electron density can be stabilized by the two electron rich alkoxyl groups. This occurs because in the chain system, all bonds are free to rotate, and rotation of the C–O bond can place the oxygen's lone-pair electron orbital parallel to the radical orbital on the carbon atom resulting in a more stabilized carbon radical.

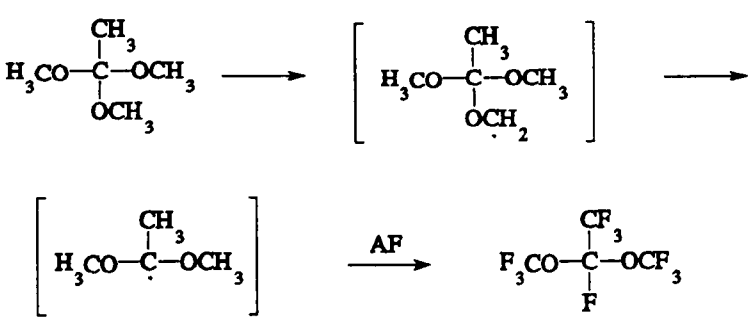

Scheme 16

In contrast to the acyclic orthoesters, successful perfluorination of cage orthoesters is achieved without significant beta scission. In cage orthoesters (Structure 16 and 17), all atoms are held in a rigid system. No free bond rotation is allowed. The orientation of the nonbonding orbitals on oxygen can not be antiperiplanar to any C–H bond being broken. The possibility of oxygen-assisted hydrogen abstraction is severely limited by the rigid structures. Even if the hydrogen abstraction does occur without the assistance of a non-bonding electron pair on oxygen, the radical orbital on the carbon cannot be anti-periplanar to any nonbonding orbital on oxygen. Consequently, the carbon radical can not be stabilized.

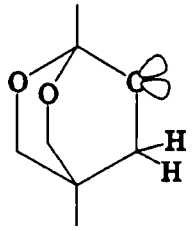

Structure 16

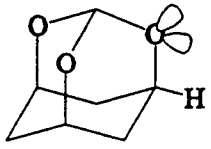

Structure 17

3.4.3 ^{13}C NMR and ^{19}F NMR

The ^{19}F NMR spectra of compounds 13', 14' and 15' (Table 14) are simple due to the high symmetry of these molecules. At position 3, 5 and 8 in each of the three compounds, the fluorine atom peaks are split by the trifluoromethyl group at position 9. The result is a set of quartet peaks with coupling constant J = 9.2 Hz. On the other hand, the trifluoromethyl group resonance is split into a septet. In

compound 13', fluorine atoms at position 1 show through-space spin-spin coupling with fluorine atoms at positions 3, 5 and 8. The fluorine atom resonance at position 1 is split into a septet with a coupling constant J = 2.4 Hz. The resonance of fluorine atoms at position 3,5 and 8 is split into a quartet of doublet peaks. Tier[82] first observed the AB splitting pattern of axial and equatorial fluorines in perfluorocyclohexane at low temperatures in 1960. Their results showed that the F–F coupling over two bonds were unresolved. In this work, the ^{19}F NMR of compound 16' and compound 17' are more interesting (Table 16). In compound 16', axial and equatorial fluorines at position 6, 8 and 9 have the same chemical shifts and do not exhibit an AB pattern. Interestingly fluorines at position 6, 8 and 9 are split into a quartet by the fluorine atoms at positions 1, 5 and 7. The fluorine atoms

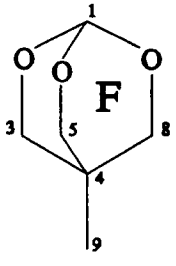

13'

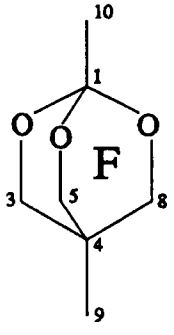

14'

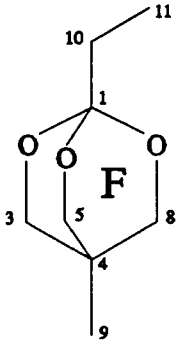

15'

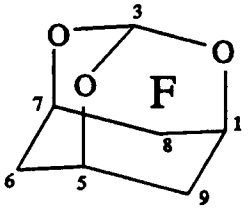

16'

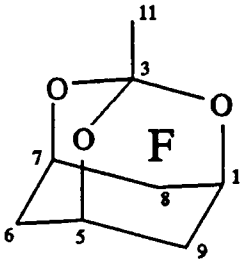

17'

at positions 1, 5 and 7 exhibit a septet with coupling constant J = 9.2 Hz. These multiplicities result from virtual coupling (discussed in 3.3.4).

In contrast, a clear AB splitting pattern is observed in compound 17'. Here axial and equatorial fluorine atoms have different chemical shifts. F_{ax} and F_{eq} couple to each other forming two doublet peaks with coupling constant ^2J = 262.5 Hz. F–F coupling over two bonds is unresolved for methylene fluorine. The three bridge-head fluorine atoms are observed as a septet with coupling constant J = 5.6 Hz.

Unlike the ^{19}F NMR spectra, ^{13}C NMR spectra of perfluorinated compounds are usually difficult to interpret because the coupling constants between C and F are large, giving rise to significant peak overlap. Compounds 13' through 17' have C_{3v} symmetry and the ^{13}C NMR spectra are relatively simple.

Della and coworkers have reported[79a] a series of coupling constant $^1J_{C-F}$ values of bridgehead monofluorinated cage compounds. Their results showed that in unstrained cage compounds, the coupling constants $^1J_{C-F}$ were around 180 Hz. In highly strained cage compounds, $^1J_{C-F}$ could rise to 330 Hz. The strain energies in compounds 13' through 17' are relatively low due to the unstrained adamantane and bicyclo[2.2.2] structures. However, the $^1J_{C-F}$ values of compounds 13' through 17' are relatively high, ranging from 260 to 280 Hz. The $^2J_{C-F}$ values are also higher than the $^2J_{C-F}$ values in the monofluorinated compounds (Tables 15 and 17). It has been suggested[79a] that the magnitude of the vicinal coupling constant $^3J_{C-F}$ is a function of the dihedral angle. In compound 13', the dihedral angle between C_1-O and C_3-F bonds is 120°. Therefore, the ^{13}C NMR spectrum of compound 13' has a

Table 14 ^{19}F NMR Chemical Shift (in ppm) and Coupling Constants (in Hz) of 13'-15' ($CFCl_3$ as Reference).

compd.	1	3,5,8	9	10	11
13'	-85.7 (sep) J=2.4	-71.6 (q-d) J_1=9.2 J_2=2.4	-62.8 (sep) J=9.2		
14'		-70.3 (q) J=9.2	-62.4 (sep) J=9.2	-84.9 (s)	
15'		-70.4 (q) J=9.2	-62.3 (sep) J=9.2	-128.6 (s)	-80.6 (s)

Table 15 ^{13}C NMR Chemical Shift (in ppm) and Coupling Constant (in Hz) of 13'-15'($CDCl_3$ as Reference).

comp	1	3,5,8	4	9	10	11
13'	116.8 (d-sep) ^{1}J=235.1 ^{3}J=3.1	116.4 (t)* ^{1}J=289.2	55.1 AB_6C_3 pattern	118.7 (q-sep) ^{1}J=282.9 ^{3}J=1.9		
14'	105.7 (q-sep) ^{2}J=41.5 ^{3}J=1.4	116.7 (t-q) ^{1}J=289.4 ^{3}J=1.9	55.2 AB_6C_3 pattern	118.9 (q-sep) ^{1}J=279.4 ^{3}J=1.9	115.9 (q) ^{1}J=282.8	
15'	106.8 (t)** ^{2}J=30.4	116.4 (t-q) ^{1}J=282.9 ^{3}J=1.9	55.4 AB_6C_3 pattern	118.7 (q-sep) ^{1}J=282.9 ^{3}J=1.9	106.3 (t-q) ^{1}J=267.3 ^{2}J=39.5	117.0 (q-t) ^{1}J=286.1 ^{2}J=32.3

* triplet with unresolved peaks.
** triplet with unresolved peaks.

Table 16 ^{19}F NMR Chemical Shift (in ppm) and Coupling Constant (in Hz) of 16' and 17' ($CFCl_3$ as Reference).

compd.	1,5,7	6,8,9	3	11
16'	−165.7 (sep-d) J_1=9.2 J_2=1.5	−138.8 (q) J=9.2	−83.0 (q) J=1.5	
17'	−162.8 (sep) J=5.6	−136.3 AB pattern (2−d) ^2J=262.5		−84.1 (s)

Table 17 ^{13}C NMR Chemical Shift (in ppm) and Coupling Constant (in Hz) of 16' and 17' ($CDCl_3$ as Reference).

compd.	3	1,5,7	6,8,9	11
16'	115.7 (d−q) ^1J=236.5 ^3J=9.1	101.6 (d)* ^1J=269.0	107.3 (t−t)** ^1J=274.7 ^2J=21.1	
17'	105.3 (q−q) ^2J=42.0 ^3J=5.7	102.1 (d−quin)*** ^1J=271.8 ^2J=19.1	107.1 (t−t)** ^1J=276.1 ^2J=20.0	116.0 (q) ^1J=283.7

* doublet with unresolved peaks.
** triplet−triplet with unresolved peaks.
*** doublet-quintet with unresolved peaks.

smaller $^3J_{C-F}$ (3.1 Hz) at C_1. In compound 16', C_3-O is antiperiplanar to the C_1-F bond (180°), thus C_3 has a larger $^3J_{C-F}$ value (9.1 Hz). In compounds 16' and 17', the coupling constants $^3J_{C3-F}$ decrease from 9.1 Hz to 5.7 Hz when CF_3 is substituted for F on C_3.

3.5 Reduction and Oxidation at the Bridgehead of 1-Substituted F-Adamantanes

3.5.1 Introduction

The C–F bond is the strongest single bond in organic compounds. As a result perfluorinated groups are extremely stable and are difficult to derivatize. In order to study the chemistry of perfluorinated adamantane derivatives, it is important to understand the reactivity of substituents at different positions in the adamantane skeleton, especially at the bridgehead position, which is a tertiary position, and not as many side reaction can occur at this tertiary position.

1-Hydryl-F-adamantane is a good synthon for the synthesis of other F-adamantyl derivatives. The synthesis of 1-hydryl-F-adamantane was achieved in our laboratory several years ago.[38] 1-chloro-F-adamantane was reduced by zinc in dioxane solution, or by tributyltin hydride, or even by photochemical reduction in CH_3OH solution (Scheme 17).

1-Hydryl-F-adamantane easily forms 1-lithio-F-adamantane in the presence of methyllithium.[83] It seems that 1-lithio-F-adamantane is stable at 0°C as long as no other reactive species is present. A series of F-adamantyl compounds can be synthesized by adding corresponding reagents. For example, 1-bromo-F-adamantane

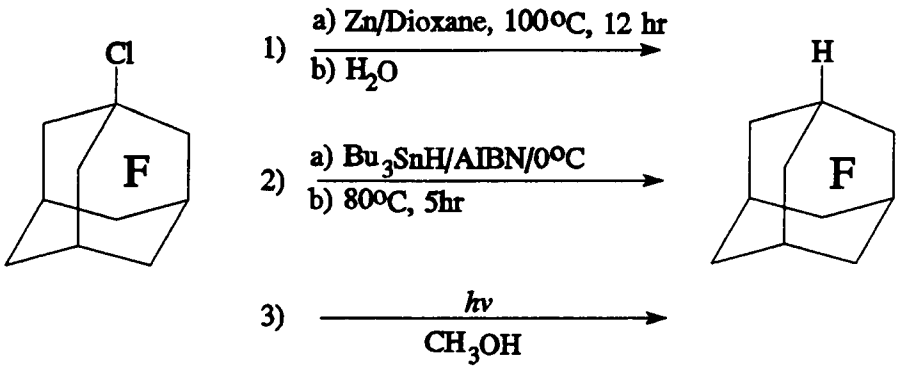

Scheme 17

was obtained by adding bromine; 1-iodo-F-adamantane was obtained by adding iodine; 1-trimethylsilyl-F-adamantane was obtained by adding trimethylchlorosilane (Scheme 18).[83]

The F-adamantyl group is nearly spherical in shape with the fluorine atoms around it. Due to the strong electron withdrawing effect of the fluorine atoms, the negative charge of the F-adamantyl anion can by delocalized over the spherical surface. Secondly, elimination of F^- to form bridgehead olefins is unfavorable. Therefore, 1-lithio-F-adamantane is a very stable species. The stability of F-adamantyl anion makes it a useful synthon. By contrast, we conducted the following reactions to examine the potential cationic reactions of this stable moiety.

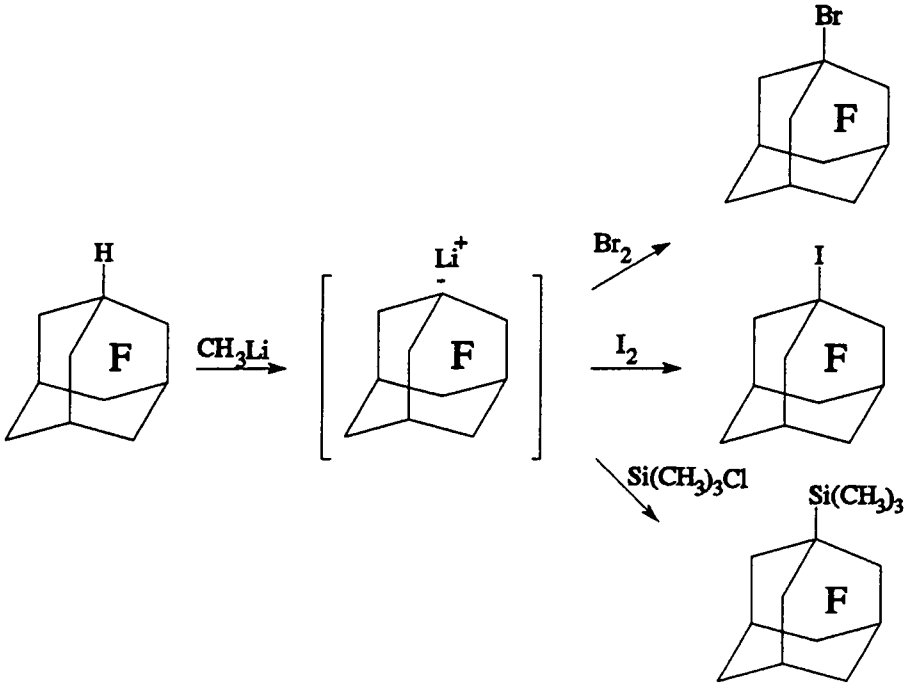

Scheme 18

3.5.2 Oxidation Reaction of 1-Hydryl-F-adamantane

According to the literature, many strong oxidizing reagents can oxidize a tertiary hydrogen to form a tertiary alcohol.[84] In the attempt to synthesize F-adamantan-1-ol, 1-hydryl-F-adamantane was reacted with a series of strong oxidation reagents, such as $CrO_3/Ac_2O/AcOH$, $KMnO_4/OH^-$, HNO_3 (70%), and HNO_3 (fuming, 90%) (Scheme 19).

^{19}F NMR spectra was used to follow the oxidation reactions. In all four reactions, however, only the starting material appeared in the spectra over two days of reaction time. No oxidation products were detected. These results suggest that the oxidation of the C–H bond in 1-hydryl-F-adamantane is unlikely to occur under

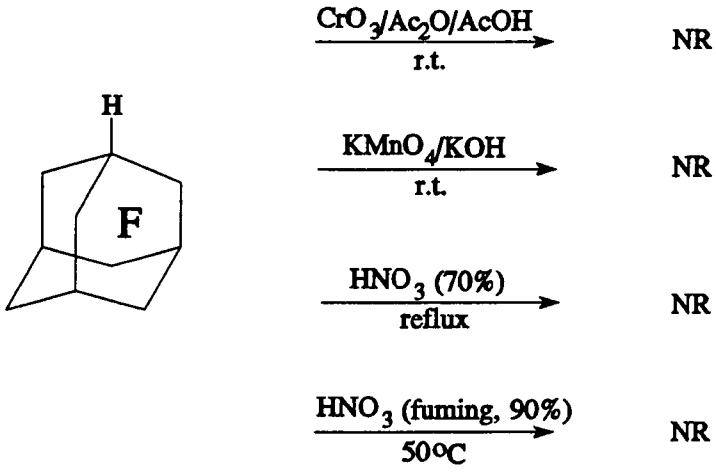

Scheme 19

normal strong oxidation conditions.

3.5.3 Novel Hydrolysis Reaction of F-Adamantyl Chlorides

Alkyl chlorides can be easily hydrolyzed to form alcohols in basic aqueous solution. In the attempt to carry out this hydrolysis reaction, 1-chloro-F-adamantane in benzene solution was added to a potassium hydroxide aqueous solution with catalytic amount of 18-crown-6. The reaction mixture was heated to 120°C for 48 hours. Instead of the hydrolysis product, 1-hydryl-F-adamantane was obtained as the only product (Scheme 20).

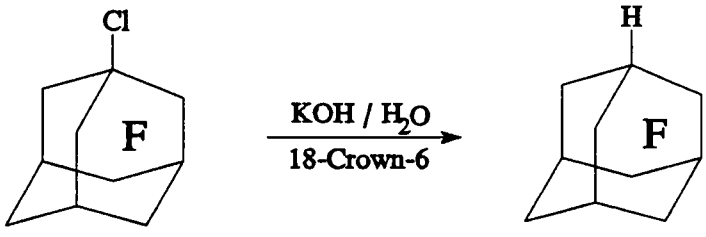

Scheme 20

When the reaction mixture was heated to 80°C, only the starting material was obtained. If 18-crown-6 is not utilized, only starting material was obtained. However, if tetraethylene glycol dimethyl was used as solvent, 1-hydryl-F-adamantane is obtained without the use of 18-crown-6. In all cases, if no potassium hydroxide was used, no reaction occurred. When 1,3,5-trichloro-F-adamantane was used in the hydrolysis reaction under the same conditions, 1,3,5-trihydryl-F-adamantane was obtained after 5 days.

These results suggest that the hydrolysis is an anionic reaction. Because of the high stability of the F-adamantyl anion, it is impossible to have a chloride anion as a leaving group. Here chlorine is acting as an electrophile. The hydroxyl group attacks the chlorine and chlorine loses a pair of electrons to the F-adamantyl. The F-adamantyl anion captures a proton from water to form 1-hydryl-F-adamantane.

Based on the results from sections 3.4.2 and 3.4.3, we can conclude that the F-adamantyl group is an extremely strong electron withdrawing group. The F-adamantane cation reactions are unlikely to occur under normal reaction conditions.

3.5.4 Synthesis of 5-Hydryl-F-adamantan-2-one

In an attempt to reduce 5-chloro-F-adamantan-2-one in our laboratory,[40] the reduction methods that were used to reduce 1-chloro-F-adamantane were applied to 5-chloro-F-adamantane. None of the reduction methods including tributyltin hydride,[40] photochemical reduction,[40] and KOH/H_2O/18-crown-6 produced the

reduced product, 5-hydryl-F-adamantan-2-one. None of these three reagents are particularly strong reduction reagents. Because the hydrogen can not be easily oxidized as shown previously, we decide to use a strong reducing reagent, $LiAlH_4$ to reduce both the carbonyl to hydroxyl and the chlorine to hydrogen, and then to oxidize the hydroxyl group back to the carbonyl group (Scheme 21).

The reaction was simple and the final product, 5-hydryl-F-adamantan-2-one

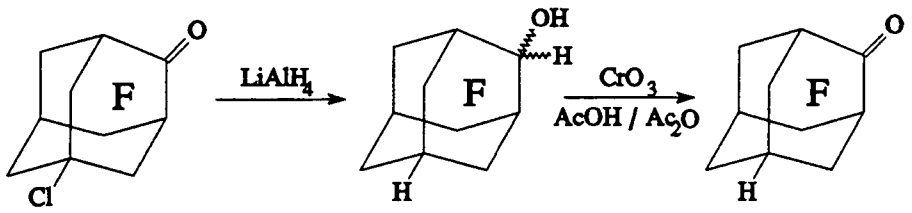

Scheme 21

was produced in fairly good yield. The reduction of 5-chloro-F-adamantane by $LiAlH_4$ forms a pair of isomers, E,Z-2,5-dihydryl-F-adamantan-2-ol. Preparative GC could not separate these two isomer. The ^{19}F NMR spectrum shows two sets of bridgehead fluorines (Figure 13, Structure 18). The small peak on the left side

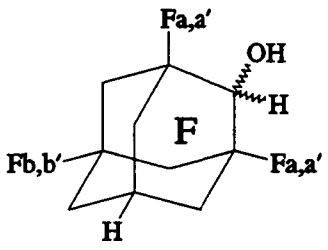

Structure 18

belongs to impurity. Fa and Fb belong to the Z isomer and Fa'and Fb' belong to the

E isomer. 15 minutes after addition of the oxidation reagent, 5-hydryl-F-adamantan-2-one is formed quantitatively. 5-Hydryl-F-adamantan-2-one is an achiral compound, therefore, the ^{19}F NMR coalesces; the bridgehead fluorine now has only one set of fluorine resonance. The interesting observation is that the two isomer are in about 40:60 ratio rather than in 50:50 ratio. Both the starting material and the reducing reagent are achiral compounds. However, the products are chiral compounds. There must be a preferential mode (*syn* or *anti)* for delivery of hydride to the carbonyl group (Structure 19). The stereo effect is not the major role in this molecule since chlorine is not a bulky atom and it is located at the γ position of the carbonyl group. Instead, hyperconjugative stabilization is the major reason for the preference of the hydride delivery. Further investigation is continuing in Professor le Noble's laboratory at the State University of New York, Stony Brook.[39]

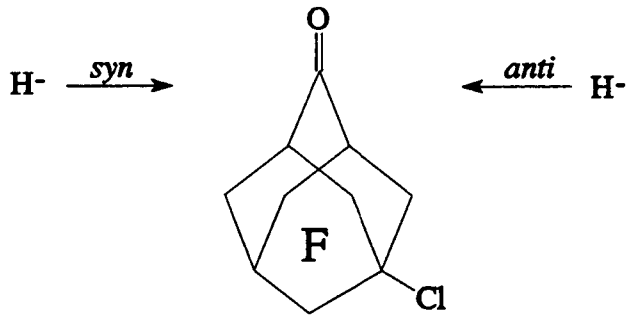

Structure 19

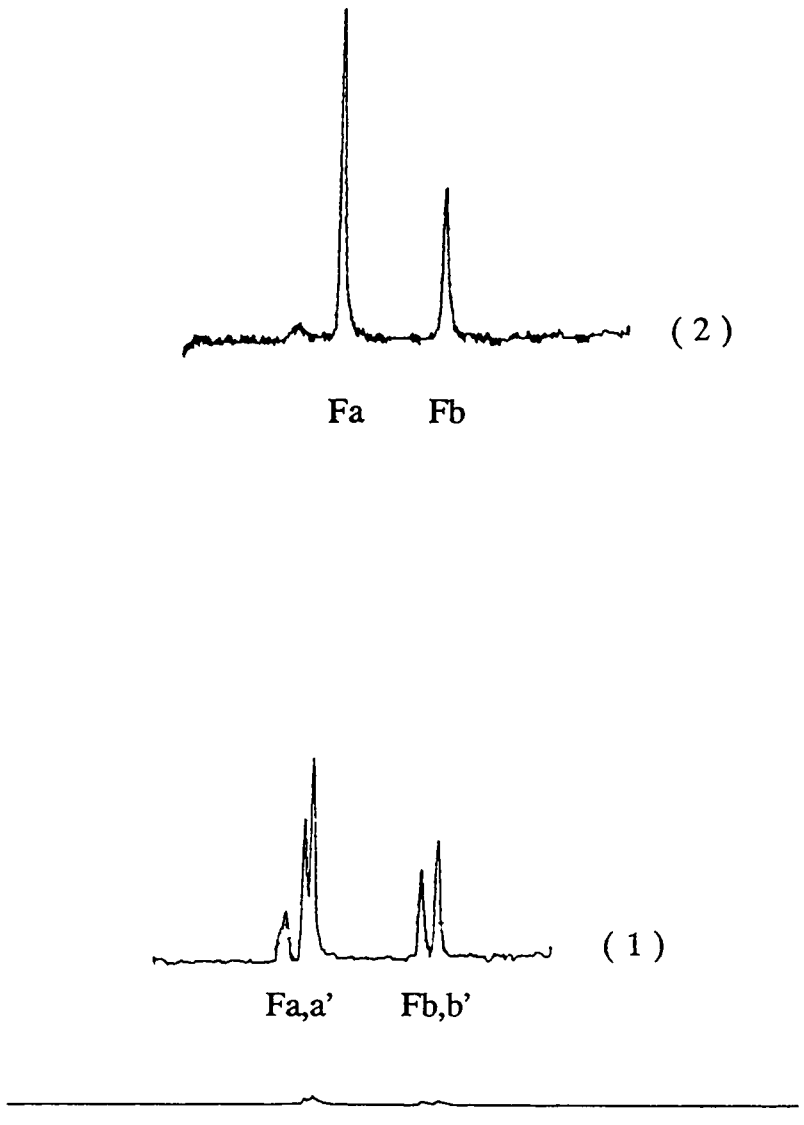

Figure 13 ^{19}F NMR Spectra of E,Z-2,5-Dihydryl-F-adamantan-2-ol and 5-Hydryl-F-adamantan-2-one

REFERENCES

References

1. Pauling, L. "*The Nature of the Chemical Bond*", 3d ed., Cornell Univ. Press, Ithaca, N.Y., **1960.**

2. Smart, B. "*Chemistry of Functional Group, Supplement D, The Chemistry of Halides, Pseudohalides and Azides*"; Patai, S; Rapoport, Z. Eds.; J. Wiley; New York, NY, **1983**, p.603-655.

3. Bondi, A. *J. Phys. Chem.*, **1964**, *68*, 443.

4. Kortum, G.; Vogel, W.; Andrussow, K. "*Dissociation Constants of Organic Acids in Aqueous Solution*", Butterworths, London, **1961.**

5. Sharts, C. M. *J. Chem. Ed.*, **1968**, *45*, 185.

6. Lagow, R. J.; Margrave, J. L. "*Progress in Inorganic Chemistry*", Lippard, S. J., Ed; Wiley: New York, **1979**; *Vol. 26*, p161.

7. Burford, W. B.; Fowler, R. D.; Hamilton, J. M.; Anderson, H. C.; Weber, C. E.; Sweet, R. G. *Ind. Eng. Chem.* **1947**, *39*, 319; Burdon, J.; Knights, J. R.; Parsons, I. W.; Tatlow, J. C., *Tetrahedron*, **1976**, *32*, 1041.

8. Simons, J. H. *U.S. Pat. 2519983*, (**1948**), Minnesota Mining & Manufacturing Co.; *Chem. Abstr.* **1951**, *45*, 51h.

9. March, J. "*Advanced Organic Chemistry*", 4th. John Wiley: New York, **1991.**

10. Bockemuller, W. *Justus Liebigs Am. Chem.*, **1933**, *506*, 20.

11. Calfee, J. D.; Bigelow, L. A. *J. Am. Chem. Soc.* **1937**, *59*, 2072; Fukuhara, N.; Bigelow, L. A. *J. Am. Chem. Soc.* **1941**, *63*, 788.

12. Tyczkowski, E. A.; Bigelow, L. A. *J. Am. Chem. Soc.* **1955**, *77*, 3007.

13. Adcock, J. L.; Horita, K.; Renk, E. B. *J. Am. Chem. Soc.* **1981**, *103*, 6937.

14. Adcock, J. L.; Cherry, M. L. *Ind. Eng. Chem. Res.*, **1987**, *26*, 208.

15. Adcock, J. L.; Cherry M. L. *J. Fluorine Chem.* **1985**, *30*, 343.

16. Shimp, L. A.; Lagow, R. J. *J. Org. Chem.* **1977**, *42*, 3437.

17. Maraschin, N. J.; Catsikis, B. D.; Davis, L. H.; Jarvinen, G.; Lagow, R. J. *J. Am. Chem. Soc.* **1975**, *97*, 513.

18. Adcock, J. L.; Robin, M. L. *J. Org. Chem.* **1983**, *48*, 3128.

19. Adcock, J. L.; Luo, H. *J. Org. Chem.* **1992**, *57*, 2162.

20. Adcock, J. L.; Robin, M. L. *J. Org. Chem.* **1984**, *49*, 191.

21. Adcock, J. L.; Robin, M. L.; Zuberi, S. *J. Fluorine Chem.* **1987**, *37*, 327.

22. Cherry, M. L., Ph.D. Dissertation, The University of Tennessee at Knoxville, **1986**.

23. (a) Adcock, J. L.; Robin, M. L. *J. Org. Chem.* **1983**, *48*, 2437; (b) Adcock, J. L.; Luo, H. *J. Org. Chem.* **1992**, *57*, 4297.

24. Ruff, O.; Pitochelli, A.; Lustig, M. *J. Am. Chem. Soc.* **1966**, *88*, 4531; *J. Am. Chem. Soc.* **1967**, *84*, 2481; Hohorst, F. A.; Shreeve, J. M. *Inorg. Synth.* **1968**, *11*, 143.

25. Adcock, J. L.; Robin, M. L. *J. Org. Chem.* **1984**, *49*, 1442.

26. Adcock, J. L.; Evans, W. D. *J. Org. Chem.* **1984**, *49*, 2719.

27. Adcock, J. L.; Luo, H. *J. Org. Chem.* **1993**, *58*, 1704.

28. Baklan, V. F.; Klil'chevskii, A. N.; Kukhar, V. P. *Zhur. Org. Khim.* **1984**, *20*, 2238.

29. Geluk, H. W.; Schlatmann, J. L. M. A. *Tetrahedron*, **1968**, *24*, 5369.

30. Lunn, W. H. W. *J. Chem. Soc. (C)* **1970**, *16*, 2124.

31. Geluk, H. W.; Schlatmann, J. L. M. A. *Rec. Trav. Chim.* **1971**, *90*, 516.

32. Morat, C.; Rassat, A. *Tetra. Lett.* **1979**, *45*, 4409.

33. Steeter, H.; Krause, M.; Last, W. D. *Chem. Ber.* **1969**, *102*, 3357.

34. Tolstikov, G. A.; Lerman, B. M.; Arefjeva, Z. Y. *Tetra. Lett.* **1972**, *31*, 3191.

35. Doering, W. von.; Levy, L. K. *J. Am. Chem. Soc.* **1955**, *77*, 509.

36. Bertrand, R. D.; Compton, R. D.; Verkade, J. G. *J. Am. Chem. Soc.*, **1970**, *92*, 2702.

37. Bohlmann, F.; Sucrow, W. *Ber.* **1964**, *97*, 1839.

38. Adcock, J. L.; Luo, H. *J. Org. Chem.* **1992**, *57*, 4749.

39. LeNoble, W. and Adcock, J. L., *et al*, to be published.

40. Adcock, J. L.; Luo, H., unpublished result.

41. Luo, H., Ph.D. Dissertation, The University of Tennessee at Knoxville, 1992.

42. Chambers, R. D. "*Fluorine in Organic Chemistry*", John Wiley & Sons, New York, **1973.**

43. Weinmayr, V. *U.S. Pat. 3,317,616*, (1967); *Chem. Abs.* **1967**, *67*,63753.

44. Filler, R.; Schure, R. M. *J. Org. Chem.*, **1967**, *32*, 1217.

45. Knunyants,I. L.; Dyatkin, B. L. *Bull. Acad. Sci., U.S.S.R.*, **1964**, 863.

46. Tamborski, C.; Burton, W. H.; Breed, L. W. *J. Org. Chem.*, **1966**, *31*, 4229.

47. Brenuan, M., Master Thesis, The University of Tennessee at Knoxville, 1987.

48. Adcock, J. L. and Zhang, H., to be published on *J. Org. Chem.*

49. Middleton, W. J.; Lindsey, R. V. *J. Am. Chem. Soc.* **1964**, *86*, 4948.

50. Mentel, T. F.; Luck, W. A. *J. Phys. Chem.* **1991**, *95*, 68; Schriver, L.; Schriver, A.; Peil, S.; Schrems, O. *Can. J. Chem.* **1991**, *69*, 1520; Luck, W. A. P.; Peil, S. *J. Molecular Str.* **1990**, *224*, 175.

51. Jursic, B; Ladika, M.; Sunko, D. E. *Tetra. Lett.* **1985**, *26*, 5323.

52. Schuster; Zundel; Sandorfy "*The Hydrogen Bond*", 3 vols., North Holland Publishing Co., Amsterdam, 1976.

53. Taylor, R.; Kennard, O.; Versichel, W. *J. Am. Chem. Soc.* **1984**, *106*, 244.

54. Glasstone, S. *Trans. Faraday Soc.*, **1937**, *33*, 200.

55. Gordy, W. *J. Chem. Phys.* **1939**, *7*, 136; Stanford, S. C.; Gordy, W. *J. Am. Chem. Soc.*, **1941**, *63*, 1094.

56. Hamilton, W. C.; Ibers, J. A. "*Hydrogen Bonding in Solid*", W. A. Benjamin; New York, 1968.

57. Green, R. D., "*Hydrogen Bonding By C—H Groups*", John Wiley & Sons, New York, 1974.

58. Chuen, L; Sammes, M. *J. Chem. Soc. Perkin Trans. I*, **1983**, 1303.

59. Sammes, M. P.; Harlow, R. L.; Simonsen, S. H. *J. Chem. Soc., Perkin II*, **1976**, 1126; 1130.

60. Slasinski, F. M.; Tustin, J. M.; Sweenet, F. J.; Armstrong, A. M.; Ahmed, Q. A.; Lorand, J. P. *J. Org. Chem.* **1976**, *41*, 2697.

61. Pinchas, S. *Anal. Chem.*, **1955**, *27*, 2.

62. Evans, D. F. *J. Chem. Soc.* **1963**, 5575.

63. Adcock, J. L.; Luo, H.; Zuberi, S. S. *J. Org. Chem.* **1992**, *57*, 4748.

64. (a) Al-Mansour, A. I.; Al-Showiman, S. S.; Al-Najjar, I. M. *Spectrochimica Acta.*, **1988**, *44A*, 643; (b) Burns, R. C.; Devereux, L. A.; Granger, P.; Schrobilgen, G. J. *Inorg. Chem.* **1985**, *24*, 2615; (c) Hogben, M. G.; Graham, W. A. G. *J. Am. Chem. Soc.* **1969**, *91*, 283.

65. Allerhand, A.; Schleyer, P. von R. *J. Am. Chem. Soc.*, **1963**, *85*, 1715.

66. Pinchas, S. *Anal. Chem.*, **1955**, *27*, 2; **1957**, *29*, 334.

67. West, R.; Watley, L. S. *Chem. Ind.*, **1959**, 333.

68. Li, Chuen; Sammes, M. *J. Chem. Soc., Perkin Trans. I*, **1983**, 2193.

69. March, J. "*Advanced Organic Chemistry*", Forth ed., John Wiley & Sons, New York, 1991.

70. Adcock, J. L.; Zhang, H., unpublished result.

71. Adcock, J. L.; Guak, A., unpublished result.

72. Prelog, V.; Siewerth, R. *Ber.*, **1941**, *74*, 1644; Webster, O. W.; Sommer, L. H. *J. Org. Chem.* **1964**, *29*, 3103; Vogt, B. R.; Suter, S. R.; Hoover, J. R. E. *Tetra. Lett.*, **1968**, *13*, 1609.

73. Sauers, R. R.; Kelly, K. W. *J. Org. Chem.* **1970**, *35*, 3286.

74. (a) Geluk, H. W.; Schlatmann, J. L. M. A. *Rec. Trav. Chim.* **1971**, *90*, 516. (b) Morat, C.; Rassat, A. *Tetra. Lett.* **1979**, *45*, 4409.

75. Musher, J. I.; Corey, E. J. *Tetrahedron*, **1962**, *18*, 791.

76. Bovey, F. A. *"Nuclear Magnetic Resonance Spectroscopy"*; Academic Press: San Diego, **1988**, p441.

77. Saika, A.; Gutowsky, H. S. *J. Am. Chem. Soc.* **1956**, *78*, 4814.

78. Crapo, L.; Sederholm, C. H. *J. Chem. Phys,* **1960**, *33*, 1583.

79. (a) Della, E. W.; Cotsaris, E.; Hine, P. T. *J. Am. Chem. Soc.*, **1981**, *103*, 4131; (b) Olah, G. A.; Shih, J. G.; Krishnamurthy, V. V.; Singh, B. P. *J. Am. Chem. Soc.* **1984**, *106*, 4492; (c) Talbott, R. L. *J. Org. Chem.*, **1967**, *32*, 834.

80. Talbott, R. L. *J. Org. Chem.*, **1967**, *32*, 834.

81. Hayday, K.; Mckelvey, R. D. *J. Org. Chem.*, **1976**, *41*, 2222.

82. Tiers, G. V. D. *Proc. Chem. Soc.*, **1960**, 391.

83. Adcock, J. L.; Luo, H. *J. Org. Chem.*, **1993**, *58*, 1999.

84. Carruthers, W. "*Some Modern Methods of Organic Synthesis*", 3rd edition, Cambridge University Press, **1987**.

APPENDICES

APPENDIX 1

Aerosol Direct Fluorination

Parameters

Table 1-1

Aerosol Fluorination of 1-Adamantyl Acetate

Fluorination Parameters		
Fluorine Flows (ml/min)	Module 1-1	8
	Module 1-2	64
	Module 2-1	52
	Module 2-2	6
Helium Diluent Flows (ml/min)	Module 1-1	170
	Module 1-2	170
	Module 2-1	170
	Module 2-2	170
Helium Carrier (ml/min)	Main carrier	760
	Primary hydrocarbon carrier	55
	Secondary hydrocarbon carrier	760
Reaction Temperature (°C)	Module 1-1	−10
	Module 1-2	−2
	Evaporator	110
	Injector	105
Reaction Condition	Hydrogen:Fluorine	1:4
	Injection rate (ml/hr)	1.5
Yield	Hydrocarbon input (g)	2.4
	Product weight (g)	$0.58^{*} + 0.66^{**}$
	Yield (%)	$9.4\%^{*} + 10.3\%^{**}$

* 1-[2-hydryl-F-adamantyl]trifluoroacetate ** 1-F-adamantyl trifluoroacetate

Table 1-2

Aerosol Fluorination of 1,3-Adamantyl Diacetate

Fluorination Parameters		
Fluorine Flows (ml/min)	Module 1-1	8
	Module 1-2	60
	Module 2-1	45
	Module 2-2	7
Helium Diluent Flows (ml/min)	Module 1-1	170
	Module 1-2	170
	Module 2-1	170
	Module 2-2	170
Helium Carrier (ml/min)	Main carrier	760
	Primary hydrocarbon carrier	135
	Secondary hydrocarbon carrier	820
Reaction Temperature (°C)	Module 1-1	−12
	Module 1-2	−4
	Evaporator	162
	Injector	155
Reaction Condition	Hydrogen:Fluorine	1:3.5
	Injection rate (ml/hr)	1.5
Yield	Hydrocarbon input (g)	1.2
	Product weight (g)	0.16
	Yield (%)	6

Table 1-3

Aerosol Fluorination of 2,6-Adamantanedione

Fluorination Parameters		
Fluorine Flows (ml/min)	Module 1-1	8
	Module 1-2	60
	Module 2-1	46
	Module 2-2	7
Helium Diluent Flows (ml/min)	Module 1-1	170
	Module 1-2	170
	Module 2-1	170
	Module 2-2	170
Helium Carrier (ml/min)	Main carrier	760
	Primary hydrocarbon carrier	135
	Secondary hydrocarbon carrier	820
Reaction Temperature (°C)	Module 1-1	-10
	Module 1-2	0
	Evaporator	155
	Injector	160
Reaction Condition	Hydrogen:Fluorine	1:5.3
	Injection rate (ml/hr)	1.0
Yield	Hydrocarbon input (g)	1.0
	Product weight (g)	0.60
	Yield (%)	26

Table 1-4

Aerosol Fluorination of Adamantanone

Fluorination Parameters		
Fluorine Flows (ml/min)	Module 1-1	8
	Module 1-2	58
	Module 2-1	50
	Module 2-2	7
Helium Diluent Flows (ml/min)	Module 1-1	170
	Module 1-2	170
	Module 2-1	170
	Module 2-2	170
Helium Carrier (ml/min)	Main carrier	760
	Primary hydrocarbon carrier	135
	Secondary hydrocarbon carrier	820
Reaction Temperature (°C)	Module 1-1	−11
	Module 1-2	−3
	Evaporator	150
	Injector	155
Reaction Condition	Hydrogen:Fluorine	1:3.5
	Injection rate (ml/hr)	1.5
Yield	Hydrocarbon input (g)	2.8
	Product weight (g)	3.2
	Yield (%)	43

Table 1-5

Aerosol Fluorination of 5-Chloroadamantan-2-one

Fluorination Parameters		
Fluorine Flows (ml/min)	Module 1-1	8
	Module 1-2	62
	Module 2-1	50
	Module 2-2	7
Helium Diluent Flows (ml/min)	Module 1-1	170
	Module 1-2	170
	Module 2-1	170
	Module 2-2	170
Helium Carrier (ml/min)	Main carrier	760
	Primary hydrocarbon carrier	135
	Secondary hydrocarbon carrier	820
Reaction Temperature (°C)	Module 1-1	−10
	Module 1-2	−4
	Evaporator	160
	Injector	155
Reaction Condition	Hydrogen:Fluorine	1:4.0
	Injection rate (ml/hr)	1.5
Yield	Hydrocarbon input (g)	2.7
	Product weight (g)	1.8
	Yield (%)	30

Table 1-6

Aerosol Fluorination of 4-Methyl-2,6,7-trioxabicyclo[2.2.2]octane

Fluorination Parameters		
Fluorine Flows (ml/min)	Module 1-1	8
	Module 1-2	50
	Module 2-1	36
	Module 2-2	6
Helium Diluent Flows (ml/min)	Module 1-1	170
	Module 1-2	170
	Module 2-1	170
	Module 2-2	170
Helium Carrier (ml/min)	Main carrier	760
	Primary hydrocarbon carrier	55
	Secondary hydrocarbon carrier	760
Reaction Temperature (°C)	Module 1-1	−12
	Module 1-2	−3
	Evaporator	115
	Injector	110
Reaction Condition	Hydrogen:Fluorine	1:3.4
	Injection rate (ml/hr)	1.5
Yield	Hydrocarbon input (g)	2.2
	Product weight (g)	0.66
	Yield (%)	13

Table 1-7

Aerosol Fluorination of 1,4-Dimethyl-2,6,7-trioxabicyclo[2.2.2]octane

Fluorination Parameters		
Fluorine Flows (ml/min)	Module 1-1	8
	Module 1-2	50
	Module 2-1	36
	Module 2-2	6
Helium Diluent Flows (ml/min)	Module 1-1	170
	Module 1-2	170
	Module 2-1	170
	Module 2-2	170
Helium Carrier (ml/min)	Main carrier	760
	Primary hydrocarbon carrier	55
	Secondary hydrocarbon carrier	760
Reaction Temperature (°C)	Module 1-1	−10
	Module 1-2	−3
	Evaporator	108
	Injector	108
Reaction Condition	Hydrogen:Fluorine	1:3.0
	Injection rate (ml/hr)	1.5
Yield	Hydrocarbon input (g)	2.1
	Product weight (g)	0.8
	Yield (%)	15

Table 1-8

Aerosol Fluorination of 1-Ethyl-4-methyl-2,6,7-trioxabicyclo[2.2.2]octane

Fluorination Parameters		
Fluorine Flows (ml/min)	Module 1-1	8
	Module 1-2	52
	Module 2-1	40
	Module 2-2	7
Helium Diluent Flows (ml/min)	Module 1-1	170
	Module 1-2	170
	Module 2-1	170
	Module 2-2	170
Helium Carrier (ml/min)	Main carrier	760
	Primary hydrocarbon carrier	55
	Secondary hydrocarbon carrier	760
Reaction Temperature (°C)	Module 1-1	−10
	Module 1-2	−2
	Evaporator	110
	Injector	105
Reaction Condition	Hydrogen:Fluorine	1:3.0
	Injection rate (ml/hr)	1.5
Yield	Hydrocarbon input (g)	2.2
	Product weight (g)	1.1
	Yield (%)	18

Table 1-9

Aerosol Fluorination of 2,4,10-Trioxaadamantane

Fluorination Parameters		
Fluorine Flows (ml/min)	Module 1-1	8
	Module 1-2	48
	Module 2-1	40
	Module 2-2	6
Helium Diluent Flows (ml/min)	Module 1-1	170
	Module 1-2	170
	Module 2-1	170
	Module 2-2	170
Helium Carrier (ml/min)	Main carrier	760
	Primary hydrocarbon carrier	135
	Secondary hydrocarbon carrier	820
Reaction Temperature (°C)	Module 1-1	−12
	Module 1-2	−2
	Evaporator	155
	Injector	150
Reaction Condition	Hydrogen:Fluorine	1:3.4
	Injection rate (ml/hr)	1.5
Yield	Hydrocarbon input (g)	0.82
	Product weight (g)	0.21
	Yield (%)	11

Table 1-10

Aerosol Fluorination of 1-Methyl-2,4,10-trioxaadamantane

Fluorination Parameters		
Fluorine Flows (ml/min)	Module 1-1	8
	Module 1-2	56
	Module 2-1	44
	Module 2-2	6
Helium Diluent Flows (ml/min)	Module 1-1	170
	Module 1-2	170
	Module 2-1	170
	Module 2-2	170
Helium Carrier (ml/min)	Main carrier	760
	Primary hydrocarbon carrier	55
	Secondary hydrocarbon carrier	760
Reaction Temperature (°C)	Module 1-1	−10
	Module 1-2	−2
	Evaporator	115
	Injector	110
Reaction Condition	Hydrogen:Fluorine	1:3.4
	Injection rate (ml/hr)	1.5
Yield	Hydrocarbon input (g)	0.40
	Product weight (g)	0.13
	Yield (%)	14

APPENDIX 2

Characterization of Compounds

Table 2-1

Characterization of 1-F-Adamantyl Trifluoroacetate

Structure	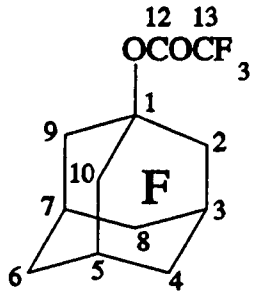				
^{19}F NMR ($CFCl_3$)	label	δ (ppm)	mult.	J (Hz)	integral
	13	−74.4	s		3
	2,9,10	−114.6	s		6
	4,6,8	−121.1	s		6
	3,5,7	−221.7	s		3
IR (film)	ν in cm^{-1} (inten.)				
	1848 (s)				

Table 2-2

Characterization of 1-[2-Hydryl-F-adamantyl] Trifluoroacetate

Structure	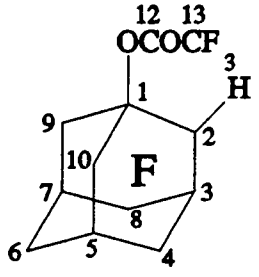				
^{19}F NMR	label	δ (ppm)	mult.	J (Hz)	integral
	13	−74.9	s		3
($CFCl_3$)	4,6,8,9,10	−111.7 to −126.2	unresolved		10
	3	−212.5	s		1
	2,5,7	−221.6 to −223.0	unresolved		3
^{1}H NMR	label	δ (ppm)	mult.	J (Hz)	
($CDCl_3$)	3	6.55	d-q	^{2}J = 46.2 ^{5}J = 6.2	
IR (film)	ν in cm^{-1} (inten.)				
	3021 (w), 1829 (s).				

Table 2-3

Characterization of 1,3-[2-Hydryl-F-adamantyl] Bis-Trifluoroacetate

Structure	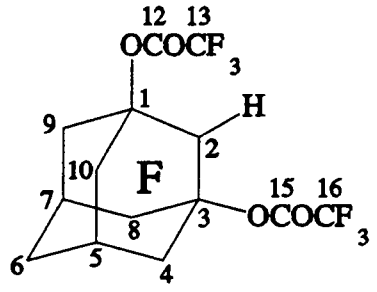				
^{19}F NMR	label	δ (ppm)	mult.	J (Hz)	integral
	13,16	−74.9	s		6
($CFCl_3$)	4,6,8,9,10	−112.0 to −121.3	unresolved		10
	2,5,7	−218.8 to −221.4	unresolved		3
^{1}H NMR	label	δ (ppm)	mult.	J (Hz)	integral
($CDCl_3$)	2	7.70	d-t	^{2}J = 43.5 ^{5}J = 5.8	1
IR (film)	ν in cm^{-1} (inten.)				
	3051 (w), 1832 (w).				

Table 2-4

Characterization of F-2,6-Adamantanedione

Structure	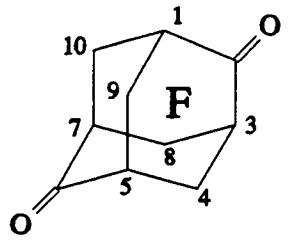				
MS	m/z (inten., indent.)				
	380 (2.8, M^-); 352 (1.8, $M^- - 10$); 341 (2.0, $C_9F_{10}O^-$); 295 (89, $C_9F_9O^-$); 267 (85, $C_8F_9^-$); 248 (100, $C_8F_8^-$).				
^{19}F NMR ($CFCl_3$)	label	δ (ppm)	mult.	J (Hz)	integral
	4,8,9,10	−123.8	s		8
	1,3,5,7	−215.9	s		4
IR (vapor)	ν in cm^{-1} (inten.)				
	1817 (s)				

Table 2-5

Characterization of F-4-Methyl-2,6,7-trioxabicyclo[2.2.2]octane

Structure	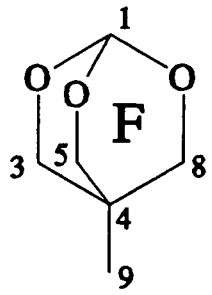				
MS	m/z (inten., indent.)				
	291 (3, $M^+ - F$); 244 (25, $M^+ - OCF_2$); 225 (24, $M^+ - F - OCF_2$); 181 (100, $CF_3CCF_2CF_2$).				
^{19}F NMR ($CFCl_3$)	label	δ (ppm)	mult.	J (Hz)	integral
	1	−85.7	sep	^4J = 2.4	1
	3,5,8	−71.6	q-d	^4J = 9.2 ^4J = 2.4	6
	9	−62.8	sep	^4J = 9.2	3
^{13}C NMR ($CDCl_3$)	label	δ (ppm)	mult.	J (Hz)	
	1	116.8	(d-sep)	^1J = 23.5 ^3J = 3.1	
	3,5,8	116.4	t	^1J = 289.2	
	4	55.1	unsolved		
	9	118.7	q-sep	^1J = 282.9 ^3J = 1.9	
IR (film)	ν in cm^{-1} (inten.)				
	1427 (m), 1245 (s), 1204 (m), 1025 (s), 669 (w).				

Table 2-6

Characterization of F-1,4-Dimethyl-2,6,7-trioxabicyclo[2.2.2]octane

Structure	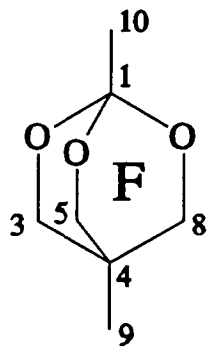				
MS	m/z (inten., indent.)				
	341 (3, $M^+ - F$); 294 (5, $M^+ - OCF_2$); 275 (15, $M^+ - F - OCF_2$); 181 (100, $CF_3CCF_2CF_2$).				
^{19}F NMR ($CFCl_3$)	label	δ (ppm)	mult.	J (Hz)	integral
	3,5,8	−70.3	q	^4J = 9.2	6
	9	−62.4	sep	^4J = 9.2	3
	10	−84.9	s		3
^{13}C NMR ($CDCl_3$)	label	δ (ppm)	mult.	J (Hz)	
	1	105.7	q-sep	^2J = 41.5 ^3J = 1.4	
	3,5,8	116.7	t-q	^1J = 289.4 ^3J = 1.9	
	4	55.2	unresolved		
	9	118.9	q-sep	^1J = 279.4 ^3J = 1.9	
	10	115.9	q	^1J = 282.8	
IR (film)	ν in cm^{-1} (inten.)				
	1337 (s), 1297 (s), 1121 (s), 1022 (s), 985 (m), 816 (w), 764 (w)				

Table 2-7
Characterization of F-1-Ethyl-4-methyl-2,6,7-trioxabicyclo[2.2.2]octane

Structure	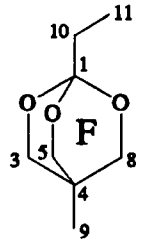				
MS	m/z (inten., indent.)				
	391 (2, M^+-F); 344 (2, M^+-OCF_2); 325 (10, $M^+-F-OCF_2$); 181 (100, $CF_3CCF_2CF_2$).				
^{19}F NMR ($CFCl_3$)	label	δ (ppm)	mult.	J (Hz)	integral
	3,5,8	−70.4	q	^4J = 9.2	6
	9	−62.3	sep	^4J = 9.2	3
	10	−128.6	s		2
	11	−80.6	s		3
^{13}C NMR ($CDCl_3$)	label	δ (ppm)	mult.	J (Hz)	
	1	106.8	t	^2J = 30.4	
	3,5,8	116.4	t-q	^1J = 282.9 ^3J = 1.9	
	4	50.4	unresolved		
	9	118.7	q-sep	^1J = 282.9 ^3J = 1.9	
	10	106.3	t-q	^1J = 267.3 ^2J = 39.5	
	11	117.0	q-t	^1J = 286.1 ^2J = 32.3	
IR (film)	ν in cm^{-1} (inten.)				
	1332 (s), 1296 (s), 1253 (s), 1151 (m), 1030 (s), 908 (m), 814 (m)				

Table 2-8

Characterization of F-2,4,10-Trioxaadamantane

Structure	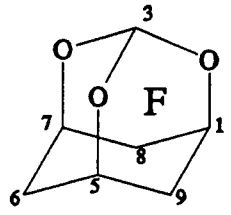				
MS	m/z (inten., indent.)				
	322 (2, M^+); 303 (1, $M^+ - F$); 131 (28, $C_3F_5^+$); 97 (25, $OCCF_3$); 69 (100, CF_3^+).				
^{19}F NMR ($CFCl_3$)	label	δ (ppm)	mult.	J (Hz)	integral
	1,5,7	−165.7	sep-d	J_1 = 9.2 J_2 = 1.5	3
	6,8,9	−138.8	q	J = 9.2	6
	3	−83.0	q	J = 1.5	1
^{13}C NMR ($CDCl_3$)	label	δ (ppm)	mult.	J (Hz)	
	3	115.7	d-q	^1J = 236.5 ^3J = 9.1	
	1,5,7	101.6	d	^1J = 269.0	
	6,8,9	107.3	t-t	^1J = 274.7 ^2J = 21.1	

Table 2-9

Characterization of F-1-Methyl-2,4,10-trioxaadamantane

Structure	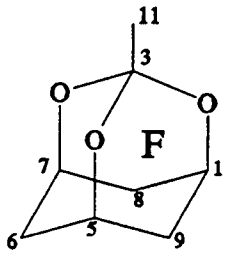				
MS	m/z (inten., indent.)				
	372 (12, M^+); 353 (27, $M^+ - F$); 131 (100, $C_3F_5^+$); 97 (25, $OCCF_3$); 69 (100, CF_3^+).				
^{19}F NMR ($CFCl_3$)	label	δ (ppm)	mult.	J (Hz)	integral
	1,5,7	−162.8	sep	J = 5.6	3
	6,8,9	−136.3	2d	^2J = 262.5	6
	11	−84.1	s		3
^{13}C NMR ($CDCl_3$)	label	δ (ppm)	mult.	J (Hz)	
	3	105.3	q-q	^2J = 42.0 ^3J = 5.7	
	1,5,7	102.1	d-quin	^1J = 271.8 ^2J = 19.1	
	6,8,9	107.1	t-t	^1J = 276.1 ^2J = 20.0	
	11	116.0	q	^1J = 283.7	
IR (film)	ν in cm^{-1} (inten.)				
	1211 (w), 1176 (m), 1118 (m), 1042 (m), 910 (m), 848 (s), 816 (s).				

Table 2-10

Characterization of 1-F-Adamantanol

<table>
<tr><td>Structure</td><td colspan="5"> 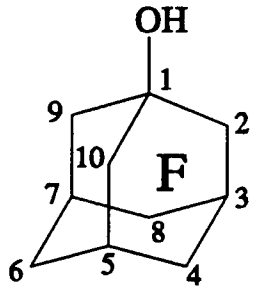
</td></tr>
<tr><td rowspan="2">MS</td><td colspan="5">m/z (inten., indent.)</td></tr>
<tr><td colspan="5">422 (17, M^+); 403 (24, $M^+ - F$); 203 (100, C_6F_6OH).</td></tr>
<tr><td rowspan="3">^{19}F NMR

($CFCl_3$)</td><td>label</td><td>δ (ppm)</td><td>mult.</td><td>J (Hz)</td><td>integral</td></tr>
<tr><td>3,5,7</td><td>−224.3</td><td>s</td><td></td><td>3</td></tr>
<tr><td>2,4,6,8,9,10</td><td>−123.0</td><td>s</td><td></td><td>12</td></tr>
<tr><td rowspan="2">IR
(film)</td><td colspan="5">ν in cm^{-1} (inten.)</td></tr>
<tr><td colspan="5">3410 (w), 3117 (w), 1281 (s)</td></tr>
</table>

Table 2-11

Characterization of 2-Hydryl-F-1-adamantanol

Structure	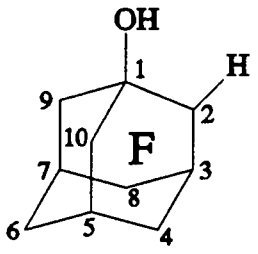				
MS	m/z (inten., indent.)				
	(EI): 404 (63, M^+); 385 (30, $M^+ - F$); 203 (100, C_6F_6OH). (EA): 404 (1, M^-); 403 (3, $M^- - 1$); 384 (100, $M^- - HF$).				
^{19}F NMR	label	δ (ppm)	mult.	J (Hz)	integral
($CFCl_3$)	4,6,8,9,10	−116.4 to −127.1	unresolved		10
	3	−213.7	s		1
	2,5,7	−222.5 to −226.3	unresolved		3
^1H NMR	label	δ (ppm)	mult.	J (Hz)	
($CDCl_3$)	2	5.23	d-q	^2J = 48.2 ^5J = 6.2	
	OH	3.40			
IR (film)	ν in cm^{-1} (inten.)				
	3379 (b), 2994 (w).				
HRMS	formula: calc. (found)				
	$C_{10}H_2F_{14}O$: 403.9882 (403.9874)				

Table 2-12

Characterization of 2-Hydryl-F-adamantan-1,3-diol

Structure	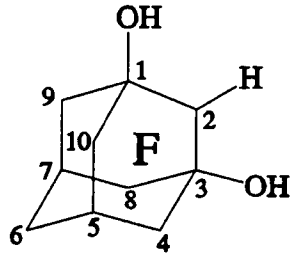				
MS	m/z (inten., indent.)				
	402 (40, M^+); 383 (12, $M^+ - F$); 69 (100, CF_3).				
^{19}F NMR	label	δ (ppm)	mult.	J (Hz)	integral
	4,6,8,9,10	−120.3 to −123.9	unresolved		10
($CFCl_3$)	2,5,7	−221.9 to −225.7	unresolved		3
^1H NMR	label	δ (ppm)	mult.	J (Hz)	integral
($CDCl_3$)	2	5.02	d-t	^2J = 47.9 ^5J = 6.3	1
	OH	3.85			
IR (film)	ν in cm^{-1} (inten.)				
	3385 (b), 2970 (w).				
HRMS	formula: calc. (found)				
	$C_{10}H_3F_{13}O_2$: 401.9926 (403.9919)				

Table 2-13

Characterization of 2-Hydryl-F-adamantan-2-ol

Structure	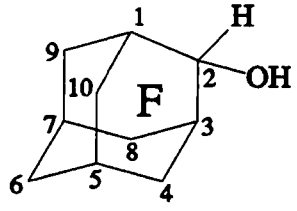				
MS	m/z (inten., indent.)				
	404 (1, M^+); 402 (13, M^+-2H); 383 (7, M^+-2H-F); 205 (100, $C_6F_7^+$).				
^{19}F NMR ($CFCl_3$)	label	δ (ppm)	mult.	J (Hz)	integral
	4,6,8,9,10	−115.0 to −126.3	unresolved		10
	1,3	−214.4	s		2
	5	−223.4	s		1
	7	−224.6	s		1
^1H NMR ($CDCl_3$)	label	δ (ppm)	mult.	J (Hz)	integral
	2	4.90	q	^5J = 6.1	1
	OH	3.3			
IR (film)	ν in cm^{-1} (inten.)				
	3500 (b), 2999 (w).				

Table 2-14

Characterization of 1-F-Adamantyl Acetate

Structure	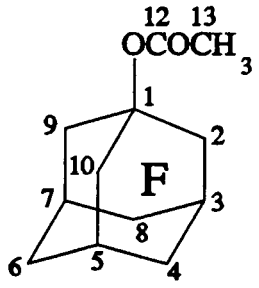				
^{19}F NMR ($CFCl_3$)	label	δ (ppm)	mult.	J (Hz)	integral
	2,9,10	−114.7	s		6
	4,6,8	−121.3	s		6
	3,5,7	−221.8	s		3
^{1}H NMR ($CDCl_3$)	label	δ (ppm)	mult.	J (Hz)	integral
	13	2.34	s		3

Table 2-15

Characterization of 1-[2-Hydryl-F-adamantyl] Acetate

Structure	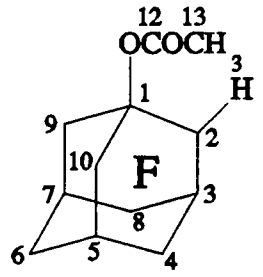				
MS	m/z (inten., indent.)				
	446 (18, M^+); 427 (14, $M^+ - F$); 386 (9, $M^+ - CH_3COOH$); 371 (11, $C_9F_{13}O$); 324 (38, C_8F_{12}); 309 (100, $C_7F_{11}O$).				
^{19}F NMR ($CFCl_3$)	label	δ (ppm)	mult.	J (Hz)	integral
	4,6,8,9,10	−111.8 to −126.6	unresolved		10
	3	−212.5	s		1
	2,5,7	−223.3 to −223.1	unresolved		3
^1H NMR ($CDCl_3$)	label	δ (ppm)	mult.	J (Hz)	integral
	13	2.32	s		3
	2	6.69	d-q	^2J = 45.9 ^5J = 6.4	1
IR (film)	ν in cm^{-1} (inten.)				
	3025 (w), 2966 (w), 2932 (w), 2870 (w), 1800 (s).				

Table 2-16

Characterization of 2-[2-Hydryl-F-adamantyl] Acetate

Structure	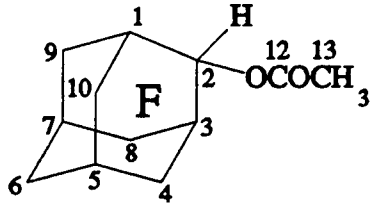				
MS	m/z (inten., indent.)				
	446 (12, M^+); 386 (18, $M^+ - CH_3COOH$); 371 (27, $C_9F_{13}O$); 324 (24, C_8F_{12}); 309 (71, $C_7F_{11}O$); 137 (100, $C_2F_5OH_2$)				
^{19}F NMR ($CFCl_3$)	label	δ (ppm)	mult.	J (Hz)	integral
	4,6,8,9,10	−116.6 to −126.7	unresolved		10
	1,3	−213.9	s		2
	7	−223.3	s		1
	5	−224.7	s		1
^1H NMR ($CDCl_3$)	label	δ (ppm)	mult.	J (Hz)	integral
	13	2.25	s		3
	2	6.29	quin	^5J = 5.6	1
IR (film)	ν in cm^{-1} (inten.)				
	2970 (m), 2866 (w), 1798 (s).				

Table 2-17

Characterization of 1-[2-Hydryl-F-adamantyl] Benzoate

Structure	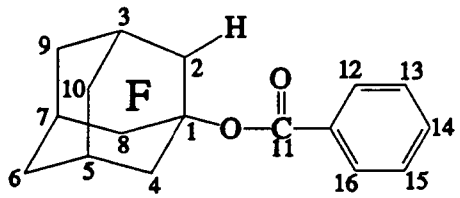				
MS	m/z (inten., indent.)				
	508 (7, M^+), 489 (2, M^+-F), 105 (97, $PhCO^+$)				
^{19}F NMR	label	δ (ppm)	mult.	J (Hz)	integral
	4,6,8,9,10	−111.3 ~ −126.0	unresolved		10
($CFCl_3$)	3	−212.0	s		1
	2,5,7	−221.8 ~ −222.5	unresolved		3
^1H NMR	label	δ (ppm)	mult.	J (Hz)	
($CDCl_3$)	2	6.90	d-q	^2J = 45.5 ^5J = 6.5	1
	12,16	8.08	d	J = 7.8	2
	4	7.63	t	J = 7.4	1
	13,15	7.48	t	J = 7.8	2
IR (film)	ν in cm^{-1} (inten.)				
	3021 (w), 1763 (s), 1597 (m), 1450 (m)				

Table 2-18

Characterization of 1-[2-Hydryl-F-Adamantyl] Methylsulfonate

Structure	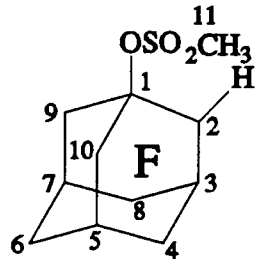				
^{19}F NMR ($CFCl_3$)	label	δ (ppm)	mult.	J (Hz)	integral
	4,6,8,9,10	−111.6 ~ −126.4	unresolved		10
	3	−212.5	s		1
	2	−218.9	unresolved		1
	7	−222.0	sep	J = 12.2	1
	5	−222.7	sep	J = 12.2	1
^{1}H NMR ($CDCl_3$)	label	δ (ppm)	mult.	J (Hz)	
	2	6.28	d-q	^{2}J = 45.9 ^{5}J = 6.2	1
	11	3.40	s		3
IR (film)	ν in cm^{-1} (inten.)				
	3017 (w), 2939 (w), 1389 (m), 1339 (m), 1226 (s)				

Table 2-19

Characterization of 1,3-[2-Hydryl-F-adamantyl] Bis-benzoate

Structure	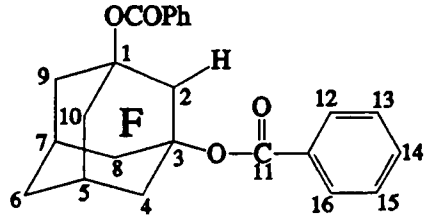				
MS	m/z (inten., indent.)				
	610 (49, M^+), 591 (8, $M^+ - F$), 488 (3, $M^+ - PhCO_2H$), 105 (100, $PhCO^+$)				
^{19}F NMR	label	δ (ppm)	mult.	J (Hz)	integral
	4,6,8,9,10	−112.5 ~ −122.1	unresolved		0
($CFCl_3$)	2	−219.9	unresolved		1
	5,7	−221.8	sep	J = 12.2	2
^1H NMR	label	δ (ppm)	mult.	J (Hz)	integral
($CDCl_3$)	2	8.31	d-t	^2J = 42.3 ^5J = 6.1	1
	12,12',16,16'	8.11	d	J = 7.2	4
	14,14'	7.69	t	J = 7.4	2
	13,13',15,15'	7.52	t	J = 7.4	4
IR (film)	ν in cm^{-1} (inten.)				
	3066 (w), 1763 (s), 1597 (m), 1451 (m)				

Table 2-20

Characterization of F-Tricyclo[3.3.0.0^{3,7}]octane

Structure	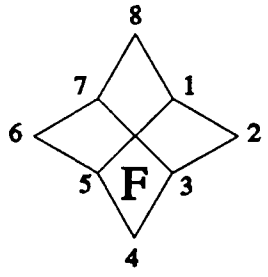				
MS	m/z (inten., indent.)				
	324 (70, M^-); 305 (27, $M^- - F$); 255 (53, C_7F_9); 205 (100, C_6F_7).				
^{19}F NMR ($CFCl_3$)	label	δ (ppm)	mult.	J (Hz)	integral
	2,4,6,8	−118.1	quin	^4J = 5.6	8
	1,3,5,7	−206.0	nonet	^4J = 5.6	4
Elemental Analysis	formula: calc. (found)				
	C: 29.65% (29.76%); F: 70.35% (70.13%).				

VITA

Huqiu Zhang had her all pre-college education in Shanghai, China. She got her BS degree in 1984 and MS degree in 1987 in Chemistry Department at Fudan University, Shanghai, China. She then worked at Fudan University as a teaching associate from 1987 to 1989. She moved to The United States in May, 1989. In 1990, she accepted a part time job as a research assistant in the Department of Chemistry, the University of Tennessee at Knoxville. She entered the graduate school of the University of Tennessee at Knoxville in 1991.

She was married to Yimin Jin in 1988. They have two children, Shee Qiu and Dong Yun.

Her hobby is travel and photography.